UNIVERSITY OF THE WITWATERSRAND, JOHANNESBURG

OPEN PIT OPTIMISATION USING MONTE CARLO SIMULATION: A CASE STUDY OF KOLOMELA MINE

S’thembile Nkambule

A research report submitted to the Faculty of Engineering and the Built Environment, University of the Witwatersrand, in partial fulfilment of the requirements for the degree of Master of Science in Engineering.

Johannesburg, September 2024

DECLARATION

I declare that this research report is my own unaided work. It is being submitted for the degree of Master of Science at the University of the Witwatersrand, Johannesburg. It has not been submitted before for any degree or examination to any other university.

I have familiarised myself with the University of the Witwatersrand Student Academic Misconduct Policy (SAMP). I hereby declare that the work I am submitting for assessment is my original work. I affirm that I have not plagiarised, misrepresented, or colluded with any other person or source. I have properly acknowledged, cited, and referenced all the sources that I have used in my work. I also declare that where I have used artificial intelligence (AI) tools it has only been as a means of guidance. The ideas and arguments presented in my work are my original thoughts and interpretations. I acknowledge that any academic misconduct, such as plagiarism or collusion will result in serious consequences. According to the SAMP, these consequences may include a reduced grade, a fail mark, or disciplinary action. The Faculty of Engineering and the University of the Witwatersrand have my consent to investigate any potential academic misconduct in my work. This investigation may include the use of similarity and AI detection software to check the originality of my work. I undertake to abide by the decision of any such investigation.

.

________________________________ ___30/09/2024_______

Signature of Candidate Date

ABSTRACT

Iron ore grade and price are among the input variables in the open pit optimisation process. Kumba Iron Ore (KIO) uses the widely used deterministic approach whereby average input variables are used to determine open pit limits. This approach assumes that the estimated variables are known with certainty. However, the input variables are associated with uncertainty. For example, the grade of a mineral deposit is estimated by interpolating relatively limited data from exploration drilling results. This means that the estimated grade is not entirely a true representation of the entire mineral deposit. This can be a significant source of uncertainty. Also, iron ore prices have proven to be highly variable in the past years which can also be a significant source of uncertainty. If uncertainty of these two variables is not well understood and quantified, this can result in sub optimal or overly estimated pit limits. The effect of not understanding uncertainty can lead to poor decisions that can result in loss of revenues or additional cost and thus can impact the net present value (NPV) and life of a mine (LOM) of a mineral project. KIO, like all mining companies, is increasingly concerned with the effects of risk on NPV because of the chosen final pit shells. The aim of this research was to model the uncertainty of iron ore price and grade associated with open pit optimisation.

Isatis software was used to produce ten realisations of the case study orebody and Monte Carlo Simulation was used to model iron ore prices. The economic block values of the ten block model realisations were calculated using four prices which were P75, P50, P25 and P5. The ‘P’ in P75, P50, P25 and P5 refers to probability of exceeding a certain iron ore price point. A P50 value is a median value, which means that it is expected that 50% of the time, the iron ore price will be above the P50 value, and 50% of the time, it will be below the P50 value as simulated from @Risk software. Forty pit shells and high-level schedules were then generated using Deswik Pseudoflow. NPVs of the forty pit shells were determined and were compared to the NPV of the deterministic pit shell.

The study showed that there are benefits in doing probabilistic iron ore grade estimation as opposed to deterministic estimation. The highest difference in ore tonnages between the deterministic block model and the simulated block models was 15%. The probabilistic pit shell with the highest ore tonnages had lower strip

ratios and an additional year of mining. This resulted in the pit shell producing the highest NPV.

Results of the study also showed that iron ore price has a huge impact on NPV. The P5 price ($170.89/t), which was the highest price with a low probability, produced bigger pit shells and higher NPVs. The P75 price ($70.84/t) which was the lowest price with higher probability, produced smaller pit shells and lower NPVs when compared to NPV of the deterministic pit shell produced at $78.5/t. The study interpolated NPVs of the probabilistic pit shells and showed that KIO deterministic pit shell was planned at P71. This shows that KIO is very conservative in their mine planning.

It is recommended that probabilistic pit optimisation be done for all pits at Kolomela Mine. In addition to iron ore grade and price, it is recommended that uncertainty of all pit optimisation input parameters be modelled. It is also recommended that the methodology demonstrated in this study be used also at Sishen Mine. Finally, it is recommended that KIO should implement this methodology annually before their medium-term planning process to assess uncertainty during pit optimisation.

DEDICATION

I dedicate this research report to my:

- Late mother, who taught me the importance of seeking knowledge.
- Husband who encourages and supports me to be the best I can be.
- Children, who are my driving force.

ACKNOWLEDGEMENTS

I would like to thank the following institution and people:

- Kumba Iron Ore, for granting me the opportunity to conduct this study and permission to publish this research report.
- My supervisor, Dr Tinashe Tholana, for all the guidance and support during the research.
- Mrs Elelwani Machaka for providing the licence for Isatis Software used in the research.
- Mrs Sarah Williams for all the support and guidance during the research.

Table of Contents

LIST OF FIGURES

LIST OF TABLES

LIST OF ACRONYNMS AND ABBREVIATIONS

ABBREVIATION	DEFINITION
Al_2O_3	Aluminium Oxide
ANN	Artificial Neural Network
CFR	Cost and Freight
DCF	Discounted Cash Flows
DMS	Dense media separation
DSO	Direct shipping ore
EBV	Economic block value
Fe	Iron ore
FOR	Freight on rail
GA	Genetic algorithm
GT	Graph Theory
KIO	Kumba Iron Ore
KSS	Kapstevel South
LG	Lerchs Grossman
LOM	Life of mine
MCA	Monte Carlo Analysis
MCAF	Mining cost adjustment factor
MCS	Modified Conditional Simulation
Mtpa	Million tonnes per annum
NPV	Net Present Value
P75	Probability of 75% of iron ore price
P50	Probability of 50% of iron ore price
P25	Probability of 25% of iron ore price
P5	Probability of 5% of iron ore price
PCAF	process cost adjustment factor
RF	Revenue Factor
ROM	Run of Mine
SiO_2	Silica Dioxide
SMU	Small Mining Unit
3D	Three dimensional
TBS	Turning Band Simulation
UHDMS	Ultrahigh density media separation
VIU	Value-in-use

1 INTRODUCTION

1.1 Overview of Chapter 1

This chapter introduces the research study. It starts by describing Kumba Iron Ore (KIO)'s mine value chain and provides a brief description of Kolomela Mine including its location and mining processes. The chapter also provides the problem statement, research questions, research aim and objectives, and the significance of the research. In this report, the phrases ultimate pit limit, final pit limit, pit boundary and optimum pit are used interchangeably.

1.2 Research background

1.2.1 Kumba Iron Ore operations

KIO is a South African iron-ore mining company, which is the fifth largest iron-ore producer in the world and the largest in Africa producing an average of 40 Mtpa of iron ore (Anglo American, 2022). KIO follows the following steps to develop a mine (Anglo American, 2022):

- Exploration and mineral resource definition: There is ongoing, and near-mine exploration and mineral resource definition drilling conducted to increase confidence in the company's geological block models which are updated annually in support of life of mine (LOM) and long-term planning processes.
- Evaluation of the geological block models: Once the updated geological block models are produced by the mineral resource department, the deposit's characteristics, such as its grade, tonnage, and metallurgical properties are evaluated. Thereafter, pit optimisation is done. Mine management uses this information to determine the best equipment and how to beneficiate the ore to produce the required finished iron ore product specification.
- Selecting a mining method: An appropriate mining method is selected to extract the mineral deposit.
- Mine design: Once a mining method is selected, planning of the mine layout is done. This includes determining the location of access roads and other infrastructure needed to support the mining operation.
- Mining: KIO currently uses the open pit mining method. The process of mining entails topsoil stripping, drilling, blasting and then extracting the iron ore.

- Beneficiation: KIO uses a combination of direct screening, dense media separation (DMS), ultrahigh density media processing (UHDMS) and jigging technologies to regulate the physical properties of the finished iron ore product, removing impurities and improving the quality of the product.
- Processing and blending iron ore products from its operations to provide niche products to the markets. The iron ore products are screened and sized to match customer requirements, and then transported through an outbound logistics chain.
- Shipping, marketing, and selling: KIO sells its iron ore internationally and none is sold locally. Export customers are in several geographical locations around the world, including China, Japan, India, South Korea, and countries in Europe.

KIO operates two mines namely Sishen Mine and Kolomela Mine. This research was focussed on Kolomela Mine which is located 12 km south-west of Postmasburg town in the Northern Cape province of the Republic of South Africa. The location of Kolomela Mine can be plotted using the following WGS84 latitude/longitude geographical coordinates: 28°23’30.05” S and 22°58’46.88” E. Figure 1 shows the location of Sishen Mine, Kolomela Mine and the logistics chain of Kolomela Mine.

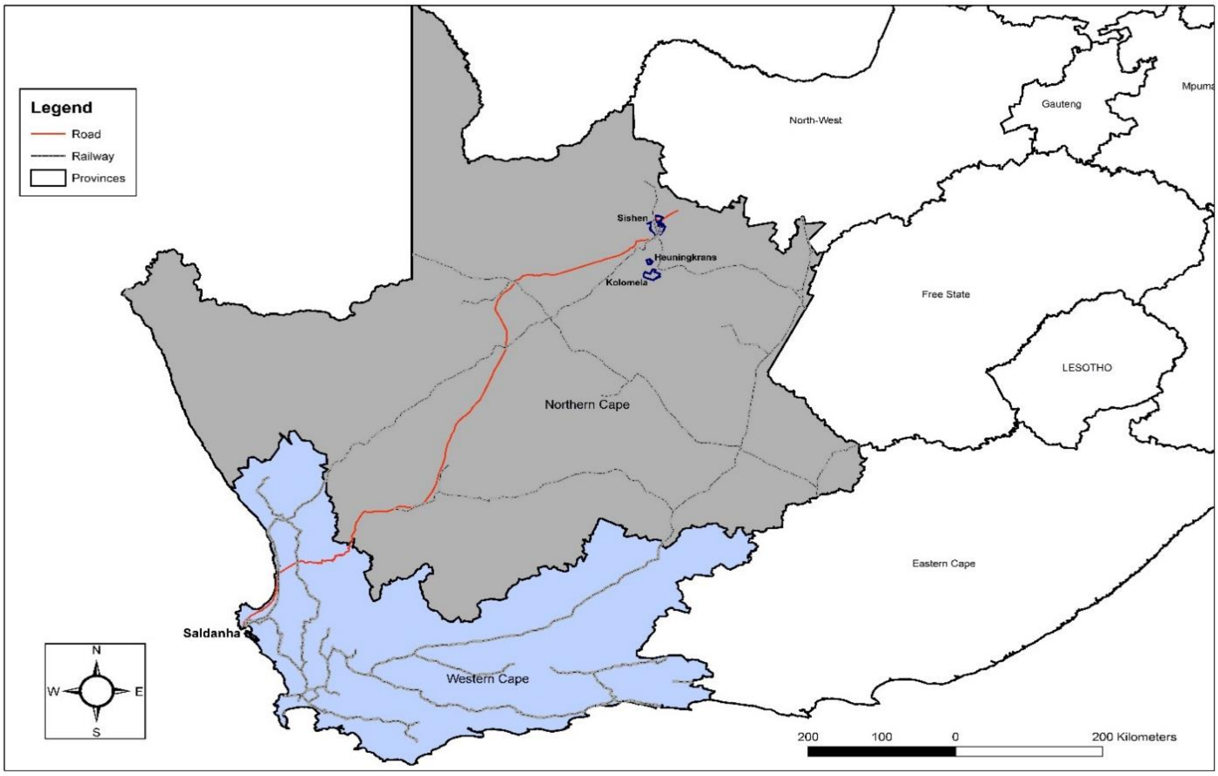

Figure 1: Location and logistics chain of Kolomela Mine

(Source: Anglo American, 2022)

1.2.2 Kolomela Mine's operational outline

Kolomela Mine currently comprises of a conventional open pit operation which consist of four active pits namely Klipbankfontein (KF), Leeuwfontein (LF), Kapstevel North (KN) and Kapstevel South (KSS) and the associated dumps called 'EF'. Figure 2 shows the arial view of Kolomela Mine and the location of each pit coloured in different colours.

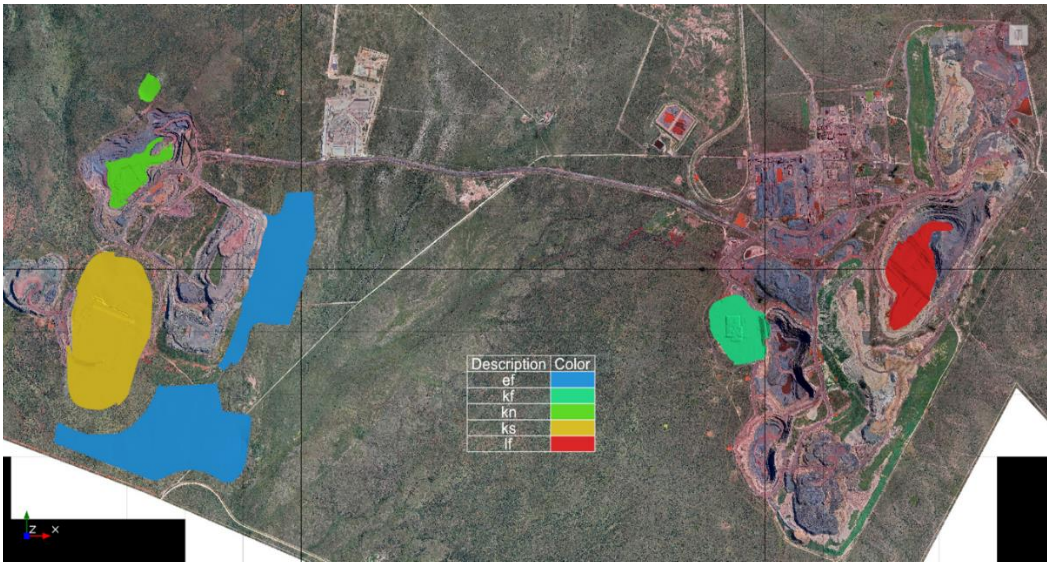

Figure 2: Kolomela Mine pits

(Source: Anglo American, 2022)

This scope of this study was limited to KSS pit which is coloured in yellow as shown in Figure 2. The pit is the latest developed pit at Kolomela Mine. Waste stripping at KSS pit started in 2021 and ore mining had not started at the time of writing this report. Kolomela Mine processes run of mine (ROM) through two facilities: a direct shipping ore (DSO) crushing and screening plant and a DMS plant, with a combined design capacity of 15 Mtpa. The costs associated with the two plants are different. The DSO plant is the lower cost plant as it only involves crushing and screening.

The current mining process at Kolomela Mine follows the KIO mining process outlined in Section 1.2.1. The iron ore is loaded to designated ROM buffer stockpiles according to a set of pre-defined grade control ore classes which are, A (high grade) and B and L (medium grade). From the stockpiles it is blended, sometimes together with direct feed from the pits as ROM. The ROM is then crushed and screened in the DSO plant to produce two types of iron ore products conforming to specific client grade specifications. These are a lump product with sizes ranging from -31.5 mm to +8 mm size and a fine product with sizes ranging from -10 mm to +0.15 mm. The medium grade iron ore, that is, the B- and L- grade ore are unsuitable as direct shipping ore. A small amount of this ore can be blended into the DSO plant feed together with the higher-grade ore, so as not to compromise grades of the blended product. The rest of the medium-grade ore is delivered as ROM to a small-scale UHDMS plant. Tailings from the processing plant are pumped into a decanter which produces a dry cake and a clean concentrate for water recovery.

1.2.3 Current open pit optimisation at Kolomela Mine

Open pit limit optimisation is a process which determines the extents within which mining is to take place for open pit mines. Thus, the process determines areas that will fall outside the limit because they will not be economic to mine. The pit optimisation process at KIO is aimed at determining areas that target the highest net present value (NPV). KIO uses the Lerchs Grossman (LG) algorithm embedded in Whittle or Deswik software to determine final pit limits. This is a deterministic approach which does not consider uncertainty associated with iron ore price and grade. Therefore, there is need for a probabilistic or stochastic approach to analyse the uncertainty in price and grade. The LG algorithm has proven to give optimum results in a reasonable amount of time of about 40 minutes for Kolomela Mine data, depending on the following attributes:

- The number of blocks in the block model and size of the block model. The KSS block model used was 3.2 gigabyte big and had 184 344 blocks after regularisation.
- The number of arcs related to slope setting. KSS pit has five domains.
- Distribution of block values.
- Computer hardware.

1.3 Problem statement and research question

The main limitation of using a deterministic approach in pit optimisation is that it does not account for any uncertainty in input factors such as iron ore price and iron ore grade. For example, Figure 3 shows the variability of iron ore prices from 2012 to 2022. According to Mineral Industry Survey (2022), 98% of iron ore produced globally is used in steelmaking. The global demand of iron ore has always fluctuated due to the unpredictability in the global steel production, mainly driven by China. This in turn resulted in fluctuating iron ore prices. KIO’s iron ore is mainly priced off the Platts IODEX 62% Fe CFR China index (Platts 62 index), which is the fines iron ore price published every day. Adjustments are made to the price depending on the Fe, SiO_2 and Al_2O_3 content of the ore, according to published Fe, SiO_2 and Al_2O_3 premia, which is also published every day. For lump ore, a lump premium is added to the price (also published by Platts).

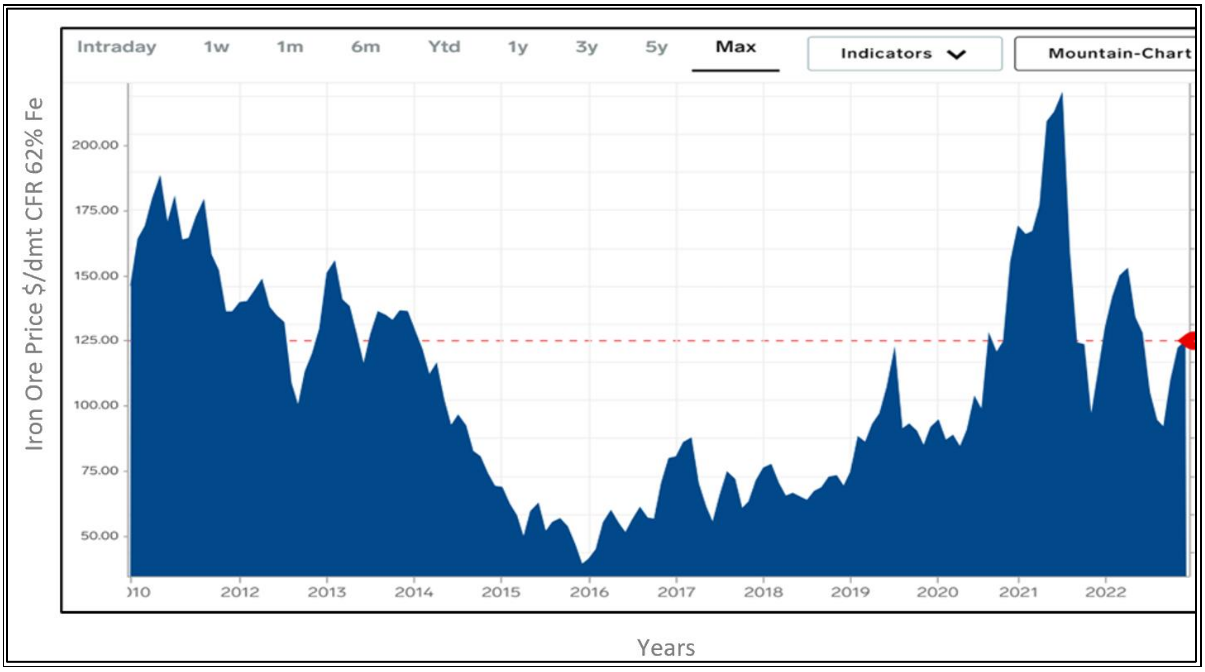

Figure 3: Ten-year historical iron ore prices

(Source: Market Insider, 2022)

Using Figure 3 as a reference, if a pit was designed in May 2012, its block value and NPV would have been calculated based on the price of $137 per tonne, while the price in February 2016 dropped to a low of $45 per tonne. The implication of this to the mine is that in 2016, the mining area would have consisted of a bigger pit with mining blocks that would not have been economic to mine at the $45 per tonne price. Therefore, the problem with a deterministic pit optimisation approach is that it determines a final pit limit based on the assumption that all blocks are mined within the same period. This is so because the same price is used for all blocks. This approach ignores the variation of commodity price with time. Uncertainty in ore grade is a major problem in open pit mines. This is general reflected by big differences between estimated grade and actual grades received by the plant. Deterministic pit optimisation assumes that all input parameters are known with certainty at the time of mine planning when in reality they are not. Therefore, this raises the question:

> *"How does the variation in iron ore price and iron ore grade affect an optimum pit"?*

1.4 Research aims and objectives

The aim of the research was to use Monte Carlo simulation and conditional simulation to model the uncertainty of iron ore price and grade associated with open pit optimisation, respectively. Kolomela Mine was used as a case study. The objectives of the research were to:

- Review relevant literature on open pit optimisation.
- Model the variability of iron ore grade using conditional simulation.
- Model the variability of iron ore price using Monte Carlo simulation.
- Illustrate the impact of variability in iron ore price and grade on optimal pit limits.
- Produce open pit shells at four price probabilities (P75, P50, P25 and P5) instead of a single pit shell estimate.

1.5 Research motivation and significance

KIO, like all mining companies, is increasingly concerned with the impacts of risk on NPV because of the chosen final pit shells. Risks should be assessed for their probability and impact using a scale such as low, medium, and high. It is important that the company evaluates the probability of the risk associated with chosen pit shells to plan for the impact it would have if it does happen. The current global mining business environment characterised by increased competition, low ore grades, increasing production cost, and stricter environmental regulations, requires that to be profitable, mining companies must optimise their processes. Final pit limit optimisation is one of the activities in the mining value chain, which is critical for optimal economic value creation. Although the deterministic LG-based pit optimisation approach is widely used in the industry including at KIO, it is unable to quantify the inherent risk associated with the stochastic pit optimisation problem.

Figure 3, shows that iron ore price is volatile hence uncertain. Therefore, probabilistic and stochastic methods should be used in open pit optimisation. These methods can incorporate the uncertainty associated with input parameters. In contrast to deterministic methods which result in static final pit limits, probabilistic and stochastic methods result in a range of possible final pit limits. Using a method to represent uncertainty in open pit optimisation at KIO is important as it will quantify risks associated with chosen optimum pits.

Results of the research will assist KIO to produce final pit limits and pit schedules that incorporate uncertainty in iron ore price and grade hence reduce the company's susceptibility to price variation and geological risk. Four optimal pit shells were created at different probabilities (P75, P50, P25 and P5) instead of a single shell estimate currently being done at the mine. Modelling uncertainty in the final pit will help the company to:

- Have a view of the potential LOM and its uncertainty.
- Derive NPV as a probability distribution from an output of simulations, which will give managers a view of the probability of mining operations successfully.
- Make informed decisions regarding infrastructure placement and available areas for stockpiling especially if the approved mining rights area is limited.

1.6 Summary of Chapter 1 and report outline

The report is structured in five chapters. Chapter 1 introduced KIO's value chain and gave a brief introduction of Kolomela Mine, which is the focus of this study. The chapter also provided the location and briefly described mining processes at Kolomela Mine. The problem statement, research questions and research aim, and objectives were also outlined in the chapter.

Chapter 2 reviews literature on open pit optimisation describing all the input factors that are required to determine final pit limits. A geological block model is one of the key inputs into the pit optimisation process. Geological block modelling and the conversion of a geological block model into a mining block model is discussed in the chapter. The chapter then discusses the application of modifying factors to convert a mining block model into an economic block model. This chapter also reviews some of the currently available open pit optimisation techniques including stochastic methods.

Chapter 3 describes the research approach and methodology used for the research. This chapter describes data that was used in the research and how the data was collected. The data include the geological block model, modifying factors, geo-metallurgical model, economic data including costs and iron ore prices. A summarised discussion is given on how the data was analysed.

Chapter 4 presents the results of the research study. A comparison and analyses of the deterministic and the forty probabilistic pit limits optimisation results is done. The chapter distinguishes results of the two processes and shows the different input parameters used in both processes. High level schedules and NPVs of the forty nestled pit shells were generated and compared to those of the deterministic pit shell. Chapter 5 provides key conclusions and recommendations for future work.

2 OPEN PIT OPTIMISATION

2.1 Overview of Chapter 2

Chapter 2 starts of by describing the importance of the pit optimisation process. The chapter then reviews relevant literature on open pit optimisation by describing all the input factors that are required to determine a final pit limit. The pit optimisation process follows a systematic approach. The chapter gives an overview of the steps involved in this process, which starts with geological block modelling. The geological block modelling process produces a geological block model which contains information about an orebody. The chapter discusses how the geological block model is converted into a mining block model. The chapter then discusses the application of modifying factors to convert a mining block model into an economic block model. The economic block model is an input to the pit optimisation process.

This chapter also reviews some of the relevant open pit optimisation techniques their strengths and limitations. Further, the chapter discusses uncertainty involved in open pit optimisation and sources of the uncertainty. The chapter concludes by reviewing the probabilistic and stochastic methodologies that are available for modelling mineral prices and grade uncertainty.

2.2 Open pit optimisation

As defined in Section 1.2.3, open pit optimisation is a process of determining economic mining limits for open pit mines. Mwangi *et al.* (2020) say that the ultimate pit limit optimisation plays a major role in open pit mines as it serves as the elementary foundation for all the activities in mine planning. Mukombo *et al.* (2020) further indicate that the process is one of the important steps which aims to design a pit that allows both a very good recovery of the deposit and a cost of the extracted metal as low as possible. This will ensure that the highest NPV is obtained. NPV may fluctuate significantly depending on the chosen final pit limits. According to Dagdelen (2001), a final pit limit defines and distinguishes blocks within a set boundary which should be mined and those which fall outside the pit boundary that should not be mined. Figure 4 shows a simple illustration of a final pit limit.

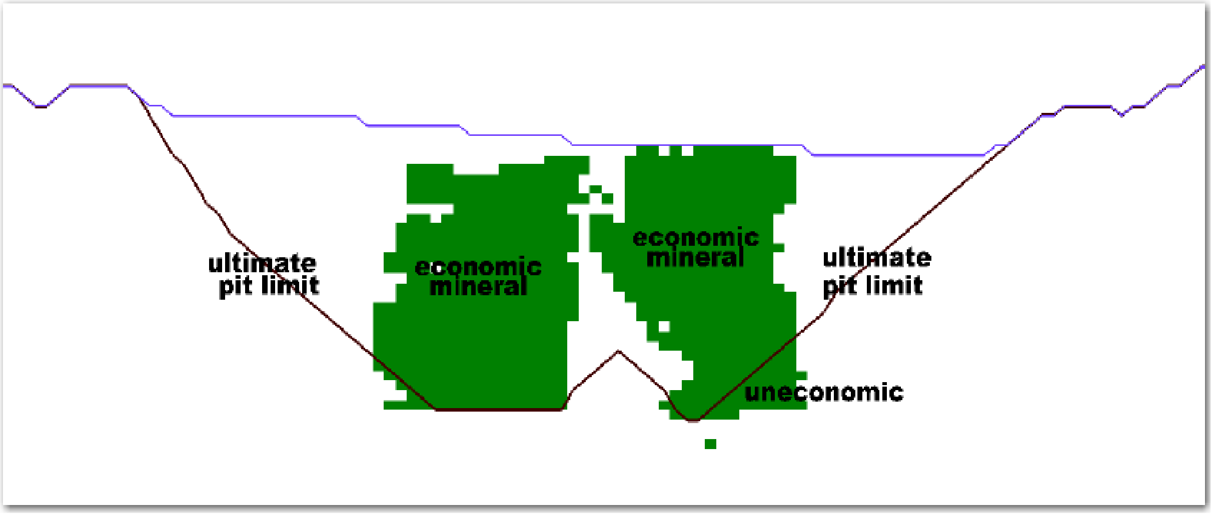

Figure 4: Final open pit limit

(Source: Songolo, 2010)

Askari-Nasab *et al.* (2009) emphasise the importance of final pit limits on long term strategic planning mentioning that:

- Understanding final pit limits is important for financial planning. It helps in estimating the costs associated with mining, processing, and extraction within the defined limits. This information allows mining companies to make informed decisions about investments and budget allocations.
- Setting final limits appropriately helps mining companies to optimise mineral resource extraction, ensuring efficient utilisation of mineral resources over the long term.

Defining final pit limits can also help in guiding the location of infrastructure, waste dumps and land acquisition strategies. Open pit optimisation follows a systematic step process which is aimed at maximising the economic value of an operation. Figure 5 shows an example of different pit shells produced at intervals of 0.5 revenue factors (RFs).

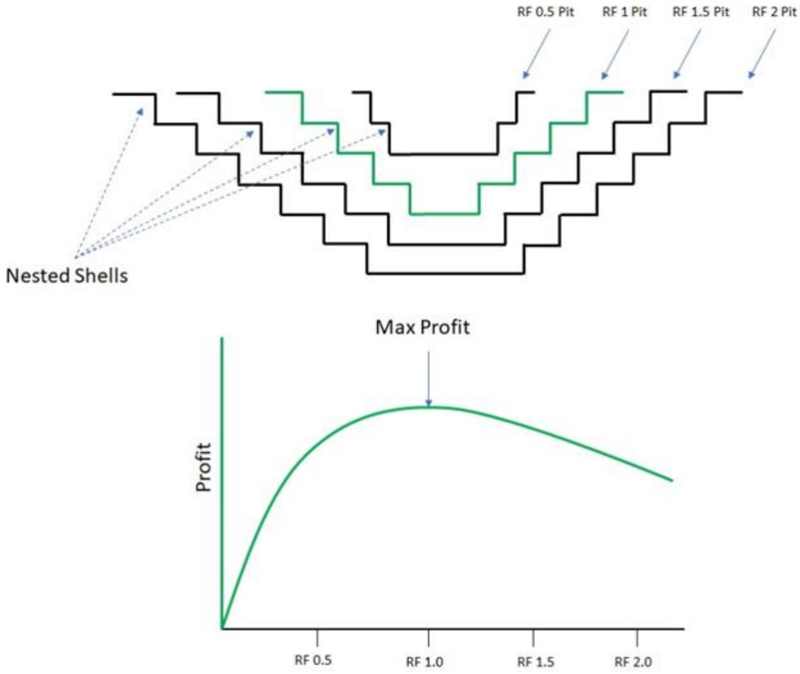

Figure 5: Nestled pit shells and revenue factors

(Source: Gauntlett, 2023)

Figure 5 shows that the pit shell with RF equal to one has the maximum profit. Profits start decreasing as RF increases beyond one. The process of choosing a final pit limit is not only based on the RF equal to one pit shell, but it also considers the time it will take to mine the pit and cashflows that will be generated. Since it is unlikely that the pit can be mined in one year, to account for the 'time value of money' the cashflows are discounted to determine the maximum NPV. This means that the final pit is always less than RF equals to one. Figure 6 shows the steps followed when doing open pit optimisation using Whittle or Deswik software.

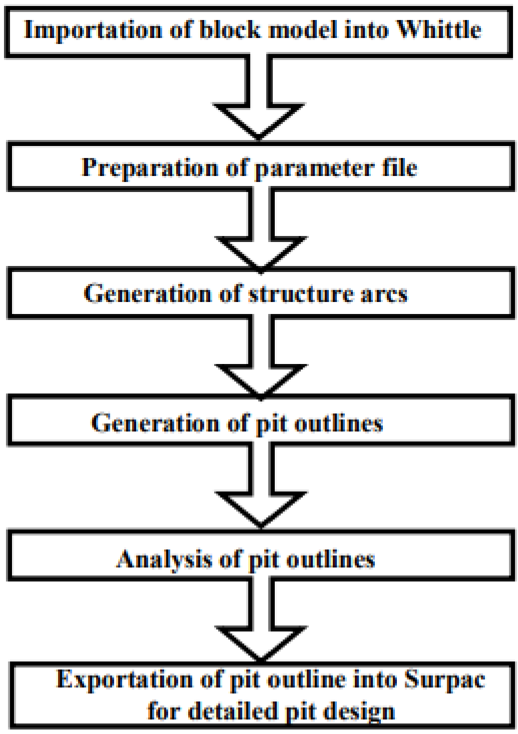

Figure 6: Open pit optimisation process

(Source: Appianing & Mireku-Gyimah, 2015)

The initial step in the open pit optimisation process is the importation of a geological block model. The geological block model can be imported in a format that Whittle or Deswik can read for example, csv files of Datamine file. A Datamine file is a block model generated using Datamine software.

2.2.1 Block modelling

Fallara *et al*. (2006) describe geological block modelling is a computerised representation of lithological, structural, geochemical, geophysical, and other diamond drill-hole data on and below the earth's surface. The process produces a geological block model. A geological block model is made up of three dimensional (3D) blocks of a mining area and each block contains assay values and corresponding geological data such as iron ore grade, oxide, contaminates among others. The assay values are estimated using geo-statistical estimation techniques such as kriging. Based on a predetermined cut-off grade, blocks of ore and waste are differentiated using their assay values.

The geological block model also known as a mineral resource block model is then converted into a mining block model. This conversion process is called block model regularisation. The process involves "up-blocking" or combining smaller blocks into bigger mining blocks. For example, 5 m x 5 m x 5 m block sizes can be converted into an operating smallest mining units (SMU) measuring 10 m x 10 m x 10 m by combining sub-blocks, including losses and dilution at source. This is done for several reasons. The first reason is to align block sizes to the SMU or shovels used at the mine. Jara *et al.* (2006) mention that SMU is the smallest size of a block that can be practically mined by shovels available at the mine. The size of the shovel is selected to match the desired production rates. These bigger blocks represent dimensions with which the shovels available at the mine can extract the blocks.

Jara *et al.* (2006) further state that the other reason is to match the mineral resource tonnages to the actual realised tonnages. The matching enables correct prediction of the tonnes of ore, tonnes of waste, and diluted iron ore grade that the plant will receive. For KSS this is closely represented by 10 m x10 m x 10 m SMU size. Therefore, SMU is an important process of pit optimisation because it enables a better representation of selectivity possible in practice. The choice of SMU has an impact on the results of the pit optimisation. A SMU block model that results in lower grades of ore after regularisation, will produce a different pit shell than the SMU block model that has higher ore grade. Once the mining block model is generated it is then converted into an economic block model by applying modifying factors.

Rupprecht (2014) defined modifying factors as considerations used to convert Mineral Resources to Mineral Reserves. These include, but are not restricted to, mining, processing, metallurgical, infrastructure, economic, marketing, legal, environmental, social and governmental factors. Ore loss and dilution factors arising from model regularisation and operational ore losses are applied to the mining block model. Breed and van Heerden (2016) state that, these modifying factors are derived from historic reconciliation. As mentioned by Wackernagel (2003), geo-metallurgy combines process mineralogy and material characterisation as a tool for predicting future metallurgical performance in beneficiation plants. Geo-metallurgy helps to determine the variability of a mineral deposit in terms of ore hardness and flotation kinetics, and impurity levels in a final product. This allows for the evaluation of different processing options based on historical samples. Geo-metallurgical algorithms help to integrate geo-metallurgical relationships in geological block models to aid mine scheduling and blending processes. In addition to the mining, processing, metallurgical modifying factors, economic factors are added to the mining block model to result in an economic block model. All these modifying factors are populated in a parameter file which is a key input for pit optimisation software.

In an economic block model, each block is expressed in economic terms by calculating each block's net worth called an economic block value (EBV). The EBV is focused on estimating the economic value of a mineral deposit. EBV which distinguishes ore and waste blocks is affected by the following factors (Nhleko *et al.,* 2018):

- Grade content of the block.
- Mining method applied.
- Location of the block which affect the cost of mining and transporting the block.
- When the block will be mined.

To calculate EBV, each block requires parameters namely, grade, tonnage, commodity price, recovery, beneficiation cost and mining cost. Many researchers including, Ataee-pour (2005); Camus (1992) and Whittle (1990) have suggested various formulae to calculate EBV. In this study, Equation 1 with simulated iron ore price and grade was used to calculate EBV (Camus, 1992):

$$EBV = GR*T*Rec*(PR-TC)-T*PC*PCAF-T*MC*MCAF \qquad (1)$$

Where: *GR* is grade, *T* is block tonnage, *Rec* is recovery, *PR* is commodity price, *TC* is total cost, *PC* is processing cost, *PCAF* is process cost adjustment factor, *MC* is mining cost and *MCAF* is mining cost adjustment factor of a block in relation to its bench elevation. Whittle *et al.* (2007) consider Equation 1 to be a deterministic approach, which results in a single EBV for each block. Tholana *et al.* (2019) mentioned that one of the main limitations of deterministic EBV calculation is that it assumes that the geological, economic, and other technical input parameters are known with certainty whilst they are uncertain.

2.2.2 Generation of structure arcs

As stated by Whittle (1993), an arc illustrates the relationship between blocks, that is, which block should be mined to expose another block of value. Structured arcs in open pit optimisation refer to predefined boundaries or areas within a mining pit that are strategically designed to enhance operational efficiency, mineral resource recovery, and overall planning of the mine. These structured arcs are used to segment the pit into separate areas (or ranges) each with specific characteristics and considerations.

Once the arcs are generated, the open pit optimisation process can be done. There are several algorithms and techniques that have been developed to generate final pit limits.

2.3 Open pit optimisation techniques

Saleki *et al.* (2019) indicated that there are two main approaches traditionally used to determine final pit limits, namely:

- The undiscounted profit maximisation approach.
- The approach of determining the optimal mining sequence of all blocks and discounting the EBVs.

Each of the approaches have different algorithms which are discussed in the next subsections. All the algorithms have a common aim of determining final pit limits which maximises NPV.

2.3.1 Lerchs-Grossman algorithm

The Lerchs-Grossman (LG) algorithm was developed by Lerchs & Grossmann (1965). Zhao & Kim (1992) mentioned that the LG algorithm was a pioneering open pit optimisation technique. The algorithm which is based on dynamic programming is used to determine final pit limits and pushbacks. It is embedded in most commercially available open pit optimisation software. For example, Whittle software provided by Dassault Systèmes GEOVIA. The algorithm is generally accepted and widely considered as an industry standard (Dimitrakopoulos *et al*., 2002; Askari-Nasab *et al*., 2009).

The LG algorithm is one of the few methods used in the industry to produce final pit limits. The algorithm produces different pit shells by using varying commodity price with RF but keeping costs and other factors constant. This in turns produces a logical incremental progression of economically defined pits shown in Figure 5.The algorithm is a rigorous mathematical algorithm that requires the following inputs and conditions to be able to determine the final pit limit (Dimitrakopous *et al.,* 2002):

- A set of blocks with calculated EBVs.
- The blocks' information must completely fill the space considered for mining.
- The blocks must have defined relationship (arcs).

Figure 7 summarises the steps of the algorithm.

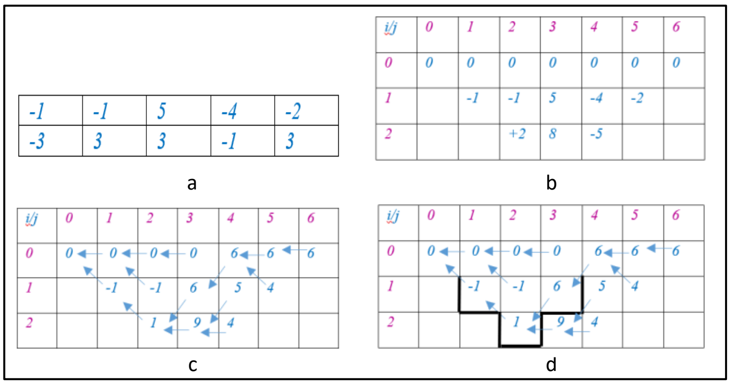

Figure 7: Summary steps of the LG algorithm

(Source: Adapted from Wright, 1987)

The following steps are followed by the algorithm (Lerchs & Grossmann, 1965):

- Step 1: One cross section of an economic block model (Figure 7a) is selected for analysis at a time and a row of blocks with zero EBVs is added at the top of the section (Figure 7b).
- Step 2: Starting from the top row, moving from left to right for each column, each block's EBV is replaced by the sum of all the block values above it (Figure 7b) calculated using Equation 2 (Lerchs & Grossmann, 1965):

$$M_{ij} = \sum_{n=1}^{i} M_{nj} \quad (2)$$

Where, M_{nj} is the block value at row number n and column number j, and M_{ij} is the cumulative EBV of a column of blocks from the surface to and including the block in row *i* and column *j*, B_{ij}.

- Step 3: P_{ij} values for each block are calculated. P_{ij} for a block is the sum of M_{ij} and the maximum EBV (optimum neighbour) among a block located on either the left row top ($B_{i-1,\ j-1}$), centre ($B_{i,\ j-1}$), and block on the lower left ($B_{i+1,\ j-1}$). P_{ij} values are calculated using Equation 3 (Lerchs & Grossmann, 1965):

$$P_{ij} = M_{ij} + \max \begin{cases} P_{i-1,\ j-1} \\ P_{i,\ j-1} \\ P_{i+1,\ j-1} \end{cases} \quad (3)$$

- Step 4: Substitute the block value with P_{ij} values and draw an arrow from B_{ij} to the optimal neighbour. This is repeated for all blocks (Figure 7c).
- The final (Step 5) is to define the final pit limit of the section by choosing the block with the highest positive value in the top row and tracing the arrows from

the highest-value block to the left of the block (Figure 7d). This forms the final pit limit for that particular section. The above steps are repeated for all sections and the final pit limit is a combination of all the optimal sections.

Even though the LG algorithm is widely used in the mining industry, it has limitations. The following are the limitations of the algorithm:

- The initial algorithm assumes static geotechnical slope angles that are ruled by the sizes of blocks (Dimitrakopous *et al.,* 2002; Khalokakaie *et al.,* 2000). Subsequent attempts to include changing slope angles have not provided an acceptable solution (Dimitrakopous *et al*., 2002).
- The 3D version of the algorithm assumes that the pit is rectangular (Lerchs & Grossmann, 1965). It is not necessarily 'wrong' that the 3D version of the algorithm assumes the pit to be rectangular, but rather a simplifying assumption made for computational efficiency and practicality. The limitation of assuming a rectangular pit is that the rectangular shape may not perfectly capture the actual topography or geological constraints of a mine site. This may result in conservative pit designs that provide a buffer against uncertainties and variations in input parameters.
- The algorithm uses a deterministic orebody model (Dowd, 1994). This means that it does not account for any uncertainty (Whittle J. , Beyond optimisation in open pit design in Computer Applications in the Minerals Industry, 1988). However, sensitivity analysis can be done though it is a very simple risk analysis method.

2.3.2 Graph Theory

Graph theory (GT) is a heuristic technique that yield optimal solutions. It was first developed by Lerchs & Grossmann (1965) to address the impracticality of the two dimensional (2D) dynamic programming algorithm in 3D. Zhao & Kim (1992, p. 423) describe the GT technique as a "technique that utilises the assets (blocks and arcs) of a block model of an open pit mine that it can be modelled as a weighted-directed graph in which the vertices represent blocks, and the arcs represent mining restrictions on other blocks". The technique applies a set of alterations to the graph's tree structures until there are no waste blocks preventing the removal of desirable ore blocks. The main advantage of the technique is that it can handle irregular block models (Picard, 1976). According to Zhao & Kim (1992, p. 423), the technique provides a systematic and structured approach to analysing the interdependencies of mining parameters, facilitates the visualisation of a mining operation as a network. Zhao & Kim (1992) also mention that the other advantage of the GT technique is that it enables the identification of optimal solutions based on mathematical optimisation techniques.

Despite the advantages of the technique mentioned above, the technique has limitations. One of the primary critiques noted by Hochbaum & Chen (2000), is the computational complexity of the graph theory, especially when dealing with large-scale mining operations and complex geological conditions. Additionally, the assumptions made in modelling the mining parameters as a graph may oversimplify the real-world complexities of the mining environment. The following are the other limitations of the GT technique (Hochbaum & Chen, 2000):

- Long computing time.
- High complexity.
- Large number of generated arcs.
- Difficult to assign pit slopes.
- Difficult to determine mining and processing capacities for each period.

Many research studies have been done to address the above listed limitations. These include the research by Chen (1977) which addressed the determination of an optimum pit with variable slopes and that of Zhao & Kim (1992)'s algorithm which aimed to reduce the number of generated arcs. In conclusion, the application of the graph theory algorithm in open pit optimisation has significantly contributed to the advancement of mining operations. While there are critiques and challenges associated with the use of graph theory, its advantages in providing systematic open pit optimisation solutions cannot be overlooked.

2.3.3 Moving (floating) cone method

This heuristic method for determining final open pits was developed by Carlson *et al.* (1966). The optimisation process is done by creating a cone with its slope angle consisting of mining blocks with EBVs, which are either positive or negative. If the sum of the blocks within the cone is positive, this represent a potential economic pit to be mined. Figure 8 illustrates the application of the moving cone method. The top row on the figure represents column number while the left column represents row number.

	1	2	3	4	5	6	7	8	9
1	-3	-3	-3	-3	-3	-3	-3	-3	-3
2	-4	7	-4	6	-4	-4	-4	8	-4
3	-5	-5	-5	18	-5	-5	-5	-5	-5

Figure 8: An example of the moving cone method application

(Source: Adapted from Ares *et al.* 2022)

In Figure 8, in row 1, moving from left to right, no block has a positive value, hence no pit can be mined economically. Moving to row 2, the first block with a positive economic value is B_{22}. Although the block is positive it cannot be mined since the cumulative value together with blocks B_{11}, B_{12} and B_{13}, the cone value is -2. The second block with a positive value is B_{24}. Again, the cumulative value together with blocks B_{13}, B_{14} and B_{15}, the cone value is -3. The last block with a positive value on row 2, is B_{28}. Although the block is positive it cannot be mined since the cumulative value together with B_{17}, B_{18} and B_{19}, the cone value is -1.

Moving to row 3, the first block with a positive economic value is B_{34}. The block should be mined together with B_{12}, B_{13}, B_{14}, B_{15}, B_{16}, B_{23}, B_{24}, B_{25} and the cone value is 1. Since the cone value is greater than zero, the cone is mined. The process is repeated by shifting the cone, until the cumulative economic value starts regressing, to indicate that the final pit limit has been reached. Figure 9 shows the final pit limit for the section with a cone value of 1.

	1	2	3	4	5	6	7	8	9
		-3	-3	-3	-3	-3			
			-4	6	-4				
				18					
1	-3						-3	-3	-3
2	-4	7				-4	-4	8	-4
3	-5	-5	-5		-5	-5	-5	-5	-5

Figure 9: Final pit limit using the moving cone method

(Source: Adapted from Ares *et al.* 2022)

Even though the method is simple and fast, according to Wright (1999), it does not yield an optimum pit solution. The method also has the following limitations (Wright, 1999)**:**

- Depending on the search order of cones, different solutions can be generated.

- The method cannot deal with overlapping cones (group of blocks which fall inside more than one cone.
- Two separate cones may give a total negative value, yet if combined a positive pit is obtained.

The moving cone method was later improved by David *et al.* (1974) and Wright (1999) to overcome the overlapping problem. The improved Moving Cone II method proposed the joint testing of cones to decide where to remove a cone or not. However, the improved algorithm also does not guarantee an optimal solution.

2.3.4 Network flow analysis

Network flow analysis was initially applied in transport logistics. Its first use to solve the final pit limit problem was by Johnson (1968). The research by Johnson (1968) revealed that the problem of determining the final pit limit is essentially a maximum flow problem in network flow theory. Determining the final pit limit requires a flow of maximum value (NPV) from a source to a sink without violating given constraints.

An extension of this technique was done by Picard (1976). Picard (1976) showed that solving a maximum flow problem in a network, derived from a mine graph, solves the maximal closure in the mine graph problem. The final pit limit is depicted by the minimum cut. The minimum cut is a cut of minimum capacity among all cuts. Johnson (1968) highlights the strengths of the network flow analysis to be that:

- It is a flexible modelling technique which is efficient and scalable.
- It can represent a wide variety of real-world scenarios and has a wide range of applications in computer science.

However, Picard (1976) discussed the following disadvantages of the network flow analysis technique:

- In some cases where the graph is too big and there are complex capacity constraints, the technique can be difficult to solve efficiently.
- The technique may not always provide a unique optimal solution.

Giannini *et al.* (1991) developed a software package called PITOPTIM, which integrates both the LG algorithm and a network flow method for determining the final pit limit. Later research work by Hochbaum & Chen (2000) generalised the LG algorithm to a pseudoflow network model. The pseudoflow algorithm is now available in most commercial software packages including Geovia Whittle and Deswik to name a few. The pseudoflow algorithm creates the same final pit limits achieved using the traditional LG algorithm in a far more time efficient manner.

2.4 Advances in open pit optimisation

There has been a growing focus on stochastic open pit optimisation that aims to quantify risks associated with open pit mining while maximising NPV. In both the deterministic and stochastic approaches, the chosen final pit limits and production schedules are the ones with the highest cumulative NPV. Advances in open pit optimisation are based on using a hybrid of algorithms discussed in Section 2.3 and advanced algorithms discussed in the next subsections to ensure highest cumulative NPV. Genetic algorithm (GA) is a rigorous search algorithm which is founded on evolutionary concepts of natural choice and principle of genetics. It was first employed to optimise open pit mines by Denby & Schofield (1994). GA is defined by Ahmadi and Shahabi (2018, p. 184) as “a population-based search algorithm that uses a structured but randomised approach to utilise population information in finding a search direction”.

The two advantages of using GA according to Mitchell (1999) is that it can find solutions to complex optimisation problems that involve multiple variables and constraints. The other advantage is that the algorithm can explore multiple solutions simultaneously using population-based search techniques. Ahmadi and Shahabi (2018) highlight the limitation of GA to be that it can be computationally expensive, especially for complex problems with large solution spaces and populations, requiring significant computational resources and time. Ahmadi and Shahabi (2018) also said that GA often involves setting multiple parameters which can impact its performance and may converge prematurely, settling for sub-optimal solutions. Navarro *et al.* (2024) introduced the Parallel Genetic Algorithm (PGA) to optimise pushbacks in an open-pit mine. PGA is aimed at accounting for operational space constraints, modeled as truncated cones of extraction. The algorithm is based on a genotype–phenotype model such that the genotype symbolises the base block of a truncated cone, and the phenotype represents the cone itself.

Artificial Neural Network (ANN) is another advanced approach used for open pit optimisation. According to Haykin (1994), the ANN approach is best suited for problems that relate to pattern classification, prediction, and optimisation, such as open pit limit determination. Haykin (1994) mentioned that ANN was developed because intelligent machines are capable of replicating functions of the human brain such as pattern recognition and modelling of non-linear relationships of multivariate dynamic systems. In combination with the ‘conditional simulation’ technique, Achireko & Frimpong (1996) applied ANN to optimise open pit limits due to their ability to categorise blocks into classes based on their accustomed EBVs. The other advantage of the ANN as discussed by Achireko & Frimpong (1996) is that it can incorporate the randomness associated with ore grades where previous algorithms failed to. To address this, “Modified Conditional Simulation” (MCS) methods developed by Achireko & Frimpong (1996) incorporated this randomness, based on the best linear unbiased estimation and local average subdivision techniques. Achireko & Frimpong (1996) also highlights the following limitations of ANN:

- It is computationally expensive than traditional algorithms.
- It requires much more data than traditional machine learning algorithms.
- it is very hard to understand how and why the approach comes up with a prediction or output

Further strides in this field include the work by Askari-Nasab *et al.* (2009) who determined the final pit limit with discounted block values and developed the Intelligent Open Pit Simulator software. One of the key advances in open pit optimisation is the integration of data analytics to leverage the vast amount of geological, operational, and market data available to mining companies. By employing machine learning, statistical analysis, and predictive modelling, mining engineers can gain deeper insights into the complex relationships between mining parameters, leading to more accurate pit designs and extraction strategies.

2.5 Uncertainty in open pit optimisation

Dimitrakopoulos *et al*. (2002) state that uncertainty in open pit optimisation refers to the variability and unpredictability of factors that can impact the economics and feasibility of open pit mining operations. There are several sources of uncertainty in open pit optimisation, including geological, economic, and technical sources.

Godoy (2003) developed a method to quantify geological uncertainty in long-term production scheduling of open pit mines. The research was focused on the development of a new, risk-based method for the optimisation of long-term production scheduling. Menade *et al.* (2004) mention that the true distribution of ore grades and mineralisation within an orebody is never known with certainty and can lead to uncertainty in the estimation of EBVs and ultimate pit limits. Asad & Dimitrakopoulos (2013) explain that the demand for minerals and metals can be influenced by factors such as global economic conditions, political instability, and technological advancements, introducing uncertainty in the long-term profitability of a mine. Akbari *et al.* (2008) developed an open pit optimisation model considering uncertainty of mineral price using the real options approach. Akbari *et al.* (2008) noted that future prices of commodities such as gold, copper, and iron ore can fluctuate significantly, impacting the economic viability of a mine and optimal pit designs.

Cost is another source of economic uncertainty. Inthanongsone *et al*. (2015) presented cost models for open pit mines, which included cost uncertainty. The costs of mining, processing, and infrastructure can vary based on factors such as labour, fuel prices, and equipment availability, leading to uncertainty in the financial viability of different pit designs. The accuracy of mining and processing constraints, and other technical factors used in the optimisation process can also introduce uncertainty into the process. These factors include processing recoveries, mining losses and mining dilution. One of the key challenges in open pit optimisation is accurately modelling and predicting uncertainties associated with these factors. Traditional optimisation methods often rely on deterministic models that assume fixed input parameters and known outcomes. However, these parameters are subject to uncertainty and variability, leading to suboptimal mine plans and decisions. Overall, dealing with uncertainty in open pit optimisation requires robust sensitivity analysis, scenario planning, and risk management strategies to ensure that the selected pit shell is resilient to potential changes in market conditions and technical constraints. Monte Carlo Analysis (MCA) and conditional simulation are some of the techniques that are used to model uncertainty.

2.5.1 Modelling of uncertainty using Monte Carlo Analysis

Boyle (1977) defines MCA as a mathematical technique used to model the probability of different outcomes of a dependent variable through a successive simulation process. Figure 10 illustrates the systematics of MCA.

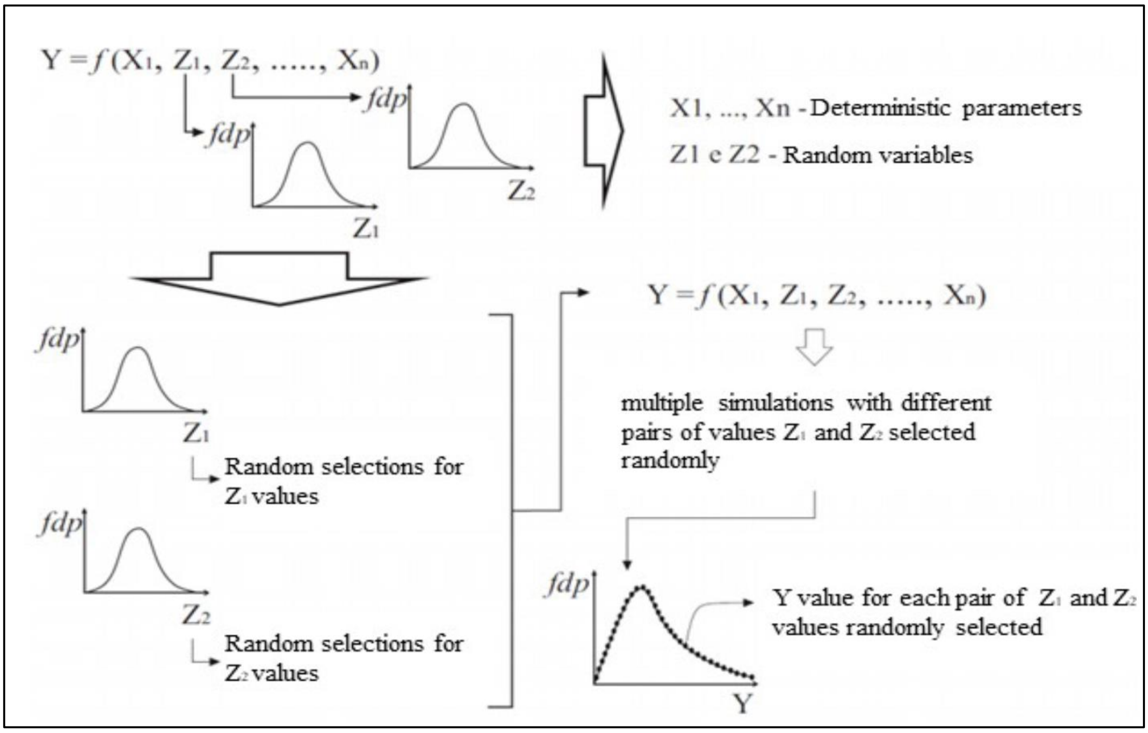

Figure 10: Systematics of Monte Carlo Analysis

(Source: Charbel, 2015)

According to Charbel (2015), in each simulation, MCA predicts a set of outcomes based on an estimated range of input values, drawn at random, as opposed to a set of fixed input values. Based on this function, probability analyses are performed on the input values. The range and likelihood of occurrence of inputs and outputs are directly related to the level of risks involved. However, MCA does not give optimal solutions. It only demonstrates the probability distribution which shows the behaviour of inputs and likelihood of occurrence of outcomes. This likelihood can be interpreted differently by different people based on their risk appetites. In this report Monte Carlo Analysis embedded in @Risk Software was used to determine the probability distribution of iron ore prices as mentioned in Chapter 1.

A case study by Baek *et al.* (2016) used the MCA method to represent uncertainty of open pit optimisation results due to variation in mineral prices in a copper-zinc deposit. The copper and zinc prices were analysed for a period of 10 years starting in January

2005 to April 2015. The study showed that uncertainty due to variations in copper and zinc prices significantly affect open pit optimisation results. Using price probabilities, mineral reserves were estimated as a function of confidence level. When confidence level was set at 90% or higher, mineral reserves were estimated to be about 76,000 tonnes, and when confidence level was set at 50% or higher, mineral reserves were estimated to be about 2,550,000 tonnes. This suggests that the MCA method can be used in mineral reserve estimation.

Gholamnejad *et al.* (2022) describe a research done on a copper mine located in Iran which was used as a case study. In the research, the probability distribution function of copper price was obtained using historical copper price. One hundred iterations of copper price were done using MCA. The simulated prices and fixed technical and other economic parameters were used to calculate EBVs. Using the EBVs and the NPV Scheduler software, a single optimal pit was obtained. Their research found that the results of the obtained optimal pit were less sensitive to changes in future copper price.

2.5.2 Modelling uncertainty in mineral price

According to Breed and van Heerden (2016), the traditional open pit optimisation methods use a fixed/known price assumption optimisation approach. However, stochastic models can be used to model future metal prices. The commonly used stochastic models to model stock prices in mining applications are the Geometric Brownian Motion and the Mean-Reversion process. According to Dixit and Pindyck (1994), the Geometric Brownian Motion is more suitable to model prices of precious metals.

The Geometric Brownian Motion was developed in 1827 by a Scottish botanist Robert Brown. Robert Brown noticed that pollen grains suspended in water move about at random even when the water appears to be very still. Metal prices are assumed to follow a continuous stochastic process like the Brownian Motion. Geometric Brownian Motion considers a constant relative growth rate. Geometric Brownian Motion involves a stochastic differential equation that describes the evolution of an asset's price over time. This equation considers the asset's drift and volatility. This model is commonly employed to understand and predict the movement of stock prices and other financial instruments over time. Equation 4 shows the Brownian Motion stochastic process (Goodman, 2012):

$$dP = \mu P dt + \sigma P dW \quad (4)$$

Where: dP represents the infinitesimal change in the asset's price over a small-time interval (dt); μ is the drift coefficient which represents the average rate of return of the asset per unit of time; σ is the volatility of the asset measuring the dispersion of returns around the average; P is the current price of the asset; dW is a Wiener process, representing the random component of the asset's price movement and μPdt accounts for the deterministic growth of the asset's price, while the term σPdW captures the stochastic (random) component of the price movement due to volatility. The Brownian Motion is used to model the inherent randomness and unpredictability in several applications in economics (Ibrahim *et al*. 2010).

Schwartz (1997) proposed the mean reverting process to model uncertainty of metal prices that exhibit some form of reversion to a long-term level. Equation 5 shows the mean reverting process (Schwartz, 1997):

$$dP = (\mu\eta - \ln P)\, Pdt + \sigma P dW \quad (5)$$

where: η is the speed of reversion, which is the speed at which the logarithm of the metal price reverts to the long-term level μ after a market shock.

In contrast from the Geometric Brownian Motion where the drift is constant, in the mean-reversion model, the drift is variable in both sign and magnitude. As shown in Equation 5, the drift varies based on the difference between the logarithms of the spot price and the long-term price μ. According to Schwartz (1997), if P is less than the long-term price, the expected drift for the next period will be positive. If P is greater than the long-term price, the expected drift will be negative. Therefore, the mean reversion model reflects the forces of supply and demand which are the main variables affecting the volatility of commodity prices. This research did not use a stochastic method like the Geometric Brownian Motion and the Mean-Reversion process to forecast the iron ore prices but used historic prices.

2.5.3 Modelling uncertainty in iron ore grade using conditional simulation

In addition to price uncertainty, it is important to understand geological uncertainty as it can also significantly affect the economics of mining. According to Dimitrakopous *et al.* (2002), one of the sources of risk in mining projects is uncertainty in ore grade. The grade of a mineral deposit is traditionally estimated by interpolating relatively limited data from exploration drilling results using geo-statistical methods such as the inverse distance and kriging methods. This means that the estimated grade is not a true representation of the entire mineral deposit. This is because it does not consider the uncertainty associated with the estimates and variability of the mineral grade. Therefore, this can be a significant source of uncertainty.

Several research on stochastic modelling of geological uncertainty has been done including by Dimitrakopous *et al.* (2002), Godoy (2003) and Menade *et al.* (2004). Dimitrakopous *et al.* (2002) developed models based on stochastic integer programming to integrate mineral grade uncertainty using a set of equally probable orebody models. Godoy (2003) developed a long term production scheduling method for open pit mines which incorporated geological uncertainty. Menade *et al.* (2004) used conditional simulation to develop a method to quantify uncertainty in EBV calculation, which results from the inherent gelogical uncertainty. This research used the conditional simulation method to simulate iron ore grade. All the research found that ignoring geological uncertainty may lead to unrealistic assessments and decisions. Figure 11 shows the traditional deterministic view, using a single estimated model, and a stochastic view using multiple probable models to account for uncertainty.

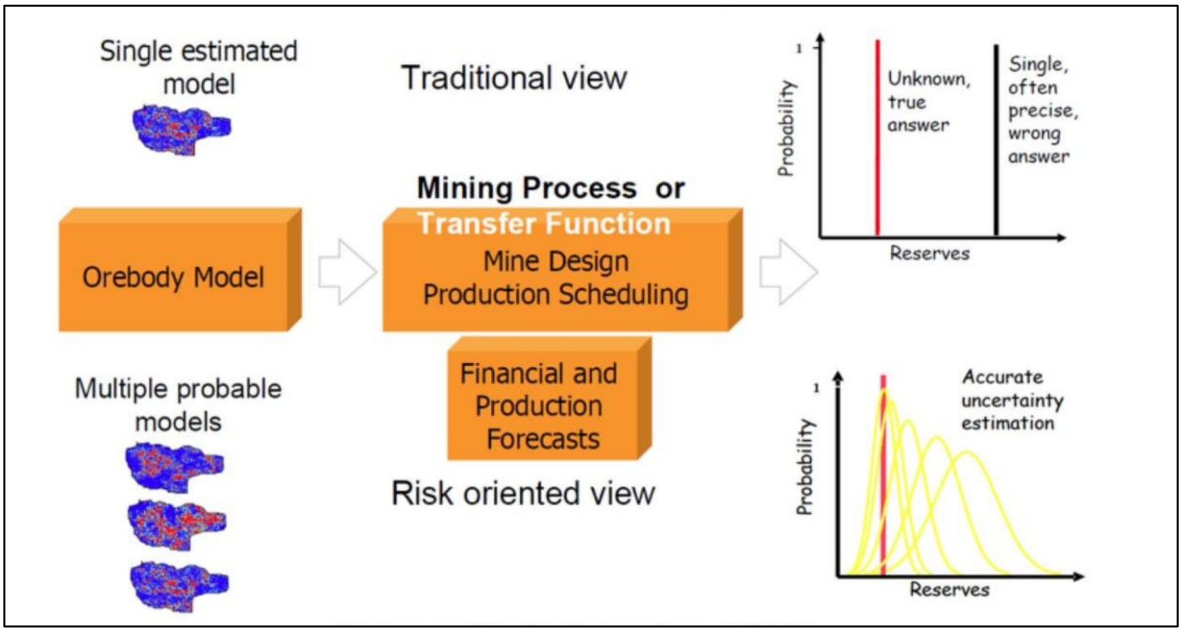

Figure 11: Quantifying uncertainty in orebody modelling

(Source: Dimitrakopoulos, 2010)

According to Dimitrakopoulos (2010), conditional simulation (Turning Band method) is a class of MCA that can be used to generate equally probable representation of in-situ orebody variability. Dimitrakopous *et al.* (2002) defines conditional simulation as a series of methods for producing models on a detailed scale to simulate spatial and statistical characteristics of mineral grade. Contrary to deterministic smooth orebody models, conditionally simulated ore bodies provide tools to quantify uncertainty in grade variability. This research study used the conditional simulation method to produce ten geological block models for each of the four probability prices. The contribution of this research study to the body of knowledge, is that it used a combination of three approaches namely, LG algorithm (pit optimisation), MCA (price probability) and conditional simulation in an iron orebody case study.

2.6 Summary of Chapter 2

Chapter 2 discussed factors that must be considered when doing open pit optimisation. This chapter described a geological block model mentioning information which is required to determine open pit limits. Once a geological block model is assessed and proved to contain all the information required, it is converted into a mining block model. This is done through a process called model regularisation or up-blocking to match the mining equipment which will be used for mining. This process results in ore loss and dilution. Additional modifying factors are applied to the mining block model based on historical performance or if it is new areas, based on benchmarking with similar mines. Geo-metallurgical factors are also included in the model to integrate geo-metallurgical relationships in block models and guide the best options of beneficiating ore. Lastly, an economic block model is derived whereby each block is expressed in economic terms by calculating each block's net economic worth.

This chapter also reviewed some of the currently available open pit optimisation techniques such as LG algorithm, GT, moving cone method, and network flow analysis. Advantages and limitations of the techniques were also discussed. Furthermore, the chapter highlighted latest advances in pit optimisation which is focused on stochastic open pit optimisation. These advances are based on using a hybrid of algorithms that ensures that the highest cumulative NPV is achieved. GA and ANN algorithms were discussed together with their advantages and limitations.

The chapter ended by discussing the sources of uncertainty in open pit optimisation and further discussed two probabilistic techniques used to model uncertainty namely MCA and conditional simulation. Stochastic modelling of mineral price techniques was also discussed. The following chapter describes the research methodology, data collection and data analysis applied in this study.

3 RESEARCH METHODOLOGY

3.1 Overview of Chapter 3

Chapter 3 describes the research approach and methodology used for the study. The chapter also discusses the data that was used in the research, how the data was collected and analysed.

3.2 Research approach

A research study can use qualitative, quantitative, or a combination of both approaches. According to Ernst (2003), the distinction between qualitative and quantitative approaches is that the quantitative approach involves the collection and analysis of numerical data while the qualitative approach involves collection of data about feelings, opinions, behaviours, experiences, and social contexts.

This research was a quantitative desktop study which was done using Kolomela Mine's data. The data include Kapstevel South (KSS) pit's block model. Even though the final pit limit is affected by uncertainty in geotechnical, geological, and economic parameters, this research study only modelled uncertainty of two variables (iron ore prices and iron ore grade). This was done by simulating iron ore price and grade, then together with other parameters, EBV for each block was calculated. The block models with the EBVs were used in Deswik Pseudoflow to determine open pit limits for different iron ore price probabilities. The research study used historically published iron ore prices obtained from Market Insider (2022).

3.3 Data collection

Data collection is the process of gathering data used to support or refute a research hypothesis. To ensure valid simulation results, data from various sources is required before a model can be built. The following subsections outline the data that was collected and how it was collected.

3.3.1 Mineral resource block model

The mineral resource block model was collected from Kolomela Mine's mineral resource department. The name of the mineral resource model that was used is KSS_0422_resource.dm. Detailed description of the KSS mineral resource model can be found on the resource report by Anglo American (2022). The data is validated and updated annually by the department. The data from new infill drilling is treated and standardised like exploration core drill hole data, in terms of logging lithologies and assayed grades. The lithological downhole interval logs within the KSS value of information have undergone numerous iterations of re-interpretation and recoding, based primarily on ongoing interval assay analysis. A total of 325 205 borehole sample log and assay data was applied in the update of the 2023 Kolomela Mine geological model. Of the data, 70% was derived from cored boreholes and 30% from percussion drilled boreholes.

Extensive iron ore and manganese-bearing lithologies are exposed in a narrow, north-south belt between Kolomela Mine and Postmasburg in the Northern Cape province. Figure 12 shows the summarised regional geology of Kolomela Mine.

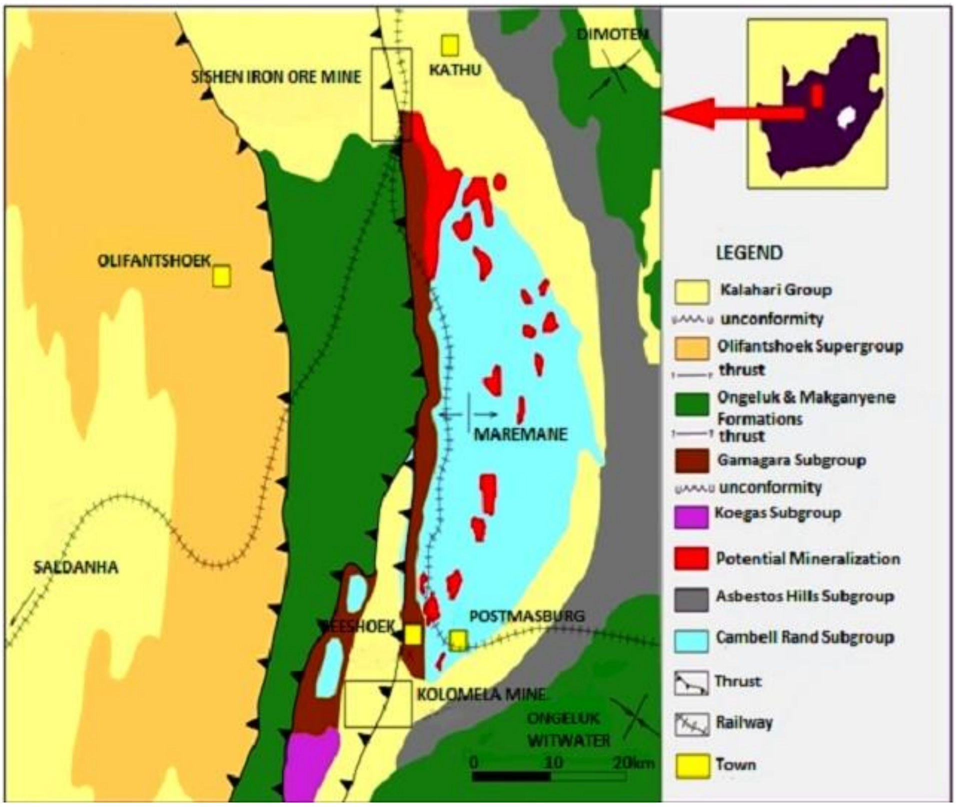

Figure 12: Summarised regional geology of Kolomela Mine

(Source: Anglo American, 2022)

The regional geology of Kolomela is discussed in detail in the report by Anglo American (2022), and a description of how the numerous shallow manganese and iron ore deposits were mined between the period 1900 and 1930. The landscape is dotted with abandoned mines along two sub-parallel ridges (the Gamagararand and Klipfonteinheuwels), which stretch from Beeshoek in the south to Kolomela Mine in the north. Currently, this ‘belt’ supplies the bulk of South Africa’s domestic iron ore market and enables the country to contribute towards the global iron ore supply.

The stratigraphy of Kolomela Mine’s local geology is schematically summarised in Figure 13. The figure shows the thickness of the modelled lithologies, the stratigraphic unit and age with which they belong to. The focus of this study was on the massive, laminated ore which ranges from 30 m to 45 m in thickness.

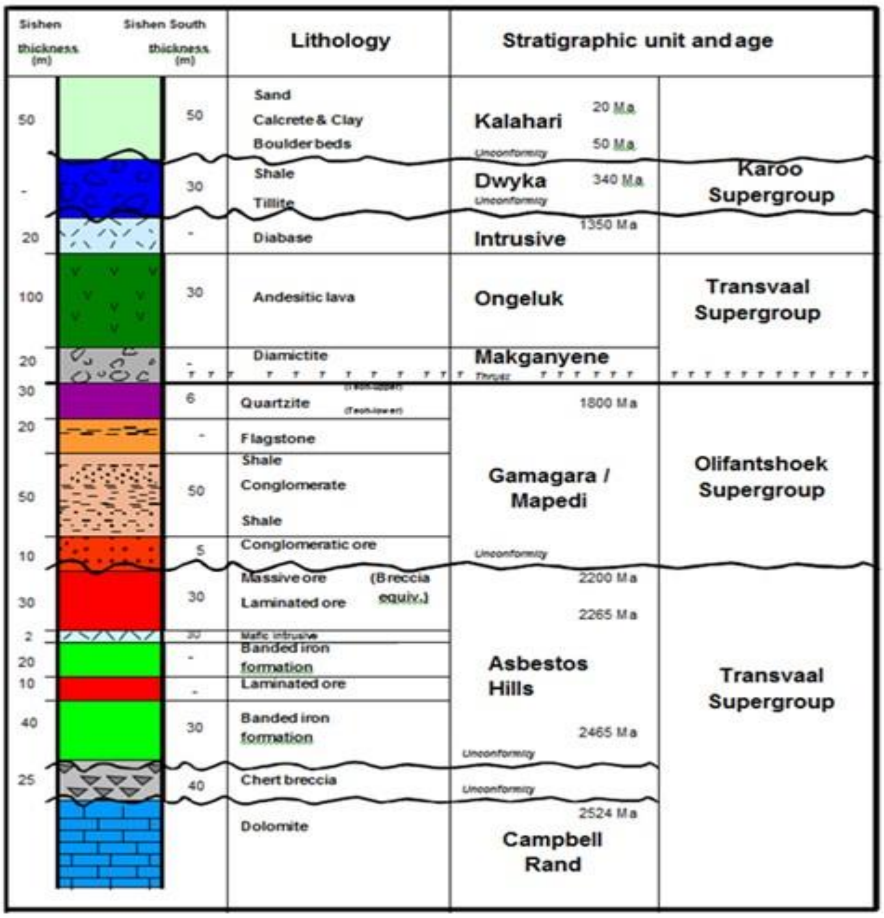

Figure 13: Stratigraphic column depicting Kolomela Mine’s local geology

(Source: Anglo American, 2022)

Anglo American (2022) states that iron ore at Kolomela Mine is associated with chemical and clastic sediments of the Proterozoic Transvaal Supergroup. These sediments define the western margin of the Kaapvaal Craton in the Northern Cape province. The stratigraphy has been deformed by thrusting from the west and has undergone extensive karstification. The thrusting has produced a series of open, north-south plunging anticlines, synclines and grabens and karstification has been responsible for the development of deep sinkholes. The iron ore at Kolomela Mine has been preserved from erosion within these geological structures. Therefore, these structures are important exploration targets and have all been modelled and given codes. Three-dimensional representation of the boundaries of the ore mass is referred to as a solid model or wireframe. These solids were divided into seventeen lithological zones. The zones are summarised in Table 1. This research focused on Zone 130 because it contains high grade iron ore and contribute 84% to the mine’s revenue, since Kolomela Mine is mainly a high-grade iron ore mine.

Table 1: Lithological zones

(Source: Anglo American, 2022)

Rocktype	Description	Code
hemcgt	Conglomeratic Ore	110
hemct	Disturbed laminated ore	120
hemlam	Rhythmic laminated ore	130
hemmas	Massive Ore	140
cgt	Conglomerate	210
qtz	Quartzite	220
sht	Gamagara Shale	240
shc	Carbonaceous Shale	260
cc	Calcrete	310
cl	Clay	320
peb	Pebble	330
bif	Banded Iron Formation	400
chert	Chert breccia	500
dol	Dolomite	600
tillite	Tillite	700
lava	Andesitic Lava	730
gabbro	Gabbro	900

The mineral resource block model and exploration data were created using Datamine software as the primary data input and then converted into a Deswik model format. Although Deswik can also run Datamine commands, the Deswik format is ideal as it reduces model size and thus increases processing speed and ensures that the model can be run using the Deswik geo commands.

3.3.2 Modifying factors

Factors such as mining dilution can reduce the overall ore recovery and affect mineral reserve estimates. Mining dilution is the inclusion of waste material in the ore and mining loss is the unrecoverable ore which is lost during mining process. These modifying factors were collected based on a three-year reconciliation process of past data. Mining dilution of 5% and mining loss of 5% each was used to estimate the total mineral reserve. Table 2 shows iron ore classification modifying factors that were collected and used for the study.

Table 2: Iron ore classification modifying factors

(Source: Anglo American, 2022)

Ore material class	Modifying factor
A1	83%
A2	100%
A3	100%
A4	100%
A5	100%
B	100%
L	100%

At Kolomela Mine an additional modifying factor is applied to the A1 classified material. The A1 material is modified using a historic modification of 83% to account for additional ore losses. This additional modification factor is derived from reconciliation process of three years of data (Anglo American, 2022) comparing the plant received A1 material tonnages versus the mining block model estimated A1 material tonnages and grade.

Metallurgical characteristics of ore such as mineralogy, ore hardness, and processing methods, determine the recoverable metal content. The recognition of geo-metallurgy as a discipline in Kumba Iron Ore is relatively new with the implementation thereof as an organisational function commencing in April 2015. A data collection protocol designed to meet the Anglo American (AA) plc geo-metallurgy requirements was finalised by the company in May 2016 with drilling and sampling commencing in 2017. The protocol prescribes the minimum drilling, sampling and testing requirements to ideally achieve the spatially representative geo-metallurgical data as per the AA plc Requirements Document. Refinement characterisation is aimed at understanding the physical and metallurgical properties of the lump fraction (-25mm to +8 mm) of the DSO plant material. The test work is conducted at the value-in-use (VIU) facility to determine the optimal processing parameters, recoverable metal content, and overall recovery rates.

Refinement characterisation allows for the marketability of the ore to be understood, that is, the characteristics of the ore during transportation and handling to the customer and how the material behaves within a blast furnace. A better understanding of these properties will allow for optimisation of the orebody and marketing strategy. One of the long-term strategies of the organisational function of geo-metallurgy is to be able to predict these characteristics through modelling them. For Kolomela Mine, refinement characterisation of the DSO plant material has been continuously done since 2017. Therefore, data is available across the different pits. During the 2022 to 2023 mineral resource cycle, these results were analysed and modelled using machine learning methods. The full report on the methodology and Quality Assurance Quality Control (QAQC) of the machine learning model (Developing_VIU_Models_Kolomela_2022) is available in Anglo American mineral resource report (Anglo American, 2022).

As mentioned earlier, Kolomela Mine process plants comprise of DMS and DSO plants. The DMS plant's beneficiation performance is estimated using densiometric algorithms which estimate the expected yield and iron ore product grade according to the type of ore, feed grade and operating cut relative density (RD) for both lump and fine fractions. The algorithms are incorporated in the geological block model through a series of Deswik scripting routines which apply the algorithms on a subblock resolution of 5 m x 5 m x 5 m according to the block's encoded ore type. All algorithms use the general expression in Equation 6 (Anglo American, 2022):

$$Y = (a + Fraction\ k) + b \times Feed\ Grade + c\ \times Feed\ Grade^2 + d \times RD + e \times RD^2 \quad (6)$$

Where a, b, c, d and e represent model constants, fraction k represents a calibration constant for the lump (l), or fine (f) fraction split, and RD represents the cut density applied. The constants are reviewed annually using sample data and updated for the mineral reserve report. The geo-metallurgical model coding calculates beneficiated attributes for a representative range of plant cut densities.

Since Kolomela Mine's DSO plant does not beneficiate ore, its product qualities are determined by the ROM qualities delivered to the plant. Metallurgical algorithms applied to the 2022 LOM plan for the DSO operation are presented in Table 3. The DSO algorithms are not built into the geological block models for Kolomela Mine but are applied on the DSO crusher feed in the Kolomela Mine LOM to produce lump and fines product volumes and qualities. At Kolomela the product lump to fine (L: F) ratio is 57:47. The research used the algorithms outlined in Table 3 to calculate and modify the saleable product tonnes from the DSO Plant.

Table 3: DSO algorithms approved for the 2022 Kolomela Mine LOM plan

(Source: Anglo American, 2022)

DSO Assumptions	2023 - 2027
Plant Capacity tonnes	12 600 000
L:F	57%
DSO Premium Lump	
ROM Criteria % Fe	Zero if %Fe in ROM is below: 63,85% Fe
% of Lump as LP	=(100/(1+EXP((1,099*64,2/0,35)*(1-ROM%Fe/64,2))))/100
DSO LP Tonnes Lump	CrusherFeed tonnes* L:F * % of Lump as LP
DSO LP Prod MOP Fe	0,444*ROM%Fe + 36,537
DSO LP Prod MOP SiO2	0,7152*ROM%SiO2 + 0,6511
DSO LP Prod MOP Al2O3	0,6959*ROM%Al2O3 + 0,1249
DSO LP Prod MOP K2O	0,8565*ROM%K2O
DSO LP Prod MOP P	1,1914*ROM%P
DSO LP Prod MOP S	1,1068*ROM%S
DSO LP Prod MOP Mn	0,9678*ROM%Mn
DSO Std Lump Tonnes Lump	CrusherFeed tonnes* L:F * (1-% of Lump as LP)
DSO Std Lump Prod MOP Fe	0,8818*ROM%Fe + 8,005
DSO Std Lump Prod MOP SiO2	0,9625*ROM%SiO2 - 0,0699
DSO Std Lump Prod MOP Al2O3	0,8083*ROM%Al2O3 + 0,0695
DSO Std Lump Prod MOP K2O	0,8161*ROM%K2O
DSO Std Lump Prod MOP P	0,9167*ROM%P+0,007
DSO Std Lump Prod MOP S	0,8194*ROM%S+0,012
DSO Std Lump Prod MOP Mn	0,9694*ROM%Mn+0,02
DSO Tonnes Fine	CrusherFeed tonnes* (1-%L:F)
DSO Fine Prod MOP Fe	1,0917*ROM%Fe - 7,0176
DSO Fine Prod MOP SiO2	1,0403*ROM%SiO2 + 0,2338
DSO Fine Prod MOP Al2O3	1,2327*ROM%Al2O3 - 0,0586
DSO Fine Prod MOP K2O	1,2167*ROM%K2O
DSO Fine Prod MOP P	1,0977*ROM%P+0,008
DSO Fine Prod MOP S	1,2552*ROM%S+0,008
DSO Fine Prod MOP Mn	1,0244*ROM%Mn+0,02

The Kolomela Mine DMS modular plant crushes B-grade material into lump (L) and fine (F) product. With very little spatial densiometric geometallurgical data available, beneficiation algorithms per ore type or per mixture of ore and waste type have not yet been developed to enable the estimation of yield and iron ore product grades from B-grade and L-grade material. Therefore, a fixed yield prediction of 60.0% on B-grade ROM and 55% on L-grade ROM were applied for the UHDMS modular plant in the

2022 LOM as indicated in Table 4. Table 4 shows DSO and DMS algorithms for the 2022 Kolomela Mine LOM. The research used the algorithms outlined in the table to calculate and modify the saleable product lump and fine grades for the B grade material. B grade material is classified as medium grade ore, and it requires a higher processing cost than A grade material to beneficiate it to acceptable marketing qualities.

Table 4: DSO and DMS algorithms for the 2022 Kolomela Mine LOM

(Source: Anglo American, 2022)

DMS Assumptions	**2023 – 2027**
ROM Capacity tonnes	1 500 000,00
Product Capacity tonnes	900 000,00
L:F	60%
Product Yield	60% and (55% for L-grade)
DMS Std Lump Tonnes Lump	CrusherFeed * Product Yield * L:F
DMS Std Lump Prod MOP Fe	64,4
DMS Std Lump Prod MOP SiO2	-1,4484*Lump%Fe + 98,642
DMS Std Lump Prod MOP Al2O3	0,063*Lump%Fe - 2,71318
DMS Std Lump Prod MOP K2O	0,0064*Lump%Fe - 0,2897
DMS Std Lump Prod MOP P	0,0012*Lump%Fe - 0,035
DMS Std Lump Prod MOP S	0,7885*ROM%S-0,001
DMS Std Lump Prod MOP Mn	0,9918*ROM%Mn-0,0107
DMS Tonnes Fine	CrusherFeed * Product Yield * (1- L:F)
DMS Fine Prod MOP Fe	63,2
DMS Fine Prod MOP SiO2	-1,2084*Fine%Fe + 82,669
DMS Fine Prod MOP Al2O3	-0,1671*Fine%Fe + 12,348
DMS Fine Prod MOP K2O	-0,0309*Fine%Fe + 2,1353
DMS Fine Prod MOP P	0,0025*Fine%Fe - 0,1124
DMS Fine Prod MOP S	1,2672*ROM%S+0,0028
DMS Fine Prod MOP Mn	1,0163*ROM%Mn+0,0164

3.3.3 Economic and technical data

Appendix A shows a list scripts and formulae that were used for this research and the scripts that were used to calculate EBVs of the block models realisation used in this study. Appendix B shows a list of global costs data (such as processing cost, marketing cost, mining cost, MCAF). The costs used for the research are actual figures collected from 2022 LOM. Unit cost per tonnages for mining, processing, selling, marketing was calculated and added as global constants in the pit optimisation software. In previous years, MCAF used at Kolomela Mine in the pit optimisation process to adjust mining cost was previously based on depth adjustment. The MCAF was revised in this research study to be based on cycle time regression formulae. The cycle time regression formulae were derived from 2022 LOM that includes the identified backfill opportunities. The revised MCAF provides the pit optimisation process a new approach in evaluating future growth areas as it accounts for savings on hauling cost which are a result of backfilling. This approach reduces haulaging cost.

Historic iron ore prices for 10 years (Figure 3) were collected from Market Insider (2022). This data shows the actual iron ore prices realised per month for the past years. A 9% discount rate obtained from Anglo American (2022) was used to calculate NPVs. The final pit design must adhere to slope angle constraints to ensure the stability of pit walls and minimise the risk of slope failures. The stability and geotechnical characteristic of the final pit shell must ensure that it can safely support mining activities and structures. For this research study, the overall slope angle was assumed for all the deterministic and probabilistic pit shells to be 45 degrees to simplify the project even though KSS has five geotechnical domains.

3.3.4 Summary of data collected

Modifying factors help mining companies to enhance the accuracy and reliability of estimating their mineral reserves. Table 5 shows the summary of modifying factors applied in this study. Appendix B also shows a list of global constants which entails a detailed breakdown of the modifying factors summarised in Table 5.

Table 5: Summary of modifying factors

Parameter	Description
Mineral resource block model	February 2023 mineral resource block model was used and was up blocked to a 10 m x 10 m x 10 m SMU mining block models.
Surfaces	Pit topography, in-pit dumping, and waste dumps were updated to reflect their positions as of end December 2022.
Geotechnical slope angles	12 degrees
Price and freight	Price: $79/t CFR 62% for deterministic pit optimisation and P75, P50, P25 and P5 for the probabilistic pit optimisation.
Cost	Total cash cost of R433/t product Royalties were 4% of the freight on rail (FOR) price.
Dilution	5%.
Mining loss	5%.
Mined recovery efficiency	83% on A1 only.
Processing	A1 to A5 material is allocated to the DSO, at 99.98% yield and B&L material is allocated to the UHDMS.

3.4 Data analysis

Data analysis techniques vary depending on the amount of data, size of data set, missing, and unavailable data. For this research, mineral resource data was analysed using ISATIS modelling and pit optimisation software to produce economic block models. With a large amount of data as is the case with the 10-year iron ore prices used in this research, probabilities (P75, P50, P25 and P5) derived from Monte Carlo Analysis were used to model the uncertainty and randomness of the iron ore price.

3.4.1 Iron ore prices analysis

Monte Carlo Analysis was used to simulate the variation in iron ore prices. The following process was followed:

i. Step 1: Historic iron ore prices for 10 years (Figure 3) were used as an input. One thousand (1000) arbitrary iterations were run. The assumption to using the historic iron ore price is that it can be representative of the future.

ii. Step 2: Statistical parameters of the prices such as mean, maximum and minimum were calculated.

iii. Step 3: The class width of the iron ore price was determined, the frequency of the data included in each class was obtained by examining the iron ore prices. The relative frequency of each class was calculated by dividing the data frequency of each class by the total amount of data. Figure 14 shows the frequency of the iron ore prices for 10 years.

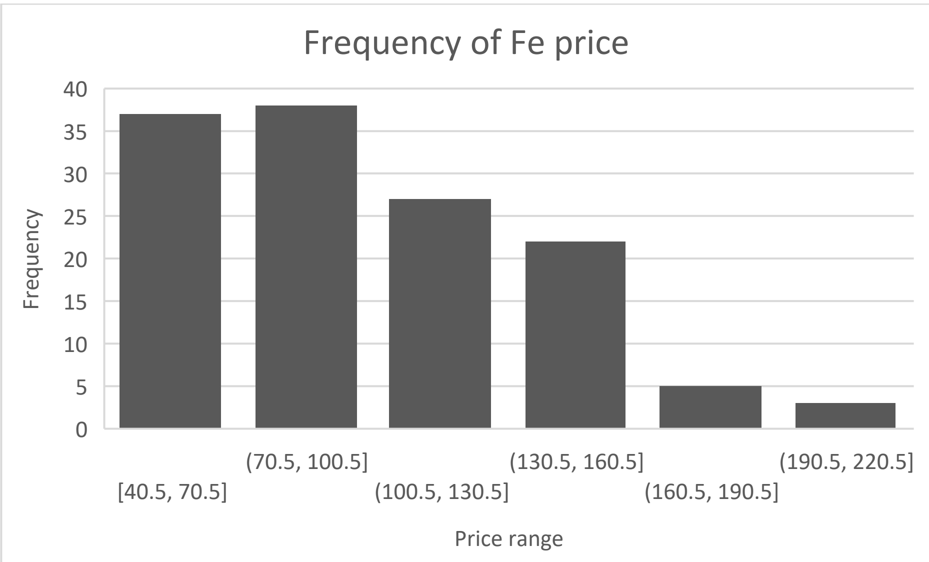

Figure 14: Frequency of iron ore price based on the 10-years data

iv. Step 4: The cumulative frequencies of the prices were then calculated using the relative frequency of each class. The cumulative relative frequency was generated by plotting iron ore prices on the x-axis and the cumulative relative frequency on the y-axis.

v. Step 5: Using the cumulative relative frequency curve of the 10 years iron ore prices that were generated in Step 3, 1000 iron ore prices were generated using Equation 7 (Charbel, 2015):

$$F(x) = P\ (X \leq x) \tag{7}$$

where F(x) is the function of the cumulative frequency curve, which gives the probability P that the iron price X will be less or equal to x. F(x) ranges from 0 to 1. Using Equation 7, the value of x can be calculated for any given value of F(x) using Equation 8 (Charbel, 2015):

$$G(F(x)) = G(r) = x \tag{8}$$

where G(F(x)) is the inverse function, r is a random real number between 0 and 1. As stated above, 1000 iron ore prices were generated using n random real numbers between 0 and 1 and then assuming each generated real numbers as the y value of the cumulative relative frequency curve and finding x values corresponding to the y values. According to Charbel (2015), MCA relies on the assumption that many random samples mimic patterns in the total population. Increasing the number of iterations in a Monte Carlo Analysis generally leads to more precise and accurate results. With more iterations, the simulation can better approximate the true distribution of possible outcomes and provide more reliable estimates of key metrics such as mean, variance, and confidence intervals. The probability distribution of the iron ore price is shown in Figure 15.

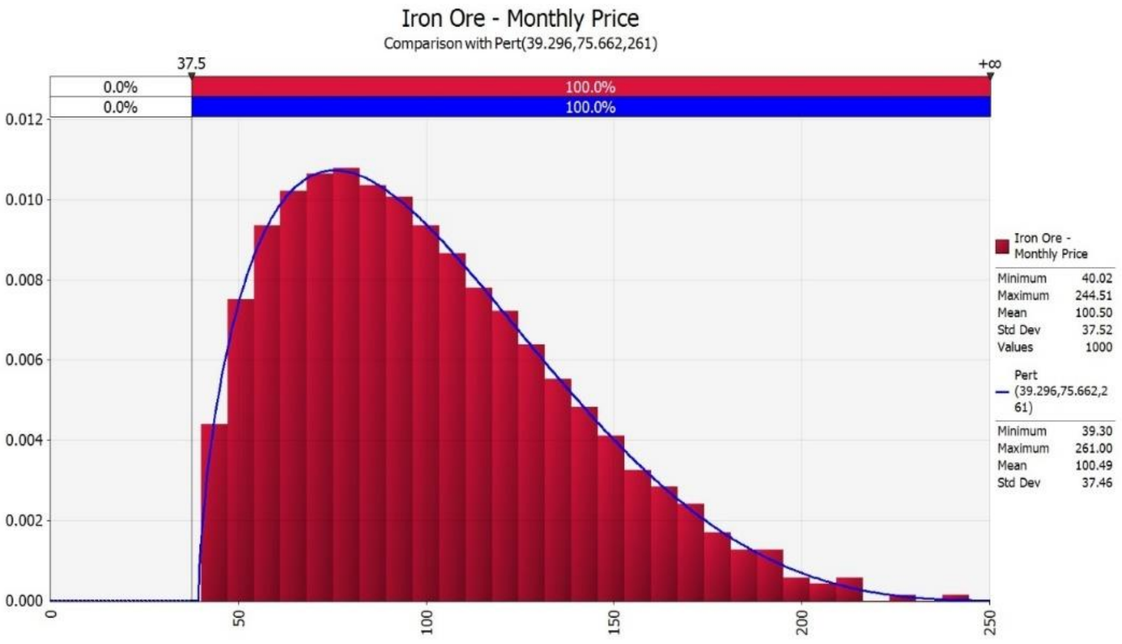

Figure 15: Probability distribution of iron ore price

Table 6 shows the detailed statistics of the 10-year iron ore price and the probability at 5% increments of that iron ore price to be realised.

Table 6: Statistical data for 10 years iron ore prices

@RISK Detailed Statistics
Performed By: Nkambule, Sthembile
Date: 07/September/2023 14:31:47

Name	Iron Ore - Monthly Price
Description	RiskPert(39.296,75.662,261,RiskName("Iron Ore - Monthly Price"))
Cell	iron-ore-180!M2
Minimum	40.01865
Maximum	244.5068
Mean	100.4994
Std Deviation	37.5151
Variance	1407.383
Skewness	0.6722432
Kurtosis	2.969199
Errors	0
Mode	69.42525
5% Perc	49.84436
10% Perc	55.81965
15% Perc	61.08573
20% Perc	66.07525
25% Perc	70.83957
30% Perc	75.43467
35% Perc	80.15984
40% Perc	84.88325
45% Perc	89.70772
50% Perc	94.63604
55% Perc	99.82581
60% Perc	105.3888
65% Perc	111.2454
70% Perc	117.5864
75% Perc	124.602
80% Perc	132.4562
85% Perc	141.8975
90% Perc	153.6403
95% Perc	170.8859

From Table 6, the following probabilities of iron ore prices were obtained, P75 iron ore price is $70.84, P50 iron ore price is $94.64, P25 iron ore price is $124.60, and P5 iron ore price is $170.89. The P75, P50, P25 and P5 probability prices represent a probability of 75%, 50%, 25% and 5% of that price being realised, respectively. The study used these four prices to calculate value per tonne of the block model realisations. The realisations were used to create pit shell limits and obtain NPV of the corresponding pit shells. This contrasts with the practice in KIO of using a single deterministic price. In this study the deterministic long-term price of $78.5 per product tonne was obtained from the mine. The P75 price of $70.8 per product tonne is lower than the deterministic long-term price. The P50, P25, and P5 prices were all higher than the deterministic long-term price.

3.4.2 Geological analysis

Geological data, including orebody models, geotechnical information, and mineralogy data, provided critical insights into the spatial distribution and characteristics of the iron ore deposits. These influence pit design and extraction strategies. The geological block model data was used to create ten block model realisations using conditional simulation.

The primary purpose of conditional simulation is to produce multiple block models, also known as realisations, to estimate grade based on a known or sampled data at a specific location. Conditional simulation models spatial variability and uncertainty at unsampled locations, using the known and sampled data points. ISATIS software was used to run conditional simulations of Kolomela Mine's KSS geological block model. Ten block model realisations were created and found to be a reasonable and sufficient number to illustrate iron ore grade variability.

The simulation only focused on laminated hematite ore (Zone 130) as explained in Section 3.3.1. To speed up the simulation process, it was decided to exclude the other rock types, except laminated hematite ore, and rather include all the contaminants (SiO_2, Al_2O_3 and P) used in the mineral resource model. Validation of the results and comparing it to the deterministic results which contained all rock types, shows that there is no notable impact of this. For this study, the following variables of interest within hemlam rock type were simulated namely Fe, SiO_2, Al_2O_3, P and RD. The process of conditional turning bands simulation embedded in ISATIS software can be summarised in the following steps (Ersoy & Yunsel, 2006):

1. A representative histogram for the input data was obtained.
2. The accumulated raw data was transformed into a standard normal distribution by anamorphisms modelling.
3. Variogram models were produced using the normalised data.
4. A conditional cumulative density function was estimated.
5. A random value from the distribution was drawn.
6. The value drawn into the conditioning data set was incorporated.
7. Steps 1 to 6 were repeated until all grid nodes were visited.
8. Steps 1 to 7 were restarted to generate another simulation.
9. The simulated data was back transformed into the original scale.
10. Results were validated using the visual aspect of the simulation, statistics, histograms and variograms.
11. Back transformed accumulation data was divided by the simulated thickness.

Figure 16 shows the flowchart from characterisation of actual data to uncertainty assessment by conditional simulation.

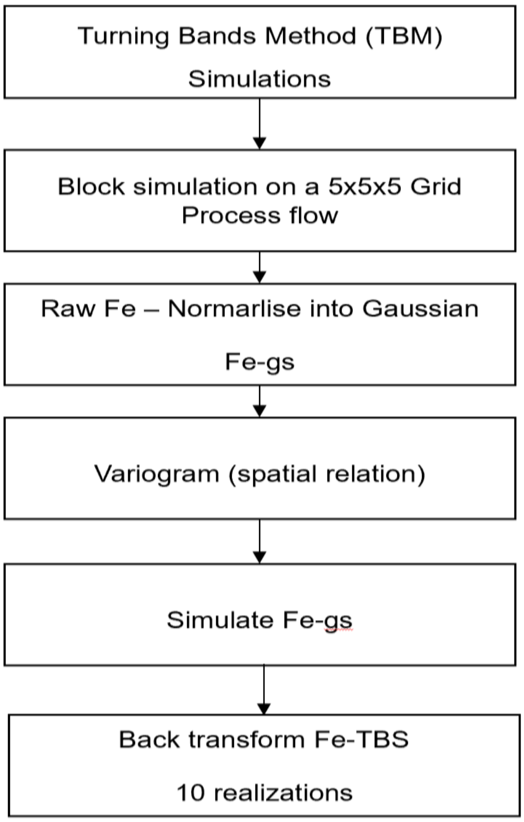

Figure 16: Conditional simulation process

Figure 17 shows the result of the accumulated raw data (Fe) that was transformed into a standard normal distribution (Fe_gs) to eventually produce the Turning Band Simulation Fe (TBS_Fe), through the process outlined in Figure 16. Appendix C shows the supporting contaminants.

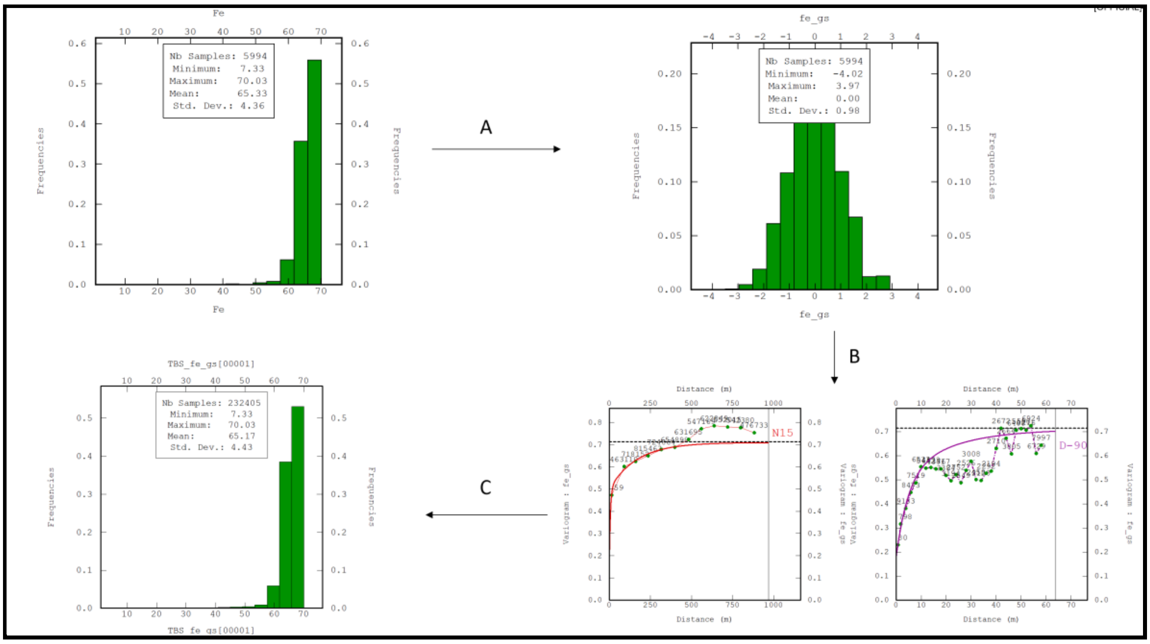

Figure 17: Conditional simulation outputs

Variogram analysis is a fundamental geostatistical process used to quantify the spatial variability of geological attributes within a mining deposit, such as ore grade. In the context of iron ore mining, variogram analysis plays a crucial role in understanding the distribution of iron ore grades, guiding mineral resource estimation, and informing pit optimisation strategies.

Regularisation was conducted for the ten block model realisations. The models were converted from a 5 m x 5 m x 5 m grid into a 10 m x 10 m x 10 m grid which is representative of the mining equipment that will be used to mine the ore. After the block models were converted into SMU models, the ore was classified based on its iron ore content and contaminants. Table 7 shows the classification criteria that is used at Kolomela Mine and in this research study, as specified by the marketing specifications.

Table 7: Iron ore classification based on grade and contaminants

Class	Fe%	Al2O3%	K2O%	P%	Additional Requirements	Use in Blend
A1	**>= 65.0%**	<= 1.8%	<= 0.18%	<= 0.056%		DSO direct feed
A2	**63.8-65%**	<= 1.8%	<= 0.18%	<= 0.056%		
A3	**61.0-63.8**	<= 1.8%	<= 0.18%	<= 0.056%		
A4	**>= 61.0%**	**> 1.8%**	<= 0.18%	<= 0.056%		DSO direct feed (lower tempo)
A4	**>= 61.0%**	<= 1.8%	**> 0.18%**	<= 0.056%		
A4	**>= 61.0%**	**> 1.8%**	**> 0.18%**	<= 0.056%		
A5	**>= 61.0%**			**> 0.056%**		
L	**50.0-61.0%**				HEM with HDW[1]	Blendable ore - very low feed to crusher
B	**50.0-61.0%**				HEM with LDW[2]	
C	**43-50%**				Waste with HEM	Stockpiled for future beneficiation
D	**0-43%**				Waste	Sterile material, can not be used in blend

Classifying ore is important as it determines which ore should be send to the DSO plant and which ore should be send to the DMS treatment plant. The operational cost of the DMS plant is higher and significantly impacts EBVs. The higher the iron ore grade and the lower the contaminants, the higher the value of the ore. Class A ore is of higher value than classes B and L ore. Appendix D shows how the material classes are different for each economic block model. This is important as it drives EBVs and eventually the pit limit and associated NPV for each block model realisation.

3.4.3 Pit optimisation results analysis

After applying all the inputs described in Section 3.3, optimal deterministic pit shell and probabilistic pit shells were created. Using each of the four price probabilities (P75, P50, P25 and P5) on each of the ten block model realisations a total of forty optimal pit shells were created. The deterministic and the forty pit shells were all scheduled to determine and compare their tonnages, LOMs and NPVs.

3.5 Summary of Chapter 3

This chapter gave an overview of the data used in the research and how the data was collected. The data discussed include the mineral resource data and modifying factors. The modifying factors include mining, metallurgical and economic factors. Monte Carlo Analysis was used to simulate and analyse the variation in iron ore prices. Ten block model realisations were simulated using conditional simulation. Variogram analysis was discussed in this chapter. The next chapter presents the pit optimisation results.

4 PIT OPTIMISATION RESULTS

4.1 Overview of Chapter 4

Chapter 4 presents the results of the research. Conditional simulation of ten block models was conducted. The results of the ten block models are compared and analysed for differences in iron ore grade curves, variograms and total iron ore tonnages. Pit optimisation was done using the ten block models in combination with the four probabilistic iron ore prices to produce forty probabilistic pit limits. A comparison and analyses of the deterministic and the forty probabilistic pit limits optimisation results is done in the chapter. The chapter distinguishes results of the two processes and shows the different input parameters used in both processes. High level schedules and NPVs of the forty nestled pit shells were generated and compared to those of the deterministic pit shell.

4.2 Conditional simulation results

Conditional simulation is a spatial characterisation process which provides a quantitative assessment of the spatial continuity and variability of ore grade. This enables delineation of high-grade and low-grade zones within a mineral deposit. Spatial variability shows how the grade values are correlated or autocorrelated across space based on the variogram model parameters. Figure 18 shows the ten block model simulation results for iron ore grade.

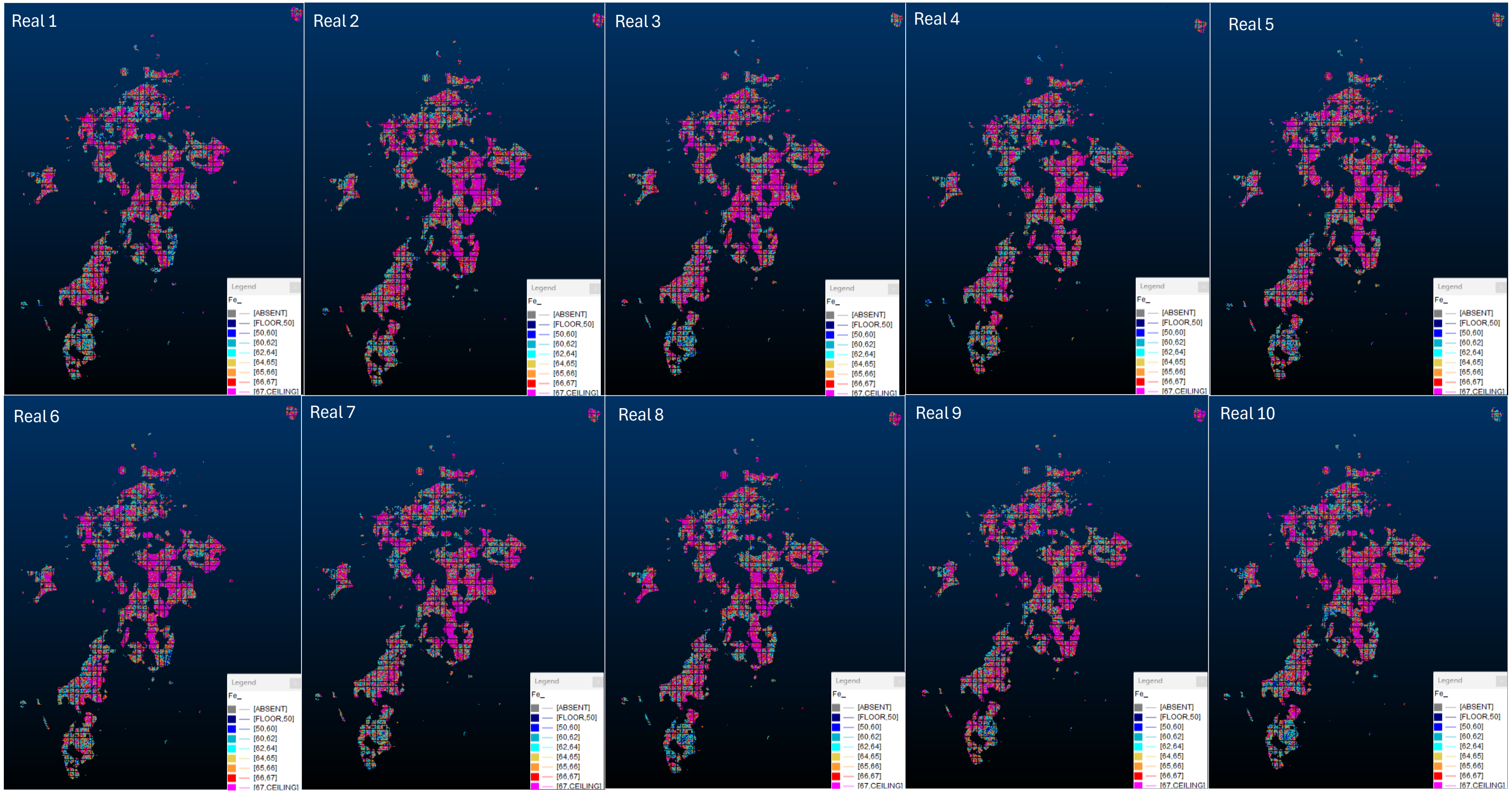

Figure 18: Spatial variability for ten block model realisations of hemlam (Zone 130) iron ore grade

Figure 18 shows that the ten block model realisations have similar spatial patterns and geographical distributions. It also shows differences in the estimated iron ore grade in the southeast and on the south directions. The iron ore grades vary from 50% to 67% in these areas as shown by the legend on Figure 18. It is expected that the statistics of the realisations should align and be consistent with the deterministic data set. Table 8 compares the raw data and conditional simulation results.

Table 8: Comparison of raw data and conditional simulation results

Raw and Realisations	Minimum grade %	Maximum grade %	Mean grade %	Standard deviation	Variance
Raw data	7.33	70.03	65.23	4.76	22.62
1	7.33	70.03	65.17	4.43	19.61
2	7.33	70.03	65.59	3.66	13.4
3	7.46	70.03	65.43	3.97	15.77
4	7.33	70.03	65.37	3.98	15.83
5	7.33	70.03	65.5	3.78	14.27
6	7.42	70.03	65.33	4.3	18.5
7	7.33	70.03	65.41	3.93	15.46
8	7.64	70.03	65.44	3.94	15.55
9	7.33	70.03	65.51	3.93	15.42
10	7.33	70.03	65.36	3.99	15.89

Variance is a measure of how spread out a set of data points are around their mean. A high variance indicates that the data points are widely dispersed from the mean, reflecting greater variability. It is expected that the variances of the simulated iron grade are close to those of the original raw iron ore grade which has a variance of 22.62. The results show that the variance of the simulated data vary from 13.4 to 19.61 which is lower than the variance of the raw data. This indicate that the simulated data has less variability compared to the raw data.

The maximum grade of the raw data and the simulated block grades are the same at 70.03%. The mean grades of the simulated data are also close to that of the raw data. This means that the normal transformation applied to the original data did not alter the intrinsic spatial characteristic of the raw data.

The cumulative frequency distribution in variograms provides a summary of the spatial correlation structure and variability of the variable under consideration. Figure 19 shows the cumulative frequency distribution of the simulated iron ore grades (TBS_Fe) data at 10 m intervals. In Figure 19, the cumulative frequency distributions of the ten block model realisations are represented by yellow lines.

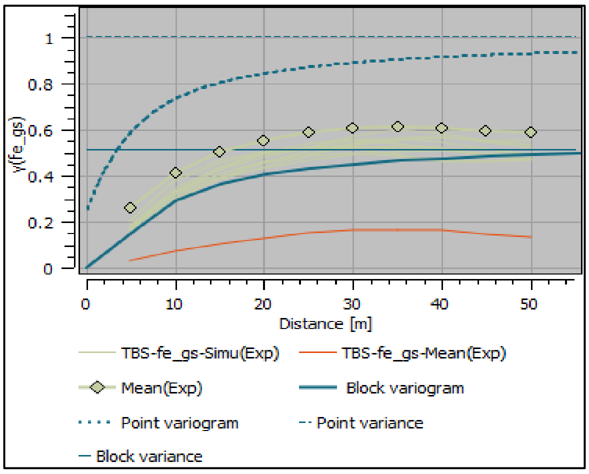

Figure 19: Cumulative frequency distribution of TBS_Fe data

Figure 19 shows that there are no major outliers since the frequency accumulates at 50 percentile and stays relatively flat. Percentiles indicate the position of a data point relative to the entire dataset. Figure 19 also shows that as distance increases, the gap between the frequency of the simulated mean (orange line) and the cumulative frequencies (yellow lines) of the ten block model realisations, increases. This increased gap indicates weaker correlation and higher variability over distance, as opposed to if the lines (yellow and orange) were closer to each other.

4.2.1 Iron ore grade curve

Figure 20 shows the frequency of the iron ore grade of the ten block model realisations (yellow lines), the frequency of the raw data (blue line) and the mean of the ten block model realisations.

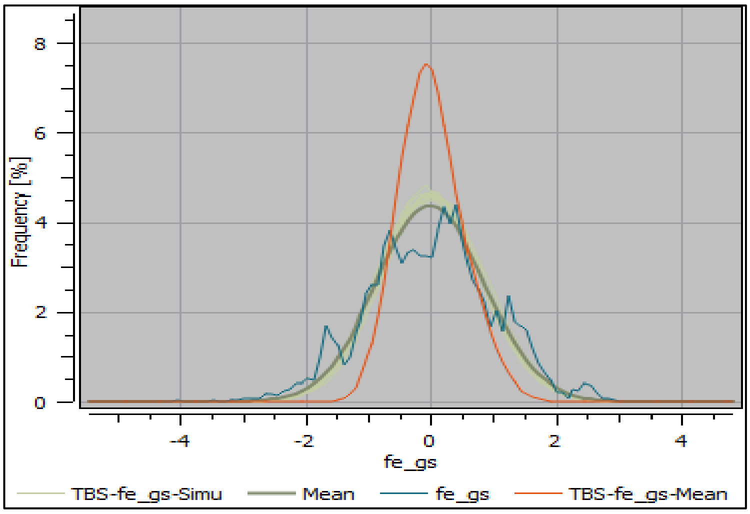

Figure 20: Curves of iron ore grade standard deviations of ten block model realisations

Figure 20 shows how well the frequency curves of iron ore grade of the ten block model realisations (yellow lines) compare with the curve of the raw iron ore grades (blue line). In all the cases, the ten block model realisations successfully reproduced the global curves, which are similar to the raw iron ore grades (blue line).

4.2.2 Variogram reproduction

Variograms for the ten block model realisations were produced and plotted with the input distance. The variogram range parameter in conditional simulation variograms indicates the distance over which values are spatially correlated. Figure 21 shows the horizontal variograms at a horizontal distance of 5000 m at a direction of 15 degrees north and at a horizontal distance of 3500 m at a direction of 285 degrees north. The solid blue line on Figure 21 represents the input model variogram while the yellow lines represent the variograms of the ten block model realisations.

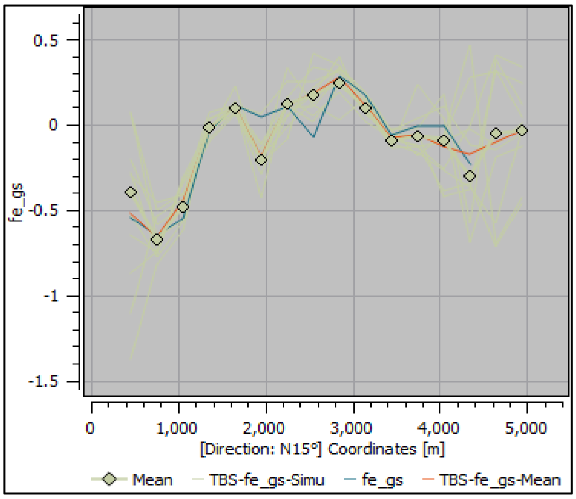

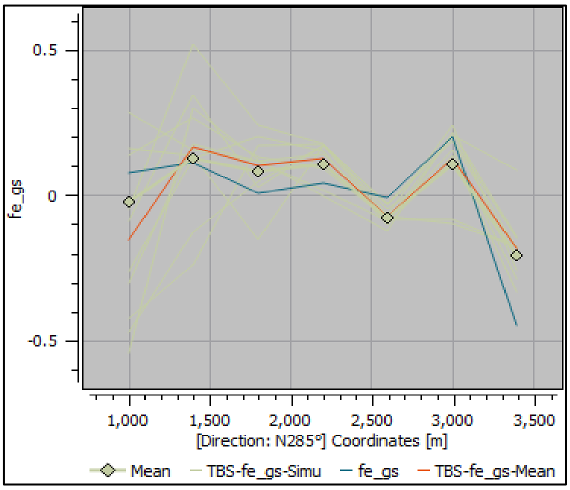

Figure 21: Horizontal variograms

Figure 21 (left) shows that the iron ore grade of the ten block model realisations (yellow lines) and the raw iron ore grade (blue line) are strongly correlated at distances less than 3500 m at a direction of 15 degrees north. However, the grade becomes highly variable at distances greater than 3500 m. Figure 21 (right) shows that the iron ore grade of the ten block model realisations and the raw iron ore grade are poorly correlated at a direction of 285 degrees north. Figure 21 (right) also shows high variability of the simulated iron ore grades.

Figure 22 shows the vertical variograms at a vertical distance of 1400 m from the surface. The solid blue line on Figure 22 represents the input model variogram (raw iron ore grade) while the yellow lines represent the variogram of the ten block model realisations.

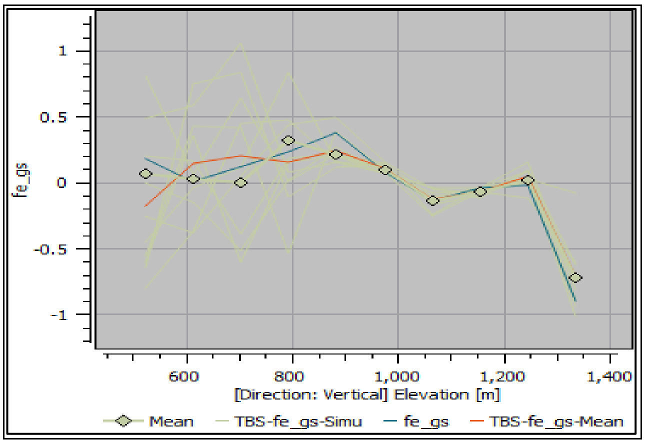

Figure 22: Vertical elevation variograms

Figure 22 shows that at surface (closer to 1400 m above sea level), the iron ore grade of the ten block model realisations and the raw iron ore grades are closely correlated, and that variability increases from 900 m below surface deeper. The ten mineral resource block model realisations shown in Table 8 were then converted into mining block models and eventually economic block models as described in Section 2.2.1. The results of the economic block models are shown in Figure 23. It shows the differing tonnages of each economic block model realisation and the corresponding iron ore grade. Figure 23 shows the accumulative tonnages in million tonnes from 68% iron ore grade to 50% iron ore grade. The cutoff grade applied at Kolomela Mine is 50%.

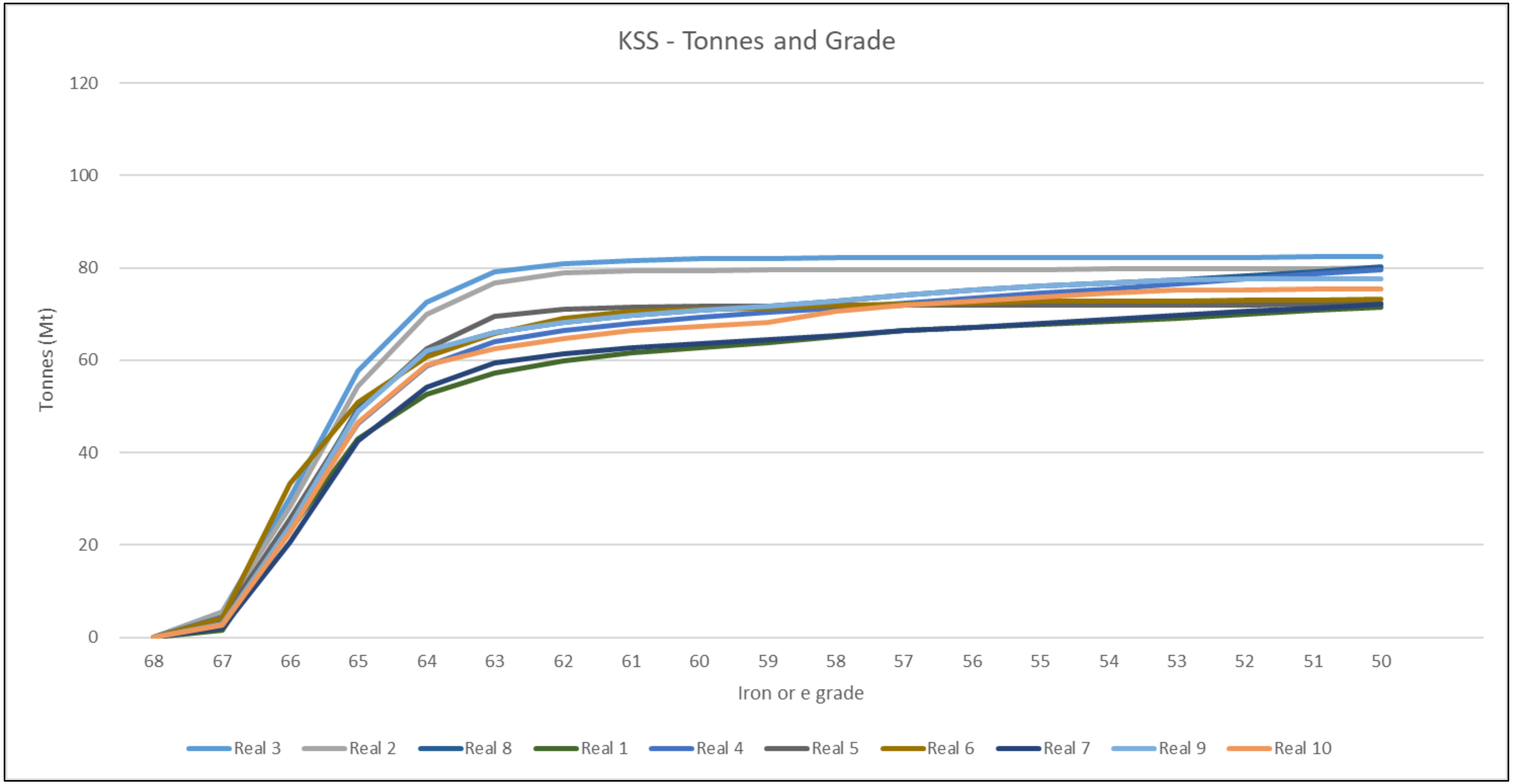

Figure 23: Tonnage and grade of the ten-block model realisations

Table 9 shows the tonnages of the deterministic economic block model and ten block model realisations that were interrogated using the 2023 KSS design. The 2023 KSS design is the design based on the deterministic pit shell.

Table 9: Tonnages of the deterministic and simulated economic block models

Block Models	Total Ore Tonnes (Mt)
Real_1	80.31
Real_2	89.79
Real_3	92.52
Real_4	89.26
Real_5	81.15
Real_6	82.07
Real_7	80.92
Real_8	90.06
Real_9	87.17
Real_10	84.55
Deterministic Pit	83.81

Table 9 shows that block model realisations 3 (Real_3) has the highest tonnage of 92.5 Mt, while block model realisation 1 (Real_1) has the lowest tonnage of 80.31 Mt. There is a 10% and -4% difference in tonnages between the deterministic block model and block model realisations 3 and 1, respectively. The difference in tonnages between Real_3 and Real_1 is 15%. This is equivalent to an additional year of mining since KSS is mined at a rate of 10 Mtpa. This shows that uncertainty in grade estimation has a significant impact on mine planning and hence the need to do probabilistic mine planning as opposed to deterministic planning. Figure 23 also shows that this variability is found between 60% and 65% iron ore grade, which is the high-grade iron ore. The tonnages of the deterministic versus Real_1 and Real_3 block models per bench level were analysed as shown in Figure 24.

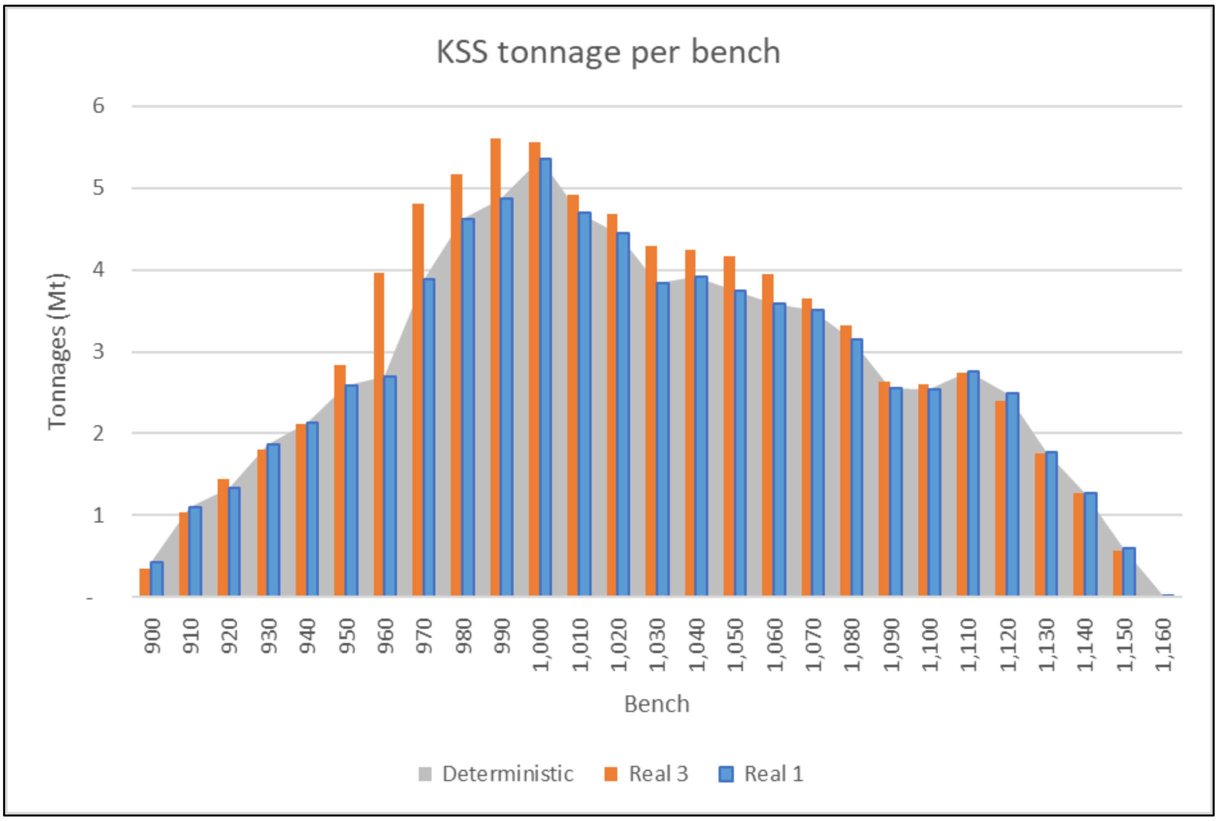

Figure 24: Comparison of deterministic versus Real_1 and Real_3 tonnages per bench

Figure 24 shows a significant difference in tonnages for the two block realisations between elevation 1080 to 950. This is important information that would not be visible if only one estimation is conducted. As mentioned in Section 3.4.3, the ten block model realisations and four price probabilities (P75, P50, P25 and P5) were used to calculate EBVs and to produce pit limit shells using Deswik Pseudoflow. The next section presents the deterministic and the probabilistic pit shell results.

4.3 Deterministic pit limit shells results

Figure 25 shows the deterministic pit shell. The blue and red boundaries represent pit shells produced in this research and by the KIO internal process at a RF equal to one, respectively. The slight difference in the two pit shells is because this research used the regression model MCAF (discussed in Section 3.3.3) instead of the depth MCAF method to better represent the cost of sending tonnages to different destinations from each mining block. The detailed results produced from this research (blue shell) are shown in Appendix E.

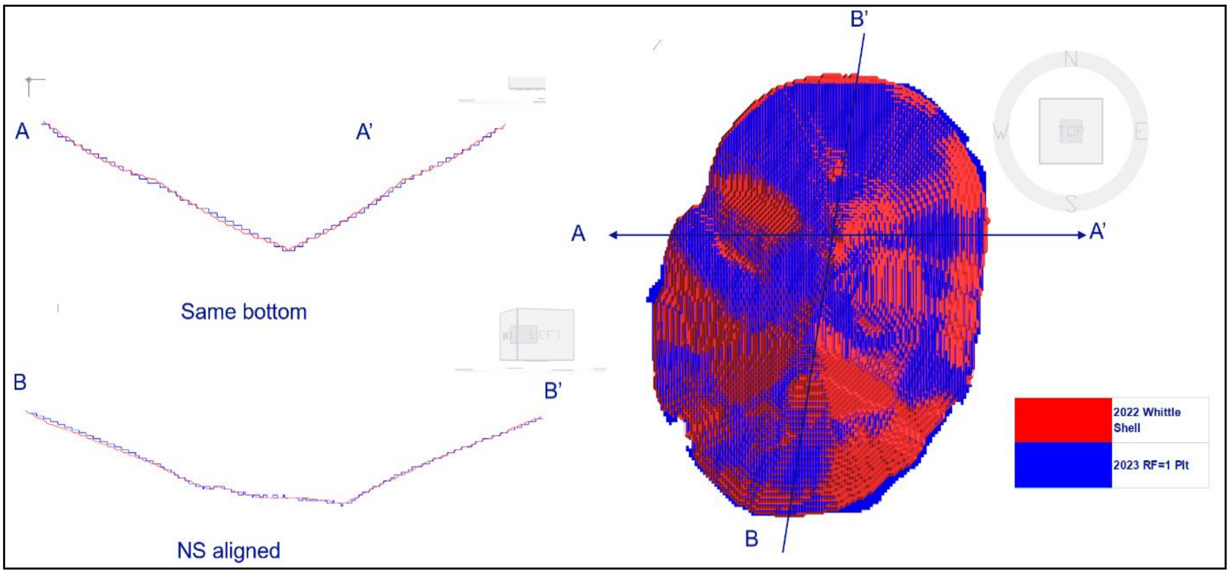

Figure 25: Cross sectional and plan views of the deterministic and KIO designed pit shells

The blue boundary represents a pit shell containing 74.7 Mt of total ore, as shown in Table 10, including B and L material. It shows the total tonnages of the RF 1 pit shells.

Table 10: Total ore tonnages of the revenue factor 1 pit shells

RF1 PIT SHELLS (Ore Tonnes)	P75 (Mt)	P50 (Mt)	P25(Mt)	P5 (Mt)
Real_1	73.10	71.58	84.44	84.46
Real_2	78.88	80.03	97.22	98.44
Real_3	81.31	82.46	83.61	84.63
Real_4	78.40	79.55	80.70	81.72
Real_5	71.18	72.33	73.48	74.50
Real_6	72.00	73.15	74.30	75.32
Real_7	70.97	72.12	73.27	74.29
Real_8	79.12	80.27	81.42	82.44
Real_9	76.54	77.69	78.84	79.86
Real_10	74.21	75.36	76.51	77.53
Deterministic Pit				**74.70**

Appendix F shows the results of the probabilistic pit shells which include the recovered ore, total mass tonnages for each RF increment and discounted cashflow (DCF). Using these results, several charts can be generated to analyse the optimisation results which include ore incremental tonnages and its relation to cost, incremental strip ratios, incremental NPV. This information helps to give more insight as to the orebody configuration and impacts on the size of the pit. Figure 26 shows the DCF compared to ore tonnes for each incremental RF for the deterministic pit shell.

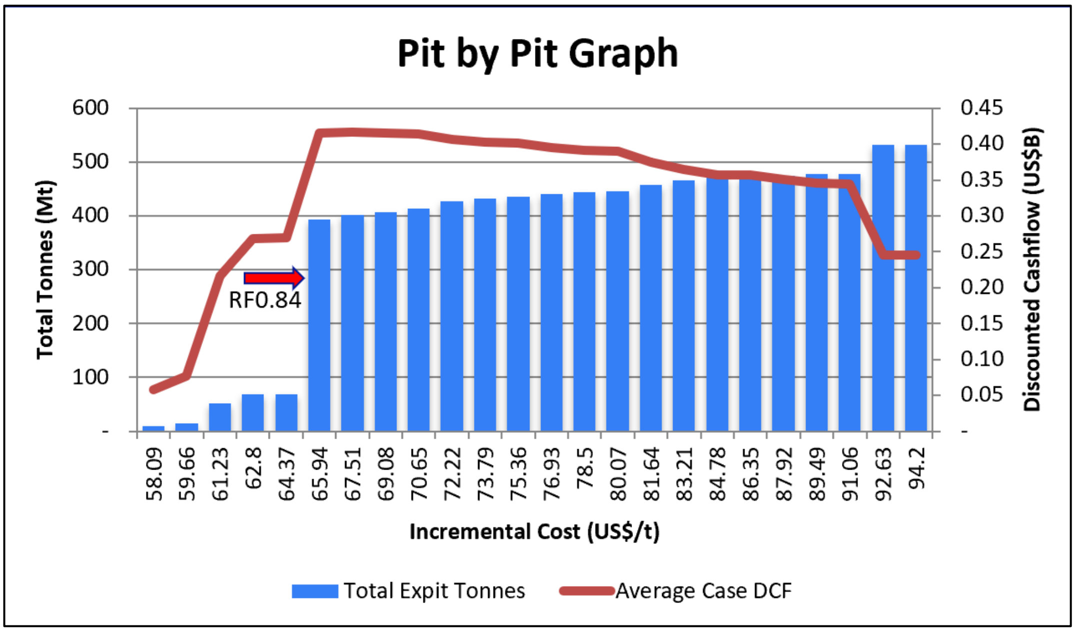

Figure 26: DCF and total tonnes of the deterministic pit shell

Figure 26 shows a big increase in total mass tonnages at RF equal to 0.84 pit which has a total mass of 393 Mt and US$0.29bn DCF. This is a big jump from the pit with RF equal to 0.8 which has a US$0.04bn DCF. This is because the ore is located deep and the jump in ore tonnages is an indication of how sensitive the pit is to price.

Figure 27 shows incremental cost plotted against ore tonnages. Incremental cost refers to the additional cost incurred for extracting each additional tonne of ore from a pit. Understanding incremental costs is essential in optimising pit design and maximising profitability.

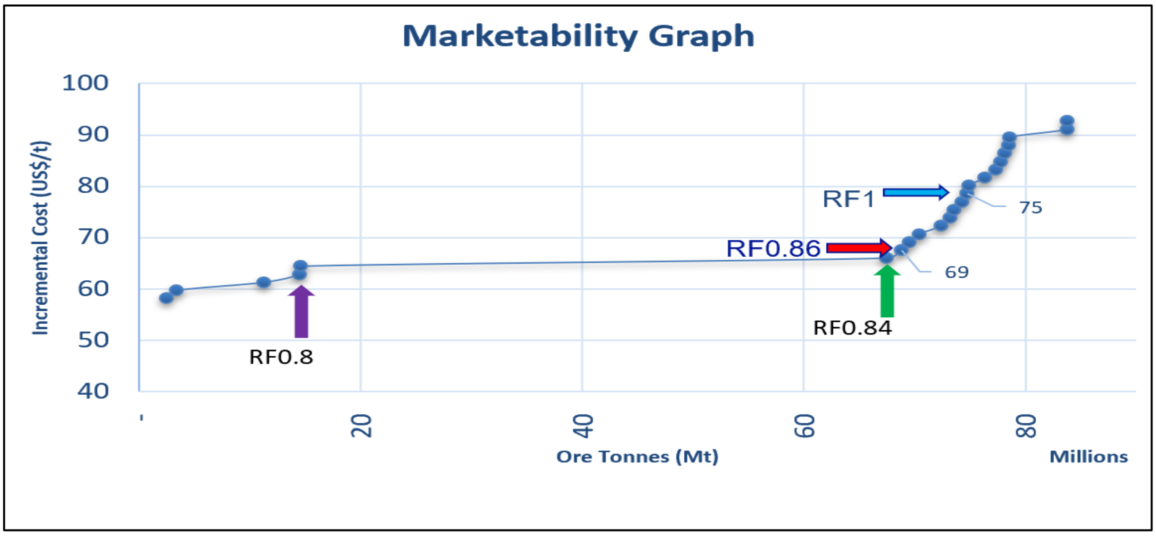

Figure 27: Deterministic marketability graph

Figure 27 shows four inflection points:

- A pit shell with RF equal to 0.8 which has 15 Mt of ore to a pit shell with RF equal to 0.84 which has 67 Mt of total ore,
- A pit shell with RF equal to one which has 74.7 Mt of total ore and a DCF of US$0.391Bn,
- A pit shell with RF equal to 0.86 with 69 Mt of total ore and the highest DCF of US$0.416Bn
- Small, high margin shell observed at RF 0.8 pit shell.

Analysing the pit optimisation results helps to gain additional insight into how sensitive the orebody is to input parameters like costs, price, and slope angles. In the deterministic pit optimisation, the pit shell with RF equal to 0.86 was chosen. For the purposes of this study, only pit shells with a RF equal to one were analysed from the forty simulated block models realisations. Their NPVs were chosen and compared to the deterministic pit shell with RF equal to one. This was done to clearly demonstrate the impact of variable grade and iron ore prices on final pit limits. The process of plotting Figure 26 and Figure 27 revealed that the orebody is highly sensitive to price equal to or less than that of RF of 0.84 ($65.9/t price). Forty probabilistic pit limits were produced and only the RF equal to one pit shells were analysed and compared to the deterministic pit shell whose RF also equal to one.

4.4 Probabilistic pit limit shells results

The same process for the deterministic optimisation was followed to generate the probabilistic pit limit shells except that instead of using a single block model, ten block model realisations produced using conditional simulation representing the variable iron ore grade were used. The price used in the deterministic pit optimisation was forecasted by Anglo American from its mineral resource report. This study used P75, P50, P25 and P5 prices simulated from MCA to calculate EBVs from the ten block model realisations. The NPVs of all forty pit shells (with RFs equal to one) were plotted and compared to the deterministic pit shell with RF equal to one to illustrate the impact of iron grade and price on pit limits.

4.4.1 P75-price pit shells results

Figure 28 shows the deterministic pit shell (white solid line around the pit solid) and the probabilistic pit shells with RF equal to one (pink solids) generated using the ten block model realisations with the P75 price ($70.8/t). The P75-price pit shells represent pit shells with low-risk profiles and high confidence levels.

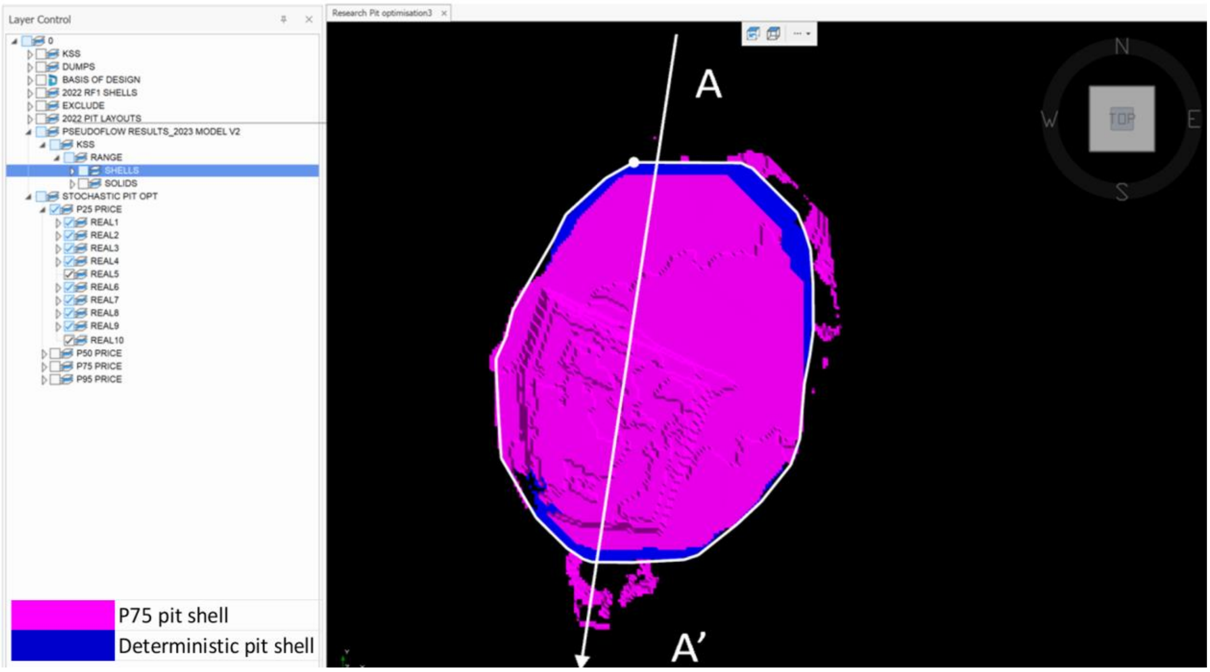

Figure 28: Deterministic and P75-price pit shells

P75-price pit shells shown in Figure 28 show a potential extension towards the northeast and south directions when compared to the deterministic pit shell. This is due to the different iron ore grade estimation of the block model realisations. The P75-price pit shells produced a pit shell bigger, in the northeast direction and in the south direction, than the deterministic pit shell even though the P75 price ($70.8/t) is lower than the price ($78.5/t) used to produce the deterministic pit shell. This was driven by the different grade estimates of the probabilistic shells. Figure 29 shows a north to south cross section view of the deterministic (blue shell) and the P75-price probabilistic pit shells.

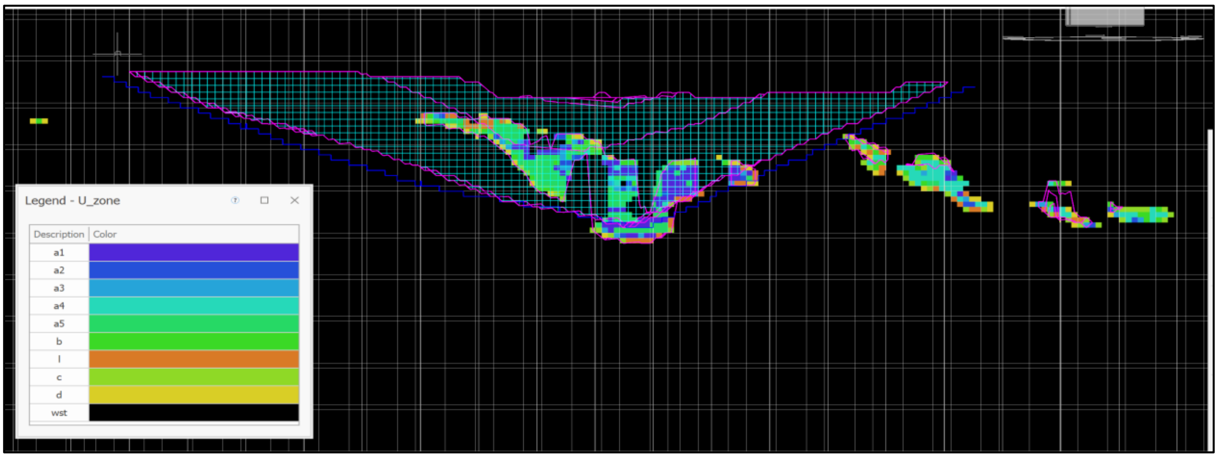

Figure 29: Cross sections of the deterministic and P75-price pit shells

Figure 29 shows that the deterministic pit shell and most of the P75-price pit shells have similar pit floors. Based on the slope angle used, both the deterministic pit shell and the probabilistic pit shells are not able to include the deeper ore. This would result in high strip ratios. A sensitivity of applying steeper slope angles could be explored later by the mine.

4.4.2 P50-price pit shells results

Figure 30 shows the deterministic pit shell (white solid line around the pit solid) and the probabilistic pit shells with RF equal to one (cyan solids) generated using the ten block model realisations with the P50 price ($94.6/t). The P50-price pit shells represent pit shells with median risk profiles and a 50% chance of realising the price.

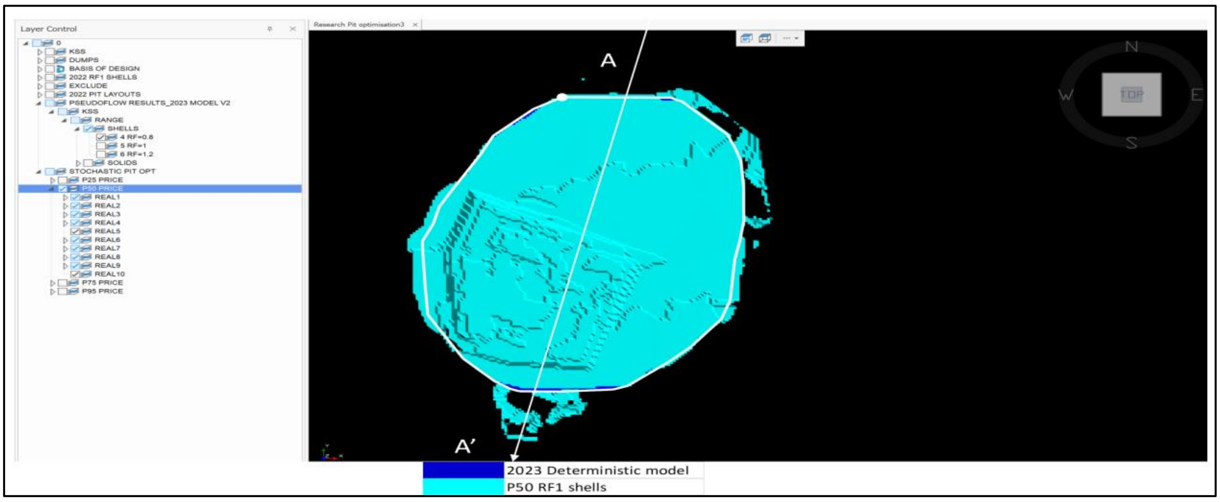

Figure 30: Deterministic and P50-price pit shells

Like the P75-price pit shells, the P50-price pit shells show a potential extension towards the northeast and south directions. The P50-price pit shell is slightly bigger on the western side when compared to the P75-price pit shell. Figure 31 shows the cross-section view of the deterministic (white solid line) and the P50-price probabilistic pit shells.

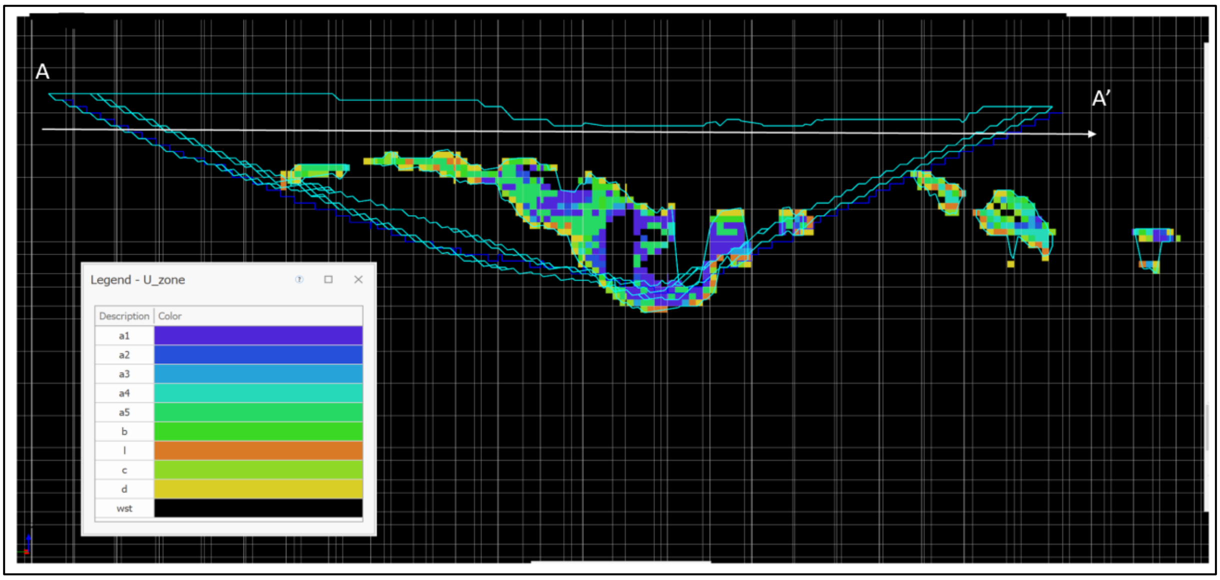

Figure 31: Cross sections of the deterministic and P50-price pit shells

The cross sections show distinctive variation in the P50-price generated pit shells in comparison to the deterministic pit shell. The P50-price pit shells are wider than the deterministic pit shell by 42 m in the northeast (A) direction. Also, P50-price pit shells have different pit floor elevations compared to the deterministic pit shell. The P50-price pit shells are 10 m deeper than the deterministic pit shells. The difference in size is because some of the P50-price block model realisations are bigger than the deterministic block model. This is also because the P50 price ($94.6/t) is higher than the deterministic price ($78.5/t).

4.4.3 P25-price pit shells results

Figure 32 shows the deterministic pit shell (white solid line around the pit solid) and the probabilistic pit shells with RF equal to one (green solids) generated using the ten block model realisations with the P25 price ($117.6/t). The P25-price pit shells represent a high-risk profile and a 75% chance of not realising the price.

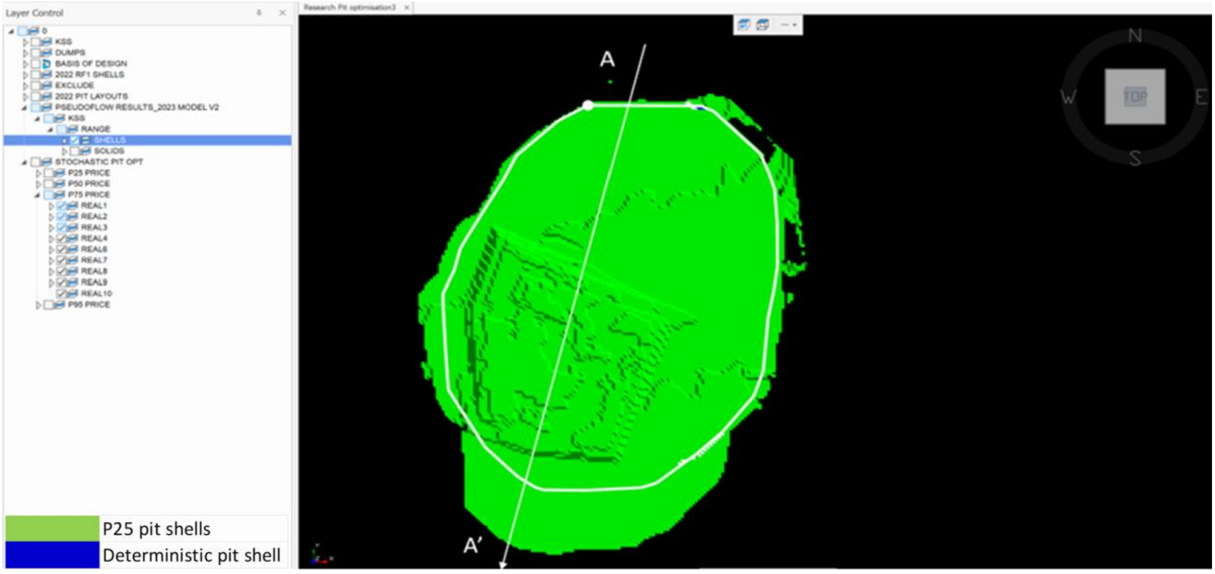

Figure 32: Deterministic and P25-price pit shells

The P25-price pit shells are notably bigger than the deterministic pit shells as they include most of the ore on the south (A') direction. They are bigger because the P25 price is 59% higher than the deterministic price. Figure 33 shows cross sections of the deterministic and P25-price pit shells.

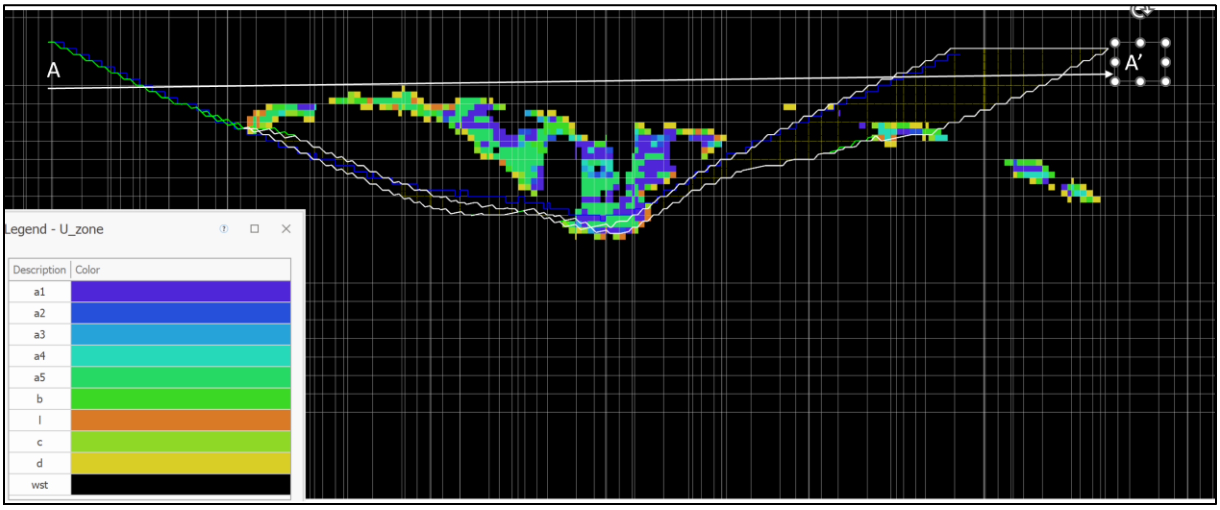

Figure 33: Cross sections of the deterministic and P25-price pit shells

The cross sections shown in Figure 33 show distinctive variation of the P25-price pit shells towards the south (A') direction. At this higher price the pit shells generated are different in pit floor elevation and width. P25-price pit shells are 10 m deeper than the deterministic pit shell. Also, they extend 123 m wider to the south. This is due to the different estimation in ore tonnages per bench as illustrated in Figure 24 and an attempt to include the pockets of iron ore on the southern side (A'). At this price point, the block model realisations which contains more ore tonnages at this depth, produce bigger pit shells. This is also because the P25 price ($117.6/t) is higher than the deterministic price ($78.5/t).

4.4.4 P5-price pit shells results

Figure 34 shows the deterministic shell (white solid line around the blue shell) and the probabilistic P5 price RF equal to one pit shells (yellow solids) generated using the ten block model realisations with the P5 price. The P5-price pit shells represent pit shells with higher risk profiles compared to previous pit shells. Also, they represent a 95% chance of not realising the iron ore price.

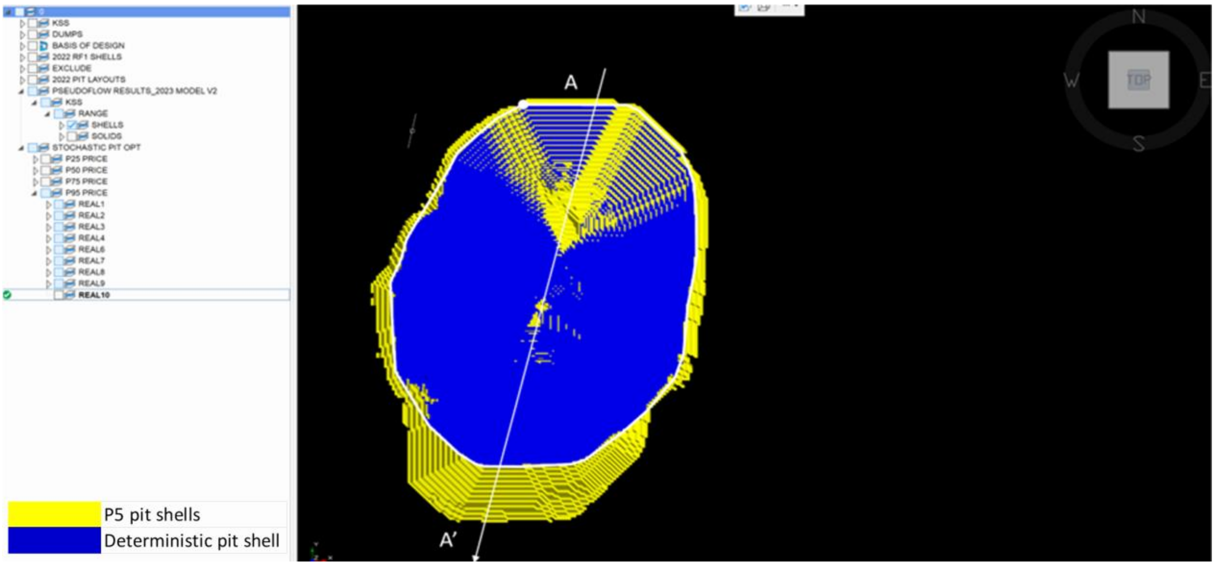

Figure 34: Deterministic and P5-price pit shells

The P5-price pit shells are notably bigger than the deterministic pit shells and bigger than the P25-price pit shells as it able to include most of the ore on the south (A') direction. The pit shells are bigger because the P5 price ($170.88) is 118% higher than the deterministic price ($78.5/t). Figure 35 shows cross sections of the deterministic and P5-price pit shells.

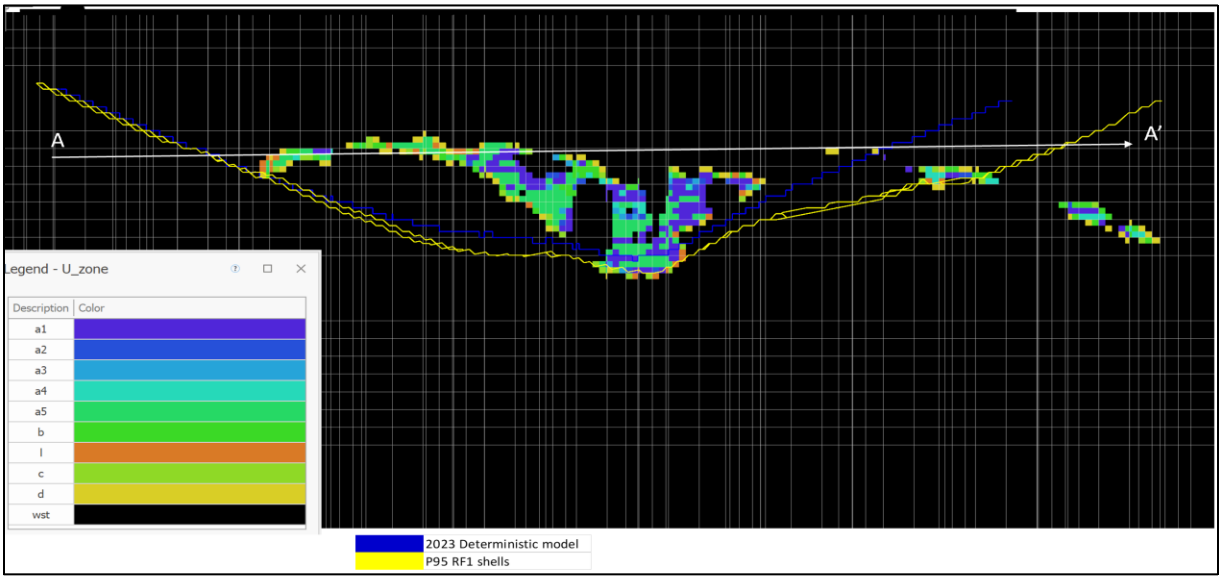

Figure 35: Cross sections of the deterministic and P5-price pit shells

The cross sections show no major distinct variation of the P5 price generated pit shells towards the south (A’) direction. At this higher P5 price, the pit shells generated are similar to P25-price pit shells, in floor elevation and width. Figure 36 shows all the forty nested pit shells and how they compare to the deterministic pit shells (white solid line around the solids).

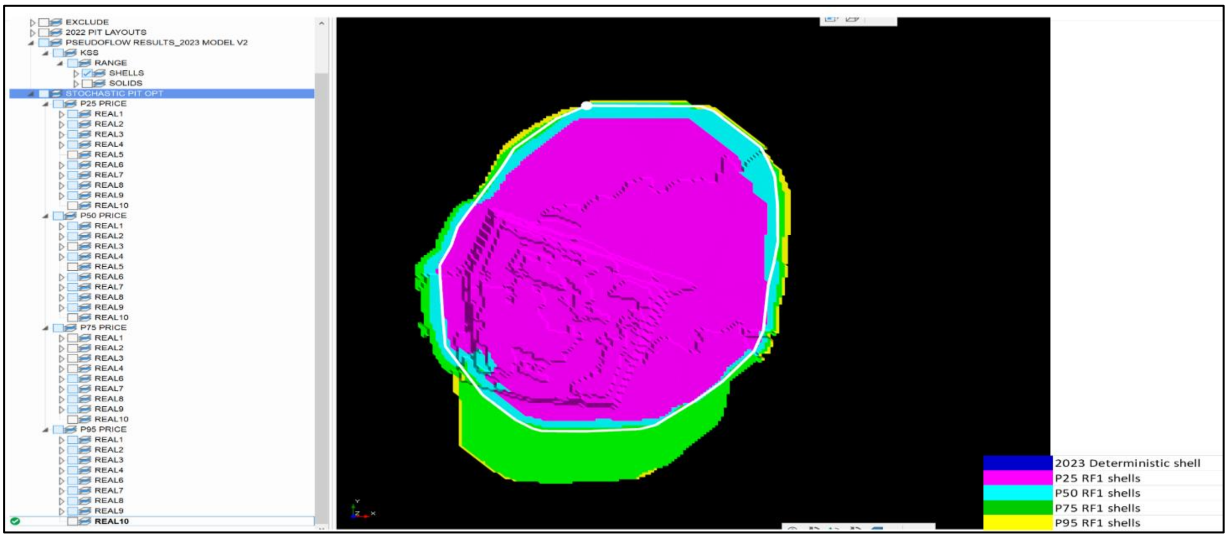

Figure 36: Nestled deterministic, P75, P50, P25 and P5 price pit shells

Figure 36 clearly shows the impact of the variability of iron ore price on the pit shells. The pit shells are sensitive to iron ore prices. The deterministic pit shell (white line) for KIO is closer to the P50-price pit shell. P50 provides a median estimate with a 50% chance of the actual outcome falling above or below the estimate. This reflects a very conservative outlook by KIO.

4.5 NPV results of all pit shells

As mentioned earlier in the report, to estimate NPV of the pits, preliminary mining schedules were generated for the deterministic and forty probabilistic pit shells. Figure 37 shows an example of a schedule with high tonnages of ore in the P50 price, which is the Real 3 pit shell.

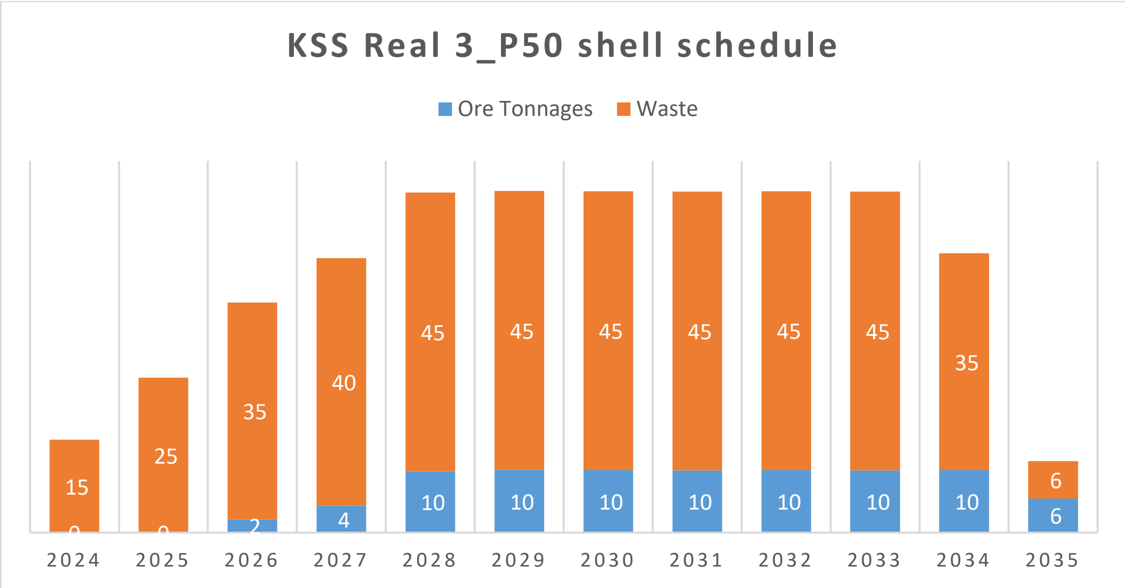

Figure 37: Schedule of KSS Real 3_P50 Shell

Figure 37 shows that the pit shell has a total of 82.46 Mt or ore at a strip ratio of 4.2. The schedule aimed for a steady state plant feed of 10 Mt, and mining will be completed in 2035.

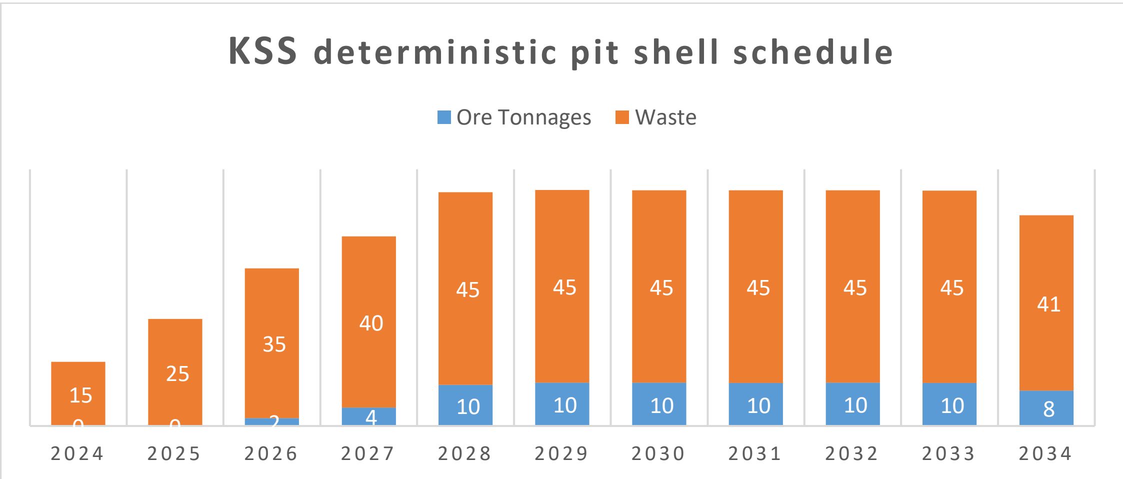

Figure 38: KSS deterministic shell schedule

Figure 38 shows a schedule for KSS deterministic pit shell. The pit shell has a total of 74.7 Mt or ore at a strip ratio of 4.94. Although the schedules reach the same tonnages of ore in the early years, mining of the deterministic pit shell will be completed in 2034 as it has 7.8 Mt less ore.

Table 11 shows the NPV results for the deterministic and forty probabilistic pit shells. Table 11 also shows the differences between the NPV of the forty probabilistic pit shells to the deterministic pit shell.

Table 11: NPV for the deterministic and all forty pit shells

RF1 Pit Shells	NPV_P75(US$Bn)	% Difference to Deterministic Pit	NPV_P50(US$Bn)	% Difference to Deterministic Pit	NPV_P25(US$Bn)	% Difference to Deterministic Pit	NPV_P5(US$Bn)	% Difference to Deterministic Pit
Real_1	2.51	**-36%**	11.35	**190%**	23.49	**501%**	44.13	**1029%**
Real_2	2.57	**-34%**	11.38	**191%**	23.66	**505%**	44.31	**1033%**
Real_3	2.92	**-25%**	11.71	**199%**	23.83	**509%**	44.48	**1038%**
Real_4	2.79	**-29%**	11.56	**196%**	23.8	**509%**	44.42	**1036%**
Real_5	2.84	**-27%**	11.63	**197%**	23.86	**510%**	44.53	**1039%**
Real_6	2.76	**-29%**	11.49	**194%**	23.74	**507%**	44.34	**1034%**
Real_7	2.73	**-30%**	11.52	**195%**	23.69	**506%**	44.3	**1033%**
Real_8	2.76	**-29%**	11.62	**197%**	23.9	**511%**	44.62	**1041%**
Real_9	2.73	**-30%**	11.56	**196%**	23.9	**511%**	44.58	**1040%**
Real_10	2.75	**-30%**	11.54	**195%**	23.79	**508%**	44.44	**1037%**
Deterministic Pit (US$Bn)	3.91							

Table 11 shows that except for the P75-price pit shells, NPVs for all the other pit shells are greater than the NPV for the deterministic pit shell. This is because P75 price is lower than the deterministic price. The key difference between P75, P50, P25 and P5 price pit shells lies in the level of confidence they represent. The P75 and P50-price pit shells represent low to medium risk profiles, while the P25 and P5 represent high-risk profiles. Table 11 also shows that there is less variation in NPV within the same probability price. However, there is a notable increase when probability price changes. Figure 39 shows the average NPVs for all the forty probabilistic pit shells plotted against their price probability.

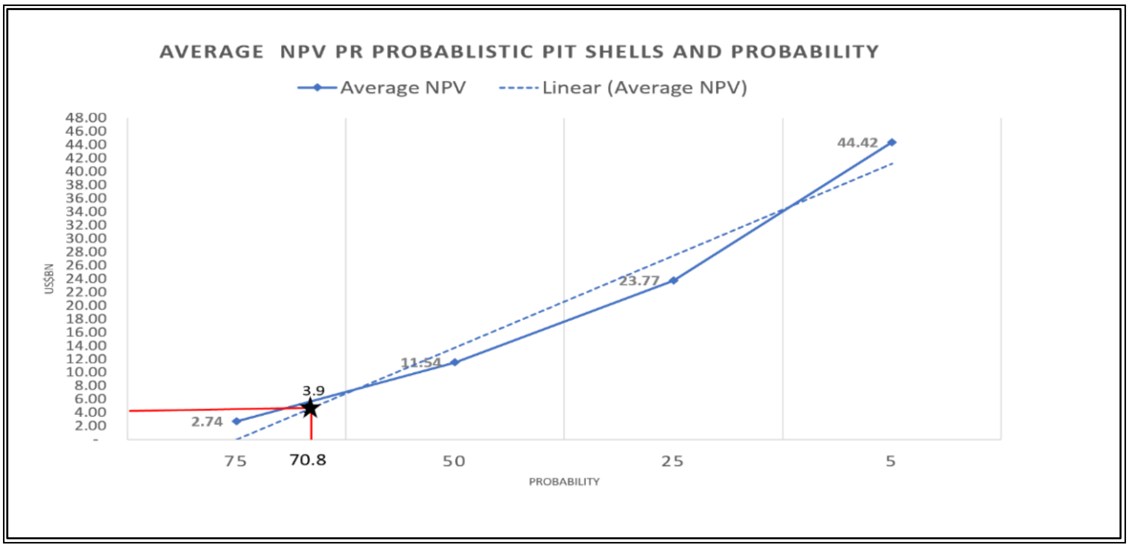

Figure 39: Average NPVs of the deterministic, P75, P50, P25 and P5 price pit shells

Figure 39 shows that the deterministic final pit limit is estimated to be at P71 price. It also shows that KIO management is very conservative in their mine planning processes. If KIO planned at the high P5 price of $170.89/t, it would produce an optimistic plan that could be riskier should the price not be realised as compared to a P75, low price of $70.84/t, which is conservative and has a high chance of being achieved. Table 11 also shows that the NPV of the deterministic pit shell was on average 195% lower than that of the P50-price pits shells. It is therefore important for mining engineers to incorporate uncertainty of commodity price when designing and planning pit shells. Since commodity price is not static, it can have significant impact on the profitability of a mine.

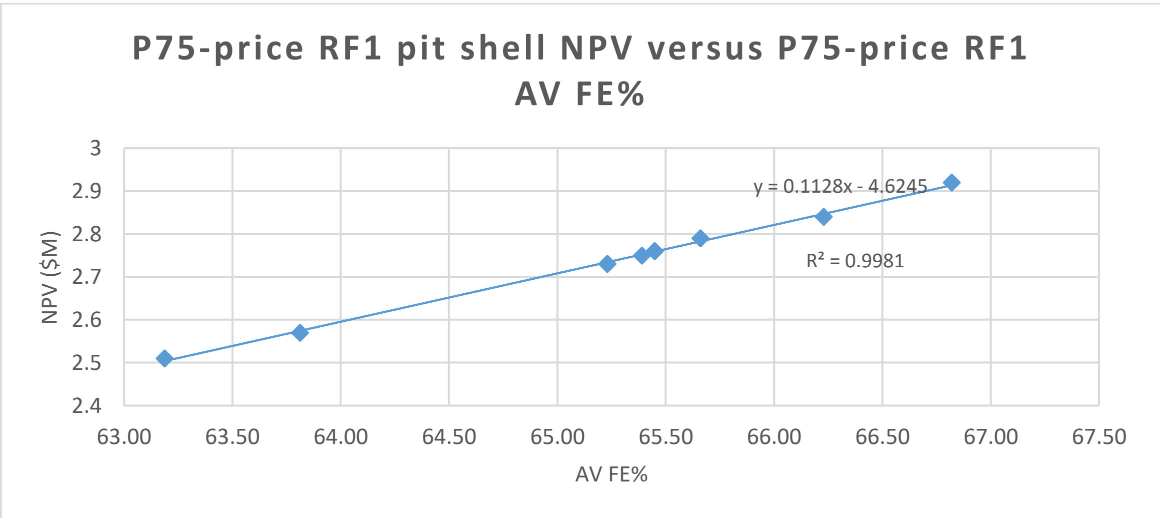

Figure 40: Linear regression of the P75 RF1 shells NPV vs. P75 RF1 Av Fe%

Figure 40 shows a linear regression analysis of iron ore grade and NPV of P75-price RF1 pit shells Figure 40 shows that there is a significant effect of varying iron grade on NPV. The higher the iron ore grade the higher the NPV. The analysis shows a very strong and positive correlation coefficient of 0.998 between iron ore grade and NPV of P75-price RF1 pit shells. Figure 41 shows a linear regression analysis of iron ore grade and NPV of P50-price RF1 pit shells.

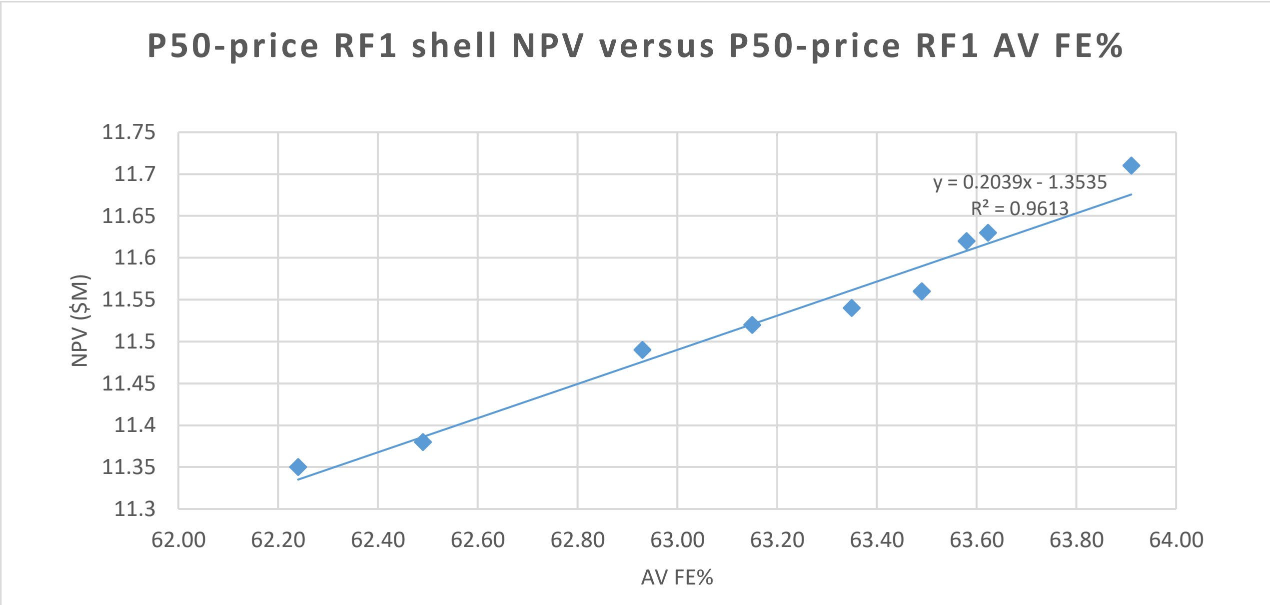

Figure 41: Linear regression of the P50 RF1 shells NPV versus P50 RF1 Av Fe%

Figure 41 shows that there is a significant effect of varying iron grade on NPV. The higher the iron ore grade the higher the NPV. The analysis shows a very strong and positive correlation coefficient of 0.961 between iron ore grade and NPV of P50-price RF1 pit shells. Looking at Figure 40 and Figure 41 it is important to note that the difference in price of $70.84 to $94.64 has an even bigger impact on NPV as a change ($23.8) resulted in a 300% increase in NPV. Table 12 shows ore tonnes, waste tonnes, strip ratio and LOM results for the P50-price probabilistic pit shells.

Table 12: P50 probabilistic pit ore and waste tonnages, strip ratio and LOM

	P50 pit shells and determistisic pit shell			
Pit shells	**Ore Tonnes (Mt)**	**Waste Tonnes (Mt)**	**Strip Ratio**	**LOM**
Real_1	71.58	354.43	4.95	7.2
Real_2	80.03	345.88	4.32	8.0
Real_3	82.46	343.40	4.16	8.2
Real_4	79.55	346.30	4.35	8.0
Real_5	72.33	353.63	4.89	7.2
Real_6	73.15	352.89	4.82	7.3
Real_7	72.12	353.91	4.91	7.2
Real_8	80.27	345.60	4.31	8.0
Real_9	77.69	348.34	4.48	7.8
Real_10	75.36	350.67	4.65	7.5
Deterministic pit shell	**74.70**	**369.16**	**4.94**	**7.5**

To simplify the study, P50-price probabilistic pit shells were analysed. The following salient points are noted from Table 12:

- Ore tonnes vary from 71.58 Mt to 82.46 Mt between the probabilistic pit shells. This illustrates the impact of iron ore grade estimation and its variability on total orebody tonnage.
- The strip ratios of the resultant probabilistic pit also vary from 4.16 to 4.95. The strip ratio of a chosen pit has an impact on mining cost and the resulting NPV. The higher the strip ratio, the higher the cost of mining. A higher mining cost erodes NPV.
- LOMs also vary between the probabilistic pit shells because of the ore tonnage estimated. The lowest LOM is 10.5 years with the highest LOM being 11.5 years. An additional year of mining would result in potential revenue gain.

4.6 Summary of Chapter 4

Chapter 4 showed that conditional simulation of the block model produced variable ore tonnages due to the different estimated iron ore grade. There was a 15% difference in ore tonnages when comparing the block model realisations with the highest ore tonnage to that with the low ore tonnage. This clearly shows the impact of variability on iron ore grade estimation. This chapter also showed that the different orebody realisation resulted in different NPVs and different pit shells. The results of the probabilistic method compared to the deterministic method is distinctly shown in the results. Through these results, the impact of variability of iron ore price and iron ore grade on NPV was demonstrated. Using the demonstrated methodology, based on their appetite from risk, managers can make informed decisions on which pit shell to choose.

5 CONCLUSSIONS AND RECOMMENDATIONS

5.1 Overview of Chapter 5

Chapter 5 discusses the salient points that were drawn from the study and the results of the study. The chapter then outlines the limitations of this study and then recommends future work and other areas that the research can be expanded to investigate.

5.2 Conclusions

This study successfully presented a method that quantitatively modelled the uncertainties in iron ore grade and price involved in open pit optimisation. The study showed that significant uncertainty exists in open pit optimisation considering the variation in iron ore prices for the past 10 years. Using P5, P25, P50 and P75 prices, forty different mineral reserves tonnages, pit shells, NPVs and LoM at RF equal to one were estimated. The NPV ranged from US$2.5Bn to US$44.6Bn for P75 and P5 prices, respectively. The NPV of the deterministic pit shell was calculated to be US$3.9Bn. The deterministic pit limit was also calculated to have a price confidence level of 70.8% as shown in Figure 39. Results from the study have shown that the uncertainty-based approach indicate the worst and the best-case scenarios in terms of mineral prices, mineral reserves tonnages and ultimately NPV. The study showed that there is less variation in NPV within the same probability price but there is a notable increase when probability price changes. This shows that iron price has more influence on NPV than iron ore grade.

5.3 Research limitations

The limitation of the study was that it used historical iron ore prices instead of forecasting the prices by using a stochastic method. Nonetheless, the study successfully highlighted the impact of using a single deterministic iron ore price on open pit optimisation. The study was based on a new pit which has not started mining and as a result the data from the study will have to wait for production so that it can be valuated against actual data.

5.4 Recommendations for future work

In future work, it is recommended that:

1. The approach be extended to simultaneously model the uncertainties of other variables which include contaminants such as SiO_2 and K_2O, costs, recoveries, mining dilution and mining losses. These variables are also uncertain hence they significantly affect optimal pit limikts. The additional information gained from assessing the uncertainty in iron ore grade estimate and iron ore prices for Kolomela Mine’s Kapstevel South Pit has indicated that this is a worthwhile exercise to do to gain insight of the impact of variability on the chosen pit and its probability.
2. Actual probability distributions of each uncertain variable can be identified, and an appropriate stochastic method be used to model uncertainty of the variables.
3. The study can be extended to all the pits at Kolomela Mine and at Sishen Mine. Information gained from the study can show all possible best and worst-case scenario for the whole KIO mineral assets. Expanding the methodology to other pits will also allow for a review of dynamic pit sequencing to maximise the value of the orebody under identified uncertain conditions.
4. The conditional simulation and economic block modelling processes can be automated using python scripts. Also, the generated pits shells/solids should be run through a tactical scheduling package instead of a strategic software. This will provide actual NPV values rather than indicative open pit values which are generated through Deswik Pseudoflow.
5. It is recommended that the methodology be also implemented at Sishen Mine before the medium-term planning process in order to understand uncertainty of grade and iron ore price of the chosen final pit shells.
6. The scope of the application can be expanded by adding the different SMU to analyse the impact of the selective mining variable on NPV.
7. Using other software such as Whittle with sensitivity analysis tools will also enable sensitivity analysis on the chosen pit to be done.

It should be noted though that the exercise is highly time consuming due to the time it takes to prepare block models (SMU up-blocking), calculate, and encode EBV calculations on all ten block realisation models. Once the block models were prepared the running of the pit optimisation software models was quick. Using python to prepare models can help reduce the time to prepare models.

REFERENCES

Achireko, P.K, & Frimpong, S. (1996). Open pit optimization using artificial neural networks on conditionally simulated blocks. *Society for Mining, Metallurgy & Exploration*, 1996.

Akbari, A., Osanloo, M., & Shirazi, M. (2008). Determination of ultimate pit limits in open mines using real option approach. *IUST IInternational Journal of Engineering Science, 19* (5), 23-38.

Anglo American. (2022). Ore reserves and mineral resources report 2022. from https://www.angloamerican.com/~/media/Files/A/Anglo-American-Group-v5/PLC/investors/annual-reporting/2022/ore-reserves-and-mineral-resources-report-2022.pdf. Retrieved October 30, 2023.

Appianing, E. J., & Mireku-Gyimah, D. (2015). Open pit optimisation and design: A stepwise approach. *Ghana Mining Journal, 15* (2), 27-35.

Asad, M., & Dimitrakopoulos, R. (2013). Implementing a parametric maximum flow algorithm for optimal open pit mine design under uncertain supply and demand. *Journal of the Operational Research Society, 64* (2), 185-197.

Askari-Nasab, H., Frimpong, H., Awuah-Offei, & K. (2009). Intelligent optimal production scheduling estimator. *Proceedings of 32nd Application of Computers and Operation Research in the Mineral Industry*, Tucson, AZ.

Ataee-Pour, M. (2005). A critical survey of the existing stope layout optimization techniques. *Journal of Mining Science, 41* (1), 447-466.

Baek, J., Choi, Y., & Park, A. (2016). Uncertainty representation method for open pit optimization results due to variation in mineral prices. *Minerals, 6* (1), 2-15.

Boyle, P. (1977). Options: A monte carlo approach. *Journal of Financial Economics, 4* (3), 323-338.

Breed, M., & van Heerden, D. (2016). Post-pit optimization strategic alignment. *Journal of of the South African Mining Institute, 116* (2), 109-114.

Camus, J. (1992). Open pit optimization considering an underground alternative. *Proceedings of the 23th International APCOM Symposium*. Littleton, Colorado: Society for Mining, Metallurgy and Exploration.

Carlson, T., Erikson, J., O'Brian, D., & Pana, M. (1966). Computer techniques in mine planning. *Mining Engineering, 18* (5), 53-56.

Charbel, P. (2015). *Gerenciamento de risco aplicado à diluição de minério, PhD. Dissertation.* Brazil: Faculdade de Tecnologia, Universidade de Brasília, Brasília.

Chen, J. (1977). 3-D pit design with variable wall slope capabilities. *In: 14th Symposium on The Application of Computers and Operations Research in the Mineral Industries. (APCOM), New York*.

Dagdelen, K. (2001). Open pit optimization-strategies for improving economics of mining projects through mine planning*. Proceedings of the 17th International Mining Congress and Exhibition of Turkey*, Ankara, 19-22 June 2001.

David, M., Dowd, P., & Korobov, S. (1974). Forecasting departure from planning in open pit design and grade control. *In: 12th Symposium on the Application of Computers and Operations Research in the Mineral Industries (APCOM),* Colorado School of Mines *2, pp. F131-F142*..

Denby, B., & Schofield, D. (1994). Open-pit design and scheduling by use of genetic algorithms. *The Institution of Mining and Metallurgy, 103*, pp. A21-26.

Dimitrakopoulos, R., Farelly, C., & Godoy, M. (2002). Moving forward from traditional optimization: grade uncertainty and risk effects in open-pit design. *Transactions of the Institutions of Mining and Metallurgy, Section A: Mining Technology, 111* (1), 82-88.

Dimtrakopoulos, R. (2010). Stochastic mine planning-methods, examples and value in an uncertain world. Dimitrakopoulo (Ed.), *Advances in Orebody Modelling and Strategic Mine Planning* (pp. 13-19). McGill University, Montreal, Québec, Canada: Springer International Publishing.

Dixit, A., & Pindyck, R. (1994). *Investment under uncertainity* (First ed.). Pronceton: Princeton Unviversity Press.

Dowd, P. (1994). Risk assessment in reserve estimation in open-pit planning. *Transactions of the Institution of Mining and Metallurgy-Section A-Mining Industry*, 103, p. A148.

Ernst, A. (2003). *Comparison of qualitative and quantitative research. GRIN Verlag*.

Ersoy, A., & Yunsel, T. (2006). Geostatistical conditional simulation for the assessment of the quality characteristics of Cayırhan lignite deposits. *Energy Exploration and Explotation, 24* (6), 371-453.

Fallara, F., Legauult, M., & Rabeau, O. (2006). 3-D Integrated geological modeling in the Abitibi Subprovince (Québec, Canada): techniques and applications. *Exploration and Mining Geology, 15* (no. 1–2.), pp. 27-41.

Gauntlett, J. (2023). *Quarry resource optimisation*., From https://www.eltirus.com/quarry-resource-optimisation. Retrieved December 28, 2023.

Gholamnejad, J., lotfi, E., Najafi, M., & Zamani, M. (2022). Designing the most probable final pit limit of open pit mines considering price uncertainty. *Journal of Analytical and Numerical Methods in Mining Engineering, 12* (32), pp. 76- 86.

Giannini, L. M., Caccetta, L. K., & P and Carras, S. (1991). PITOPTIM: A new high speed network flow technique for optimum pit design facilitating rapid sensitivity analysis. *Australasian Institute of Mining and Metallurgy (AusIMM)* 2, pp. 57-62.

Godoy, M. (2003). *The effective management of geological risk in long-term production scheduling of open pit mines. PhD Thesis*, School of Engineering, The University of Queensland.

Goodman, J. (2012). *Stochastic differential equations.* (1 ed.). New York: New York University. 2012.

Haykin, S. (1994). *Neural networks: A comprehensive foundation.* New York: Macmillan College.

Hochbaum, D., & Chen, A. (2000). Performance analysis and best implementations of old and new algorithms for the open-pit mining problem. *Journal of Operation Research, 48* (6), 894-914.

Ibrahim, S., Misiran, M., & Mohamed, F. L. (2010). Geometric fractional Brownian motion model for commodity market simulation. *Alexandria Engineering Journal, Volume 60* (1), pp. 955-962.

Inthanongsone, I., Drebenstedt, C., & Bongaerts, J. (2015). Cost estimation for open pit mines: Tackling cost uncertainties. Freiberg, Germany: Department of Mining Engineering, National University of Laos.

Jara, R., Couble, A., Emery, X., Magri, E., & Ortiz, J. (2006). Block size selection and its impact on open-pit design and mine planning. *The Journal of The South African Institute of Mining and Metallurgy, 106 (3), pp. 205-211.*.

Johnson, T. (1968). Optimum open pit mine production scheduling. Berkely: Operations Research Center.

Khalokakaie, R., Dowd, P.A, & Fowell, R.J. (2000). Lerchs–Grossmann algorithm with variable slope angles. *Mining Technology*, 109 (2), pp.77-85.

Lerchs, H., & Grossmann, I. F. (1965). *Optimum design of open pit mines.* Canada: Cananda Insitute Mining Bulletin.

Market Insider. (2022). *Iron ore prices today*., From https://markets.businessinsider.com/commodities/iron-ore-price, Retrieved March 12, 2022.

Menade, M., Foyland, G., Stone, P., & Yeates, G. (2004). Mining schedule optimisation for conditionally simulated orebodies. *Proceedings of the International Symposium on Orebody Modelling and Stategic Mine Planning: Uncertainty and Risk Management*. Perth, WA

Mineral Industry Survey. (2022). *Iron ore statistics and information*. From https://www.usgs.gov/centers/national-minerals-information-center/iron-ore-statistics-and-information#:~:text=Almost%20all%20(98%25)%20iron,one%2Dthird%20of%20total%20exports. Retrieved September 14, 2023

Mitchell, M. (1999). *An introduction to Genetic Algorithms, 1st ed.,* (1 ed.). London: First MIT Press.

Mukombo, M., Kisumpa, N. M., & Kalej, M. (2020). Literary review on optimizing open pit mining under Surpac and Whittle. *International Journal of Science and Research, 9* (6), pp. 202-204.

Mwangi, D., Jianhua, Z., Kasomo, R. M., Matidza, M., & Huang, G. (2020). Ultimate pit limit optimization methods in open pit mines: A review. *Journal of Mining Science, 56* (02), pp. 588–602.

Navarro, F., Morales, N., Contreras-Bolton, C., Rey, C., & Parada, V. (2024). Open-pit pushback optimization by a Parallel Genetic Algorithm. *Minerals, 14* (5), 438.

Nhleko, A., Tholana, T., & Neingo, P. (2018). A review of underground stope boundary optimization algorithms. *Resources Policy, 56*, pp. 59–69.

Picard, J. (1976). Maximal Closure of a graph and applications to combinatorial problems. *Management Science, 22* (11), pp. 1268-1272.

Rupprecht, S. (2014). The application of modifying factors. Southern African Institute of Mining and Metallurgy, The SARECISAMVAL.

Saleki, M., Kakaie, M., & and Ataei, M. (2019). Mathematical relationship between ultimate pit limits generated by discounted and undiscounted block value maximization in open pit mining. *Journal of Sustainable Mining, 18* (2), pp. 94-99.

Schwartz, E. S. (1997). The stochastic behavior of commodity prices: Implications for valuation and hedging. *Journal of Finance, 52* (3), pp. 923-973.

Songolo, M. (2010). *Pushback design using Genetic Algorithms.* Kalgoorlie, Australia: Western Australian School of Mines.

Tholana, T., Musingwini, C., & Ali, M. (2019, May 22-23). A stochastic block economic value model. *Proceedings of the Mine Planners Colloquium 2019: Skills for the Future—Yours and Your Mine's*. pp. 35-50.

Wackernagel, H. (2003). *Multivariate geostatistics: An introduction with applications* (3 ed.). Berlin, Heidelberg: Springer.

Whittle, G., Stange, W., & Hanson, N. (2007). Optimising project value and robustness. *Project Evaluation Conference. Australasian Institute of Mining and Metallurgy*, Melbourne. pp.147-155.

Whittle, J. (1988). Beyond optimisation in open pit design\. In Computer Applications in the Minerals Industry. Balkema, Rotterdam, pp. 331–337.

Whittle, J. (1990). *Allowing for underground mining in Four-D four dimenstional open pit.* Melbourne, Australia: Whittle Programming Pty Ltd.

Whittle, J. (1993). The use of optimisation inopen pit design. Melbourne, Australia: Whittle Programming Proprietary Limited.

Wright, A. E. (1987). The use of dynamic programming for open pit mine design: Some practical implications. *Mining Science and Technology, 4* (2), pp. 97-104.

Wright, E. (1999). Moving Cone II - A simple algorithm for optimum pit limit design. *Procedings of the 28th Symposium on the Application of Computers and Operational Research Industry (APCOM)*. Colorado School of Mines, Colorado USA. pp. 367-374.

Zhao, Y., & Kim, Y. (1992). A new optimum pit limit design algorithm. *Application of Computers and Operations Research in the Mineral Industry, 23*, pp. 423-434.

Appendix A: Block deswik scripts

Attribute	Filter	DataType	Description	Formula
Vol	<No Filtering>	Double	Calculate BM cell volume	10*10*10
Tonnes	<No Filtering>	Double	Calculate BM cell tonnage	[u_rd]*[Vol]
Drilling Cost	<No Filtering>	Double	Calculate drilling cost	[Tonnes]*GC("DC")
Blasting Cost	<No Filtering>	Double	Calculate blasting cost	[Tonnes]*GC("BC")
Hauling Cost	<No Filtering>	Double	Calculate hauling cost	[Tonnes]*GC("HC")
Loading Cost	<No Filtering>	Double	Calculate loading cost	[Tonnes]*GC("LC")
Ancilliary Cost	<No Filtering>	Double	Calculate ancilliary cost	[Tonnes]*GC("AC")
Other mining Cost	<No Filtering>	Double	Calculate other mining cost	[Tonnes]*GC("OC")
Bench	<No Filtering>	Double	Bench	[_ZC]-5
Dumpm	Waste	Double	Dump multiplier *Bench	[Bench]*GC("kss_ct_d_m")
DumpF	Waste	Double	Dumpfactor	([Dumpm]+GC("kss_ct_d_c"))/GC("RC_KL_WAST")
Plantm	Ore	Double	Plant multiplier *Bench	[Bench]*GC("kss_ct_plant_m")
PlantF	Ore	Double	Plant Factor	([Plantm]+GC("kss_ct_plant_c"))/GC("RC_KL_ORE")
MCAF	<No Filtering>	Double	MINING COST FACTOR - REGRES	[PlantF] +[DumpF]
Mining Cost	<No Filtering>	Double	Calculate mining cost	GC("MC")*[Tonnes]*[MCAF]
Recovered Ore	Ore	Double	Calculate Recovered Ore (MRE)	IF([u_zone]="a1", [*Volume]*[u_rd]*GC("MRE"),[*Volume]*[u_rd])
DSO Feed t	DSO Feed	Double	Calculate crusher feed tonnes	[Recovered Ore]
DMS Feed t	DMS Feed	Double	Calculate crusher feed tonnes	[Tonnes]
Product Calculations	<No Filtering>	String	Calculate product metal quantit	0
DSO Prod t	DSO Feed	Double	DSO Product Tonnes	[DSO Feed t]*GC("DSOYL")
DMS Prod t	DMS Feed	Double	DMS Product Tonnes	[DMS Feed t]*GC("DMSYL")
Attribute	Filter	DataType	Description	Formula
DSO PL t	Premium Product	Double	DSO Premium Lump Tonnes	[DSO Prod t]*GC("LR")
DSO PF t	Premium Product	Double	DSO Premium Fines Tonnes	[DSO Prod t]*(1-GC("LR"))
DSO SL t	Standard DSO Pro	Double	DSO Standard Lump Tonnes	[DSO Prod t]*GC("LR")
DSO SF t	Standard DSO Pro	Double	DSO Standard Fines Tonnes	[DSO Prod t]*(1-GC("LR"))
DMS SL t	Standard DMS Pro	Double	DMS Standard Lump Tonnes	[DMS Prod t]*GC("LR")
DMS SF t	Standard DMS Pro	Double	DMS Standard Fines Tonnes	[DMS Prod t]*(1-GC("LR"))
Total Product t	<No Filtering>	Double	Total Product Tonnes	SUM([DSO PL t],[DSO PF t],[DSO SF t],[DSO SL t],[DMS SF t],[DMS SL t])
DMS Standard Lump Price Ca	<No Filtering>	String	DMS Calculate Price for standar	0
DMS Standard Base Price	DMS Feed	Double	DMS Standard Base Price	GC("SL")
DMS Fe premium calc	DMS Feed	Double	DMS Fe premium calculation	(GC("DMSLFE")-GC("BFe"))*GC("PABFE")
DMS Standard Silica penalty	DMS Feed	Double	DMS Silica penality low	(GC("SIL")-GC("SIM"))*GC("SIPL")
DMS Standard Silica penalty	DMS Feed	Double	DMS Silica penality med	(GC("SIM")-GC("DMSLS"))*GC("SIPM")
DMS Standard Alumina pena	DMS Feed	Double	DMS Alumina penalty	IF(AND(GC("DMSLA")>=GC("ALL"),GC("DMSLA")<GC("ALM")), (GC("ALM
DMS Standard Lump Premiu	DMS Feed	Double	DMS Standard Lump premium	GC("DMSLFE")/100*GC("LP")
DMS Standard Lump Price	DMS Feed	Double	DMS Standard Lump price	SUM([DMS Standard Base Price],[DMS Standard Lump Premium],[DMS
DMS Standard Fines Price Ca	<No Filtering>	String	DMS Calculate Price for standar	0
DMS Standard Fines Price	DMS Feed	String	DMS Standard Base Price	GC("SL")
DMS Fines Fe premium	DMS Feed	Double	DMS Fe premium calculation	(GC("DMSFFE")-GC("BFe"))*GC("PABFE")
DMS Fines Silica penaltylow	DMS Feed	Double	DMS Silica penality low	(GC("SILF")-GC("SIM"))*GC("SIPL")
DMS Fines Silica penaltymed	DMS Feed	Double	DMS Silica penality med	(GC("SIM")-GC("DMSFS"))*GC("SIPM")
DMS Fines Alumina penality	DMS Feed	Double	DMS Alumina penalty	IF(AND(GC("DMSFA")>=GC("ALL"),GC("DMSFA")<GC("ALM")), (GC("ALM
Attribute	Filter	DataType	Description	Formula
DMS TStandard Fines Price	DMS Feed	Double	DMS Total Standard fines price	SUM([DMS Standard Fines Price],[DMS Fines Fe premium],[DMS Fines S
DSO Standard Lump Price Ca	<No Filtering>	String	DSO Calculate Price for standar	0
Standard Base Price	DSO Feed	String	DSO Standard Base Price	GC("SL")
Standard Fe premium	DSO Feed	Double	DSO Fe premium calculation	([u_fe]-GC("BFe"))*GC("PABFE")
Standard Silica penaltylow	DSO Feed	Double	DSO Silica penality low	IF(AND([u_sio2]<GC("SIL")), (GC("SIL")-[u_sio2]*GC("SIPL")),
&#09
Standard Silica penaltymed	DSO Feed	Double	DSO Silica penality med	IF(AND([u_sio2]<GC("SIL"),[u_sio2]<GC("SIM")), (GC("SIM")-[u_si
Standard Alumina penality	DSO Feed	Double	DSO Alumina penalty	IF(AND([u_al2o]>=GC("ALL"),[u_al2o]<GC("ALM")), (GC("ALM")-[u_al2o
Standard Lump Premium	DSO Feed	Double	DSO Standard Lump premium	[u_fe]/100*GC("LP")
Standard Lump Price	DSO Feed	Double	DSO Total Standard Lump price	SUM([Standard Base Price],[Standard Fe premium],[Standard Lump Pre
DSO Standard Fines Price Ca	<No Filtering>	String	DSO Calculate Price for standar	0
Standard Fines Price	DSO Feed	String	DSO Standard Base Price	GC("SL")
Fines Fe premium	DSO Feed	Double	DSO Fe premium calculation	([u_fe]-GC("BFe"))*GC("PABFE")
Fines Silica penaltylow	DSO Feed	Double	DSO Silica penality low	IF(AND([u_sio2]<GC("SIL")), (GC("SILF")-[u_sio2]*GC("SIPL")),
&#0
Fines Silica penaltymed	DSO Feed	Double	DSO Silica penality med	IF(AND([u_sio2]<GC("SIL"),[u_sio2]<GC("SIM")), (GC("SIM")-[u_si
Fines Alumina penality	DSO Feed	Double	DSO Alumina penalty	IF(AND([u_al2o]>=GC("ALL"),[u_al2o]<GC("ALM")), (GC("ALL")-[u_al2o]
TStandard Fines Price	DSO Feed	Double	DSO Total Standard fines price	SUM([Standard Fines Price],[Fines Fe premium],[Fines Silica penaltylov
Premuim Lump 62P Price Cal	<No Filtering>	String	Calculate Price for premium lun	0
Premium Base Price	Premium Product	Double	Standard Base Price	GC("SL")
Premium Fe premium	Premium Product	Double	Fe premium calculation	([u_fe]-GC("BFe"))*GC("PABFE")
Premium Silica penaltylow	Premium Product	Double	Silica penality low	IF(AND([u_sio2]<GC("SIL")), (GC("SIL")-[u_sio2]*GC("SIPL")),
&#09
Premium Silica penaltymed	Premium Product	Double	Silica penality med	IF(AND([u_sio2]<GC("SIL"),[u_sio2]<GC("SIM")), (GC("SIM")-[u_si

Attribute	Filter	DataType	Description	Formula
FPremium Fines Price	Premium Product	Double	Portion 33% Premium fines pric	SUM([FPremium High Price],[FPremium Fe premium],[FPremium Silica
TPremium Fines Price	Premium Product	Double	Total Premium fines price	SUM([FPremium Fines Price],[Premium Fines Price])
Premium Lump Revenue	Premium Product	Double	Calculate premium lump revenu	[DSO PL t]*[TPremium Lump Price]
Premium Fines Revenue	Premium Product	Double	Calculate Premium Fines reven	[DSO PF t]*[TPremium Fines Price]
DSO Standard Lump Revenue	Standard DSO Pro	Double	Calculate standard lump revenu	[DSO SL t]*[Standard Lump Price]
DMS Standard Lump Revenue	Standard DMS Pro	Double	Calculate standard lump revenu	[DMS SL t]*[DMS Standard Lump Price]
DSO Standard Fines Revenue	Standard DSO Pro	Double	Calculate standard lump revenu	[DSO SF t]*[TStandard Fines Price]
DMS Standard Fines Revenue	Standard DMS Pro	Double	Calculate Standard Fines revenu	[DMS SF t]*[DMS TStandard Fines Price]
Total Revenue	<No Filtering>	Double	Caculate total product revenue	SUM([Premium Lump Revenue],[DSO Standard Fines Revenue],[DMS St
DMS Cost	DMS Feed	Double	Calculate DMS cost	GC("DMSC")*[DMS Feed t]
DSO Cost	DSO Feed	Double	Calculate DSO cost	GC("DSOC")*[DSO Feed t]
Financial Calculations	<No Filtering>	Double	Calculate costs for each BM cell	0
Mining Cost	<No Filtering>	Double	Calculate mining cost	GC("MC")*[Tonnes]
Processing Cost	<No Filtering>	Double	Calculate total processing cost	SUM([DSO Cost],[DMS Cost])
Offshore Cost	<No Filtering>	Double	Calculate total off shore cost	[Total Product t]*GC("OSC")
Sea freight Cost	<No Filtering>	Double	Calculate total sea freight cost	[Total Product t]*GC("SF")
Marketing Cost	<No Filtering>	Double	Calculate marketing cost per tot	SUM([Offshore Cost],[Sea freight Cost])
Port Cost	<No Filtering>	Double	Calculate port cost per total pro	[Total Product t]*GC("PC")
Rail Cost	<No Filtering>	Double	Calculate rail cost per total prod	[Total Product t]*GC("RC")
Logistic Cost	<No Filtering>	Double	Calculate Logistic cost per total	SUM([Port Cost],[Rail Cost])
FOR Revenue	<No Filtering>	Double	Calculate revenue at Saldahna	[Total Revenue]-[Logistic Cost]-[Sea freight Cost]

Attribute	Filter	DataType	Description	Formula
FOR Revenue	<No Filtering>	Double	Calculate revenue at Saldahna	[Total Revenue]-[Logistic Cost]-[Sea freight Cost]
G&A Cost	<No Filtering>	Double	Calculate G&A per total plant fe	SUM([DMS Feed t],[DSO Feed t])*GC("GA")
Rehab Cost	<No Filtering>	Double	Claculate closure cost per tonne	[Tonnes]*GC("CC")
SIB Cost	<No Filtering>	Double	Calculate SIB cost (HME only) pe	[Tonnes]*GC("SIB")
Royalties Cost	<No Filtering>	Double	Calculate Royalties cost (4%)	[FOR Revenue]*GC("RY")
Total Cost	<No Filtering>	Double	Sum all cost of mining	SUM([Mining Cost],[Processing Cost],[Rehab Cost],[Royalties Cost],[SIB
Profit	<No Filtering>	Double	Calculate profit	[Total Revenue]-[Total Cost]
VPT	<No Filtering>	Double	Calcualte value per total tonne	[Profit]/[Tonnes]
VPPT	<No Filtering>	Double	Calcualte value per product ton	[Profit]/[Total Product t]
ASSIGN MATERIAL	<No Filtering>	String		0
Check Economic	<No Filtering>	String	Reset cost and revenue to zero	0
Flag Economic	<No Filtering>	String	Flag if block is profitable	if([VPT]>0,"True","False")
Set Material Value	<No Filtering>	String	Set the material value	IF([VPT]>0,"ORE","WASTE")

Appendix B : Deswik global constants

NAME	GROUP	DESCRIPTION	TYPE	VALUE
CC	CLOSURE	Closure cost ((US$t mined)	Double	0.13
Group: DMS PRODUCT SPEC				
DMSLFE	DMS PROD	DMS Lump product Fe	Double	66.00
DMSLS	DMS PROD	DMS Lump product SiO2	Double	4.66
DMSLA	DMS PROD	DMS Lump product AL2O3	Double	0.70
DMSFFE	DMS PROD	DMS Fine product Fe	Double	63.00
DMSFS	DMS PROD	DMS Fines product SiO2	Double	8.08
DMSFA	DMS PROD	DMS Fines product AL2O3	Double	0.73
Group: G&A				
GA	G&A	G&A Cost (US$t feed)	Double	9.36
Group: IPF RD				
IPFRD	IPF RD	IPF RD changed to waste rd	Double	2.40
Group: LOGISTIC				
RC	LOGISTIC	Rail cost (US$t Prod dry)	Double	11.80
PC	LOGISTIC	Port cost (US$t Prod dry)	Double	2.14
Group: MARKETING				
SF	MARKETIN	Sea Freight cost (US$t Prod)	Double	14.01
OSC	MARKETIN	Offshore Sales cost (US$t Prod)	Double	1.62
Group: MINING				
MC	MINING	Average mining cost (US$t mined)	Double	4.44
HC	MINING	Average haulage cost (US$t/hr)	Double	234.65
DC	MINING	Average drilling cost (US$t mined)	Double	0.22
BC	MINING	Average blasting cost (US$t mined)	Double	0.47
LC	MINING	Average loading cost (US$t mined)	Double	0.45
AC	MINING	Average ancilliary cost (US$t mined)	Double	0.91
OC	MINING	Average other mining cost (US$t mined)	Double	0.80
Group: MRE				
MRE	MRE	Modifying factor (MRE)	Double	0.83
Group: PROCESSING				
DSOC	PROCESSIN	DSO Processing cost (US$t feed)	Double	3.19
DMSC	PROCESSIN	DMS Processing cost (US$t feed)	Double	13.44
TPC	PROCESSIN	Total Processing cost (US$t Prod dry)	Double	4.68
Group: PROCESSING RATIO				
LR	PROCESSIN	LUMP RATIO	Double	0.57
Group: PROCESSING YIELDS				
DMSYL	PROCESSIN	DMS YIELD	Double	0.60
DSOYL	PROCESSIN	DSO YIELD	Double	1.00
Group: REGRESSION				
RC_KL_ORE	REGRESSIO	Kolomela ORE Reference cycle time (min)	Double	62.84
k_ct_d_m	REGRESSIO	KBF cycle time inpit fill _dump multiplier	Double	(0.19)
k_ct_d_c	REGRESSIO	KBF cycle time inpit fill _dump constant	Double	260.86
k_ct_plant_m	REGRESSIO	KBF cycle time plant multiplier	Double	(0.16)
k_ct_plant_c	REGRESSIO	KBF cycle time plant constant	Double	225.71
l_ct_d_m	REGRESSIO	LF cycle time inpit fill _dump multiplier	Double	(0.22)
l_ct_d_c	REGRESSIO	LF cycle time inpit fill _dump constant	Double	297.92
l_ct_plant_m	REGRESSIO	LF cycle time plant multiplier	Double	(0.11)
l_ct_plant_c	REGRESSIO	LF cycle time plant constant	Double	152.18
ksn_ct_plant_m	REGRESSIO	LF cycle time plant multiplier	Double	(0.06)
ksn_ct_plant_c	REGRESSIO	LF cycle time plant constant	Double	135.47
ksn_ct_d_m	REGRESSIO	LF cycle time dump multiplier	Double	0.12
ksn_ct_d_c	REGRESSIO	LF cycle time dump constant	Double	(105.45)
kss_ct_plant_m	REGRESSIO	LF cycle time plant multiplier	Double	(0.09)
kss_ct_plant_c	REGRESSIO	LF cycle time plant constant	Double	179.44
kss_ct_d_m	REGRESSIO	LF cycle time dump multiplier	Double	(0.15)
kss_ct_d_c	REGRESSIO	LF cycle time dump constant	Double	221.75
RC_KL_WAST	REGRESSIO	Kolomela WASTE Reference cycle time (min)	Double	45.84
Group: REVENUE				
FR	REVENUE	62P Std Fines (Base Platts Price)	Double	71.50
PF	REVENUE	65P Premium Fines (Base Platts Price)	Double	83.68
SL	REVENUE	62P Std Lump (Base Platts Price)	Double	71.59
PL	REVENUE	65P Premium Lump (Base Platts Price)	Double	83.68
BFe	REVENUE	62P Fe Threshold	Double	62.00
TFe	REVENUE	65P Fe Threshold	Double	65.00
PABFE	REVENUE	Premium above 62P Threshold	Double	1.15
SIPL	REVENUE	SIO2 Penality >=4.5	Double	1.00
SIPM	REVENUE	SIO2 Penality 4.5% -6.5%	Double	1.50
SIPH	REVENUE	SIO2 Penality 6.5% -9%	Double	1.80
ALP	REVENUE	Al2O3 Penality 1%-2.5%	Double	3.00
SIL	REVENUE	SIO2 Low range P62	Double	3.50
SIM	REVENUE	SIO2 MED rangeb P62	Double	4.50
SIH	REVENUE	SIO2 HIGH range P62	Double	9.00
ALL	REVENUE	Al2O3 low range 1%	Double	1.50
ALM	REVENUE	Al2O3 MED range 1%	Double	2.25
LP	REVENUE	Lump Premium $c/dmtu	Double	30.93
SILL	REVENUE	SIO2 Low range P65	Double	2.00
DA	REVENUE	Premium lump (DA) ratio	Double	0.33
FC	REVENUE	Premium Fines (FC) ratio	Double	0.25
SILF	REVENUE	SIO2 Low range P62 -Fines	Double	4.00
Group: ROYALTIES				
RY	ROYALTIES	ROYALTIES	Double	0.04
Group: SIB				
SIB	SIB	SIB Mining cost ((US$t mined)	Double	0.53

Appendix C: Contaminants

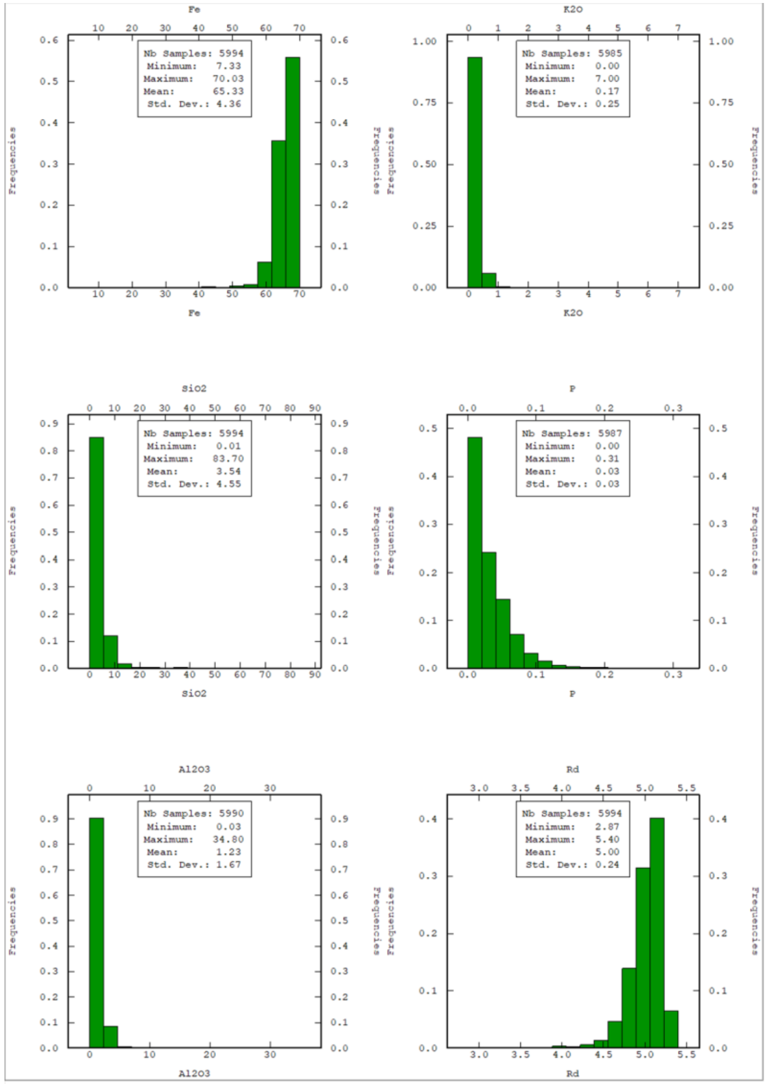

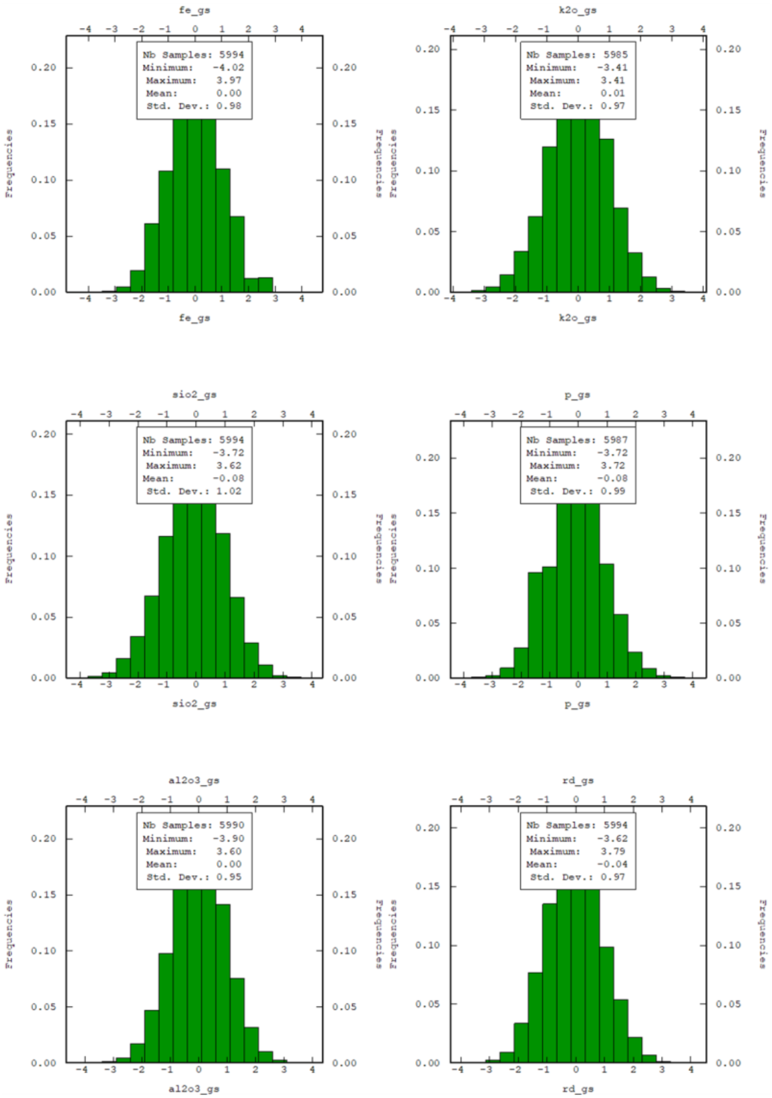

Appendix D: Material classifications of block models realisations

Block model realisation 1 results by material classification

Material Class	Volume	Tonnes	Density	u_fe	u_al2o	u_p	u_sio2	u_rd
a1	3,387,035	17,163,894	5.1	66.4	1.00	0.03	2.7	5.1
a2	762,351	3,814,549	5.0	64.5	1.06	0.03	3.3	5.0
a3	502,313	2,489,100	5.0	62.8	1.09	0.03	4.4	5.0
a4	968,948	4,818,273	5.0	64.9	2.81	0.04	3.7	5.0
a5	2,289,517	11,540,355	5.0	65.6	1.95	0.08	3.4	5.0
b	912,505	4,194,087	4.6	56.8	3.44	0.05	9.3	4.6
l	601,510	2,652,415	4.4	55.5	1.46	0.04	17.4	4.4
c	681,853	2,738,492	4.0	46.9	5.11	0.05	22.3	4.0
d	1,078,654	3,763,067	3.5	34.0	8.38	0.04	35.0	3.5
wst	140,691,115	419,506,525	3.0	20.2	11.12	0.04	48.2	3.0
Total ore	**9,424,179**	**46,672,673**	**4.96**	**64.22**	**1.68**	**0.05**	**4.57**	**4.96**
Total Waste	**142,451,622**	**426,008,083**	**2.99**	**20.47**	**11.05**	**0.04**	**47.88**	**2.99**

Block model realisation 2 results by material classification

Legend Bin	Volume	Tonnes	Density	u_fe	u_al2o	u_p	u_sio2	u_rd
a1	3,320,259	16,780,067	5.1	66.5	1.05	0.03	2.9	5.1
a2	637,723	3,176,316	5.0	64.5	1.12	0.03	3.6	5.0
a3	426,422	2,088,211	4.9	62.7	1.09	0.03	4.6	4.9
a4	1,087,227	5,405,428	5.0	65.1	2.78	0.04	3.8	5.0
a5	2,526,656	12,681,198	5.0	65.8	1.89	0.08	3.4	5.0
b	849,013	3,843,315	4.5	56.6	3.70	0.05	9.9	4.5
l	594,587	2,618,455	4.4	55.5	1.52	0.04	17.4	4.4
c	666,618	2,663,682	4.0	46.9	5.20	0.05	22.7	4.0
d	1,076,181	3,735,383	3.5	33.9	8.43	0.04	35.3	3.5
wst	140,691,115	419,506,525	3.0	20.2	11.12	0.04	48.2	3.0
Total ore	**9,441,887**	**46,592,990**	**4.94**	**64.38**	**1.73**	**0.05**	**4.65**	**4.94**
Total Waste	**142,433,915**	**425,905,589**	**2.99**	**20.46**	**11.05**	**0.04**	**47.89**	**2.99**

Block model realisation 3 results by material classification

Legend Bin	Volume	Tonnes	Density	u_fe	u_al2o	u_p	u_sio2	u_rd
a1	3,586,989	18,181,437	5.1	66.5	1.00	0.03	2.9	5.1
a2	792,162	3,964,524	5.0	64.5	1.05	0.03	3.6	5.0
a3	532,316	2,634,595	4.9	62.8	1.01	0.03	4.7	4.9
a4	856,284	4,257,348	5.0	65.0	2.59	0.04	3.8	5.0
a5	2,202,720	11,060,491	5.0	65.8	1.45	0.08	3.8	5.0
b	881,966	4,036,372	4.6	56.8	3.41	0.04	9.7	4.6
l	603,954	2,654,911	4.4	55.5	1.20	0.04	17.5	4.4
c	666,607	2,663,121	4.0	46.8	5.10	0.04	23.0	4.0
d	1,061,689	3,686,874	3.5	34.0	8.44	0.04	35.4	3.5
wst	140,691,115	419,506,525	3.0	20.2	11.12	0.04	48.2	3.0
Total ore	**9,456,390**	**46,789,679**	**4.96**	**64.36**	**1.47**	**0.05**	**4.77**	**4.96**
Total Waste	**142,419,412**	**425,856,519**	**2.99**	**20.46**	**11.05**	**0.04**	**47.89**	**2.99**

Block model realisation 4 results by material classification

Legend Bin	Volume	Tonnes	Density	u_fe	u_al2o	u_p	u_sio2	u_rd
a1	3,540,580	17,912,285	5.1	66.5	1.02	0.03	2.8	5.1
a2	673,629	3,355,977	5.0	64.5	1.10	0.03	3.4	5.0
a3	483,551	2,372,276	4.9	62.7	1.07	0.03	4.5	4.9
a4	934,014	4,640,535	5.0	64.9	2.58	0.04	3.8	5.0
a5	2,344,142	11,759,118	5.0	65.8	1.50	0.08	4.1	5.0
b	882,139	4,023,905	4.6	56.8	3.58	0.05	9.7	4.6
l	598,458	2,629,235	4.4	55.5	1.29	0.04	18.1	4.4
c	647,836	2,581,961	4.0	46.9	5.28	0.05	23.1	4.0
d	1,080,336	3,756,718	3.5	34.0	8.51	0.04	35.4	3.5
wst	140,691,115	419,506,525	3.0	20.2	11.12	0.04	48.2	3.0
Total ore	**9,456,513**	**46,693,329**	**4.95**	**64.36**	**1.54**	**0.05**	**4.81**	**4.95**
Total Waste	**142,419,288**	**425,845,204**	**2.99**	**20.46**	**11.06**	**0.04**	**47.89**	**2.99**

Block model realisation 5 results by material classification

Legend Bin	Volume	Tonnes	Density	u_fe	u_al2o	u_p	u_sio2	u_rd
a1	3,602,879	18,215,399	5.1	66.4	1.00	0.03	2.9	5.1
a2	802,864	3,993,358	5.0	64.5	1.04	0.03	3.6	5.0
a3	532,921	2,619,185	4.9	62.9	1.02	0.03	4.7	4.9
a4	785,826	3,902,530	5.0	65.1	2.67	0.04	3.9	5.0
a5	2,245,087	11,304,416	5.0	65.9	1.47	0.08	3.5	5.0
b	858,958	3,920,092	4.6	56.8	3.34	0.05	9.6	4.6
l	601,549	2,643,230	4.4	55.5	1.24	0.04	17.2	4.4
c	672,192	2,693,405	4.0	46.9	5.13	0.04	22.7	4.0
d	1,082,408	3,764,998	3.5	34.0	8.40	0.04	35.2	3.5
wst	140,691,115	419,506,525	3.0	20.2	11.12	0.04	48.2	3.0
Total ore	**9,430,086**	**46,598,210**	**4.95**	**64.37**	**1.47**	**0.05**	**4.65**	**4.95**
Total Waste	**142,445,716**	**425,964,928**	**2.99**	**20.46**	**11.05**	**0.04**	**47.88**	**2.99**

Block model realisation 6 results by material classification

Legend Bin	Volume	Tonnes	Density	u_fe	u_al2o	u_p	u_sio2	u_rd
a1	3,587,653	18,131,648	5.1	66.5	1.00	0.03	2.8	5.1
a2	820,698	4,093,923	5.0	64.5	1.07	0.03	3.5	5.0
a3	571,288	2,811,200	4.9	62.7	1.04	0.03	4.5	4.9
a4	881,111	4,382,575	5.0	65.1	2.70	0.03	4.1	5.0
a5	2,067,074	10,388,063	5.0	65.7	1.46	0.08	3.7	5.0
b	885,977	4,051,709	4.6	56.6	3.36	0.05	9.8	4.6
l	600,243	2,646,416	4.4	55.6	1.22	0.04	17.1	4.4
c	690,309	2,772,736	4.0	46.8	5.07	0.04	22.5	4.0
d	1,080,335	3,762,357	3.5	33.8	8.35	0.04	35.2	3.5
wst	140,691,115	419,506,525	3.0	20.2	11.12	0.04	48.2	3.0
Total ore	**9,414,042**	**46,505,535**	**4.95**	**64.28**	**1.49**	**0.04**	**4.70**	**4.95**
Total Waste	**142,461,759**	**426,041,617**	**2.99**	**20.47**	**11.05**	**0.04**	**47.88**	**2.99**

Block model realisation 7 results by material classification

Legend Bin	Volume	Tonnes	Density	u_fe	u_al2o	u_p	u_sio2	u_rd
a1	3,665,325	18,561,353	5.1	66.5	1.00	0.03	2.8	5.1
a2	747,828	3,723,433	5.0	64.5	1.07	0.03	3.4	5.0
a3	500,010	2,456,826	4.9	62.7	1.04	0.03	4.5	4.9
a4	856,918	4,256,132	5.0	64.8	2.63	0.04	4.0	5.0
a5	2,183,947	10,976,353	5.0	65.8	1.58	0.08	3.8	5.0
b	872,095	3,981,096	4.6	56.7	3.54	0.05	9.6	4.6
l	586,258	2,583,697	4.4	55.6	1.24	0.04	17.1	4.4
c	701,157	2,807,920	4.0	46.8	5.05	0.04	22.4	4.0
d	1,071,148	3,718,036	3.5	33.9	8.43	0.04	35.3	3.5
wst	140,691,115	419,506,525	3.0	20.2	11.12	0.04	48.2	3.0
Total ore	**9,412,381**	**46,538,889**	**4.95**	**64.38**	**1.52**	**0.05**	**4.65**	**4.95**
Total Waste	**142,463,420**	**426,032,481**	**2.99**	**20.47**	**11.05**	**0.04**	**47.88**	**2.99**

Block model realisation 8 results by material classification

Legend Bin	Volume	Tonnes	Density	u_fe	u_al2o	u_p	u_sio2	u_rd
a1	3,414,531	17,255,158	5.1	66.4	1.04	0.03	2.9	5.1
a2	618,922	3,088,258	5.0	64.5	1.09	0.03	3.6	5.0
a3	458,713	2,262,856	4.9	62.8	1.05	0.03	4.7	4.9
a4	899,770	4,469,787	5.0	65.1	2.69	0.04	3.9	5.0
a5	2,604,025	13,070,949	5.0	65.8	1.54	0.08	3.5	5.0
b	845,710	3,843,597	4.5	56.6	3.60	0.05	10.1	4.5
l	610,897	2,684,337	4.4	55.6	1.22	0.04	17.4	4.4
c	653,437	2,613,946	4.0	46.8	5.16	0.05	22.7	4.0
d	1,078,681	3,750,204	3.5	34.1	8.43	0.04	35.2	3.5
wst	140,691,115	419,506,525	3.0	20.2	11.12	0.04	48.2	3.0
Total ore	**9,452,568**	**46,674,942**	**4.95**	**64.39**	**1.56**	**0.05**	**4.73**	**4.95**
Total Waste	**142,423,233**	**425,870,676**	**2.99**	**20.46**	**11.06**	**0.04**	**47.89**	**2.99**

Block model realisation 9 results by material classification

Legend Bin	Volume	Tonnes	Density	u_fe	u_al2o	u_p	u_sio2	u_rd
a1	3,473,996	17,599,765	5.1	66.5	1.03	0.03	2.8	5.1
a2	738,896	3,684,626	5.0	64.5	1.08	0.03	3.6	5.0
a3	473,202	2,333,178	4.9	62.8	1.02	0.03	4.9	4.9
a4	791,440	3,942,510	5.0	65.0	2.54	0.04	3.8	5.0
a5	2,481,299	12,459,189	5.0	65.8	1.53	0.08	3.6	5.0
b	854,486	3,908,148	4.6	56.5	3.35	0.05	10.2	4.6
l	606,382	2,680,248	4.4	55.7	1.29	0.04	17.3	4.4
c	678,650	2,727,442	4.0	46.9	4.93	0.05	22.7	4.0
d	1,086,336	3,791,756	3.5	33.9	8.40	0.04	34.8	3.5
wst	140,691,115	419,506,525	3.0	20.2	11.12	0.04	48.2	3.0
Total ore	**9,419,700**	**46,607,665**	**4.96**	**64.37**	**1.50**	**0.05**	**4.72**	**4.96**
Total Waste	**142,456,101**	**426,025,722**	**2.99**	**20.46**	**11.05**	**0.04**	**47.88**	**2.99**

Block model realisation 10 results by material classification

Legend Bin	Volume	Tonnes	Density	u_fe	u_al2o	u_p	u_sio2	u_rd
a1	3,665,325	18,560,353	5.1	66.5	1.00	0.03	2.8	5.1
a2	747,828	3,722,433	5.0	64.5	1.07	0.03	3.4	5.0
a3	500,010	2,455,826	4.9	62.7	1.04	0.03	4.5	4.9
a4	856,918	4,255,132	5.0	64.8	2.63	0.04	4.0	5.0
a5	2,183,947	10,975,353	5.0	65.8	1.58	0.08	3.8	5.0
b	872,095	3,985,096	4.6	56.7	3.54	0.05	9.6	4.6
l	586,258	2,584,697	4.4	55.6	1.24	0.04	17.1	4.4
c	701,157	2,806,920	4.0	46.8	5.05	0.04	22.4	4.0
d	1,071,148	3,717,036	3.5	33.9	8.43	0.04	35.3	3.5
wst	140,691,115	419,508,525	3.0	20.2	11.12	0.04	48.2	3.0
Total ore	**9,412,381**	**46,538,889**	**4.95**	**64.38**	**1.52**	**0.05**	**4.65**	**4.95**
Total Waste	**142,463,420**	**426,032,481**	**2.99**	**20.47**	**11.05**	**0.04**	**47.88**	**2.99**

Appendix E: Deterministic pit optimisation results

Discount Rate	9.00%				
Mining Rate	10,000,000				
Base Price	78.5				
Revenue Factor	**Total Cost**	**Total Revenue**	**Average Case DCF**	**Incremental cost**	**Ore Tonnes (Mt)**
0.74	161,013,030	219,336,336	52,961,755	58.09	2,536,266
0.76	60,488,566	80,802,039	69,817,722	59.66	3,448,060
0.78	551,292,076	710,544,917	147,648,994	61.23	11,288,972
0.8	232,356,822	295,842,309	165,361,428	62.8	14,512,447
0.82	8,599,642	10,534,764	165,657,424	64.37	14,624,231
0.84	4,091,846,454	4,917,402,837	(150,522,122)	65.94	67,446,641
0.86	109,084,165	128,087,375	(154,189,239)	67.51	68,784,813
0.88	64,827,129	74,591,709	(156,586,279)	69.08	69,566,627
0.9	67,578,828	76,372,303	(159,032,431)	70.65	70,419,222
0.92	166,827,663	183,065,684	(165,063,397)	72.22	72,427,060
0.94	63,366,114	68,092,064	(167,309,205)	73.79	73,217,098
0.96	26,667,624	27,897,570	(168,534,533)	75.36	73,534,899
0.98	66,524,026	67,822,950	(171,159,078)	76.93	74,262,630
1	42,591,000	42,877,496	(172,807,411)	78.5	74,742,778
1.02	14,519,330	14,581,713	(173,257,572)	80.07	74,903,354
1.04	124,498,030	120,930,879	(178,276,307)	81.64	76,358,761
1.06	88,371,171	84,851,100	(181,334,853)	83.21	77,326,835
1.08	49,406,768	45,620,068	(183,376,758)	84.78	77,820,805
1.1	36,716,630	33,395,071	(183,376,758)	86.35	78,179,086
1.12	32,534,766	28,478,460	(184,835,980)	87.92	78,500,077
1.14	5,644,984	4,900,623	(186,100,715)	89.49	78,554,171
1.16	522,197,873	440,315,825	(186,280,922)	91.06	83,784,289
1.18	863,638	716,568	(205,490,076)	92.63	83,793,065

Appendix F: Probabilistic pit optimisation results

		Revenue Factor	Total Mass	Total Revenue	Total Cost	Total Revenue (Discounted)	Total Cost (Discounted)	Discounted Cash Flow	Recovered Ore	Total Product t
P5	Real 6	1	438,910,238	4,681,547,006	3,552,647,938	4,597,947,778	3,478,488,164	1,119,459,615	84,325,284	77,844,861
P5	Real 7	1	582,937,662	8,967,419,921	4,544,934,680	7,115,352,960	3,310,216,295	3,805,136,665	83,670,545	77,006,967
P5	Real 8	1	580,667,940	8,971,835,197	4,536,872,023	7,106,434,702	3,313,194,806	3,793,239,896	84,575,686	77,997,139
P5	Real 9	1	581,994,328	8,950,397,791	4,534,248,884	7,111,642,017	3,311,434,638	3,800,207,379	83,523,541	76,870,468
P25	Real 2	1	564,452,694	6,714,591,525	4,353,331,173	6,523,178,011	3,864,597,540	2,658,580,471	84,203,404	77,508,799
P25	Real 3	1	562,484,029	6,711,178,377	4,347,233,777	6,525,998,850	3,864,272,236	2,661,726,613	84,410,605	77,703,079
P25	Real 7	1	564,503,024	6,703,384,658	4,348,211,399	6,452,818,025	3,836,347,650	2,616,470,375	83,796,774	77,042,021
P25	Real 8	1	563,485,795	6,689,900,276	4,340,278,055	6,356,499,608	3,775,986,818	2,580,512,790	84,089,119	77,427,537
P50	Real 3	1	438,742,195	4,696,419,839	3,549,742,045	4,271,756,357	3,111,266,428	1,160,489,929	71,782,373	66,060,535
P50	Real 7	1	439,903,544	4,683,483,641	3,544,119,310	4,242,435,355	3,101,197,723	1,141,237,632	72,775,647	66,866,547
P50	Real 8	1	443,581,192	4,713,475,443	3,570,140,865	4,260,499,885	3,114,652,193	1,145,847,692	73,230,915	67,416,151
P50	Real 10	1	439,861,398	4,720,158,784	3,558,614,105	4,647,752,693	3,491,714,134	1,156,038,559	84,415,898	77,704,705
P75	Real 1	1	369,406,688	6,415,604,287	5,924,990,557	3,382,251,659	3,096,423,739	285,827,920	73,189,417	67,140,814
P75	Real 3	1	350,132,302	3,175,245,998	2,901,512,605	3,400,565,537	3,080,549,457	320,016,080	71,782,373	66,060,535
P75	Real 6	1	358,524,839	3,222,719,862	2,951,812,750	3,394,960,622	3,083,346,947	311,613,675	72,645,056	66,741,346
P75	Real 8	1	361,220,053	3,242,765,337	2,975,408,430	3,403,734,315	3,094,322,553	309,411,762	73,230,915	67,416,151